Optimizing Acoustic Stimulation Timing for Enhanced Deep Sleep: An Analytical Approach Using Polysomnography Data

by

Sepehr SARDOOEINASAB

MANUSCRIPT-BASED THESIS PRESENTED TO ÉCOLE DE TECHNOLOGIE SUPÉRIEURE
IN PARTIAL FULFILLMENT OF A MASTER'S DEGREE
WITH THESIS IN ELECTRICAL ENGINEERING
M.A.Sc.

MONTREAL, "DECEMBER 22, 2025"

ÉCOLE DE TECHNOLOGIE SUPÉRIEURE
UNIVERSITÉ DU QUÉBEC

Sepehr Sardooeinasab, 2025

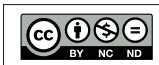

This Creative Commons license allows readers to download this work and share it with others as long as the author is credited. The content of this work cannot be modified in any way or used commercially.

BOARD OF EXAMINERS

THIS THESIS HAS BEEN EVALUATED

BY THE FOLLOWING BOARD OF EXAMINERS

Mr. Mohamad Forouzanfar, Thesis supervisor
Department of System Engineering, École de Technologie Supérieure, Montreal, Canada

Mr. Massimiliano de Zambotti, Thesis Co-Supervisor
Senior Manager, Ouraring Inc, San Francisco, US

Ms. Rita Noumeir, Chair, Board of Examiners
Department of Electrical Engineering, École de Technologie Supérieure, Montreal, Canada

Mr. Jean-Marc Lina, External Examiner
Department of Electrical Engineering, École de Technologie Supérieure, Montreal, Canada

THIS THESIS WAS PRESENTED AND DEFENDED

IN THE PRESENCE OF A BOARD OF EXAMINERS AND THE PUBLIC

ON "NOVEMBER 21, 2025"

AT ÉCOLE DE TECHNOLOGIE SUPÉRIEURE

Optimiser le moment de la stimulation acoustique pour un sommeil profond amélioré : une approche analytique utilisant les données de polysomnographie

Sepehr SARDOOEINASAB

RÉSUMÉ

La stimulation acoustique, une technique courante de neuromodulation, a montré qu'elle pouvait renforcer les oscillations lentes (SOs, *slow oscillations*) et l'activité à ondes lentes (SWA, *slow-wave activity*) pendant le sommeil profond non paradoxal (NREM). Cette amélioration soutient la fonction immunitaire, la régulation autonome, la santé cognitive, la consolidation de la mémoire et la sensation de repos au réveil. Des travaux antérieurs indiquent que l'efficacité du stimulus dépend du moment de son application par rapport aux rythmes corticaux en cours, en particulier les phases «upstate» des SOs (angles de phase compris entre 0 et 180°). Étant donné la forte connexion entre les systèmes central et périphérique pendant le sommeil, notamment au niveau cortico-cardiaque, nous avons cherché à examiner comment les phases corticales et cardiaques modulent les réponses à la stimulation et à déterminer les stratégies temporelles optimales.

Nous avons analysé des enregistrements de polysomnographie nocturne provenant de 133 adolescents, durant lesquels des sons auditifs (80 dB, 1000 Hz, 50 ms) ont été présentés à intervalles aléatoires de 15 à 30 s. Les phases instantanées des SOs de l'EEG (~0.8 Hz) ainsi que des composantes de la fréquence cardiaque (HR) en basse fréquence (LF; 0.04–0.15 Hz) et en haute fréquence (HF; 0.15–0.4 Hz) ont été extraites, et trois analyses complémentaires ont été réalisées : (1) comparaison des réponses évoquées par les sons entre les phases upstate et downstate des SOs et des composantes cardiaques ; (2) évaluation des stratégies d'ancrage de phase (*phase-locking*), en comparant des conditions unimodales (SO seul ou HR seul) et combinées EEG–HR aux conditions sans ancrage de phase et sans stimulation sonore, afin d'évaluer l'effet net de l'ancrage de phase et des sons ; et (3) analyse continue sur 360° des cycles de phase pour identifier des emplacements temporels optimaux au-delà de deux catégories de phase globales.

La stimulation pendant les phases upstate de HR-LF et les phases downstate de HR-HF a produit des amplitudes de SO significativement plus grandes (jusqu'à ~16% d'augmentation), davantage d'événements SO (jusqu'à 22%), une SWA plus élevée (jusqu'à 25%) et des réponses oscillatoires cardiaques marquées (jusqu'à 56%) par rapport aux phases opposées ($p < 0.05$). Par rapport à la stimulation sans ancrage de phase, l'ancrage sur les composantes cardiaques a augmenté l'amplitude des SOs d'environ 22 μV et la SWA de 12%, tandis que l'ancrage exclusivement sur les phases upstate des SOs a accru l'amplitude des SOs d'environ 18 μV et la SWA de 19%. Les effets maximaux ont été observés lorsque les phases cardiaques optimales coïncidaient avec les phases upstate des SOs, entraînant une augmentation de ~38 μV de l'amplitude des SOs et de 32% de la SWA. L'analyse continue de phase a en outre révélé que les réponses culminaient juste avant le pic de phase upstate de HR-LF et le creux de phase downstate de HR-HF.

Ces résultats démontrent que les phases oscillatoires corticales et périphériques fournissent des repères temporels robustes pour la stimulation auditive en boucle fermée. La combinaison des informations de phase EEG et HR permet un ciblage plus précis, mettant en évidence le couplage cerveau–cœur comme mécanisme d'optimisation des stratégies adaptatives de stimulation pour améliorer le sommeil profond et ses bénéfices physiologiques et cognitifs associés.

Mots-clés: électroencéphalogramme, ondes lentes, activité à ondes lentes, fréquence cardiaque, stimulation acoustique, couplage cerveau–cœur, neuromodulation, sommeil profond

Optimizing Acoustic Stimulation Timing for Enhanced Deep Sleep: An Analytical Approach Using Polysomnography Data

Sepehr SARDOOEINASAB

ABSTRACT

Acoustic stimulation, a common neuromodulation technique, has been shown to enhance slow oscillations (SOs) and slow-wave activity (SWA) during deep non-rapid eye movement (NREM) sleep. This enhancement is associated with improved immune function, autonomic regulation, cognitive health, memory consolidation, and restfulness upon awakening. Prior work indicates that stimulus efficacy depends on timing relative to ongoing cortical rhythms, especially SO upstates. Given the close connection between central and peripheral systems during sleep, particularly at the cortico-cardiac level, we aimed to investigate how cortical and cardiac phases shape responses to stimulation and to determine optimal timing strategies.

We analyzed overnight polysomnography data from 133 adolescents, during which auditory tones (80 dB, 1000 Hz, 50 ms) were presented at random 15–30 s intervals. Instantaneous phases of EEG SOs (~0.8 Hz) and heart-rate (HR) low-frequency (LF; 0.04–0.15 Hz) and high-frequency (HF; 0.15–0.4 Hz) components were extracted, and three complementary analyses were performed: (1) comparison of tone-evoked responses during upstate vs. downstate phases of cortical SOs and HR components; (2) evaluation of phase-locking strategies, contrasting unimodal (SO-only or HR-only) and combined EEG–HR phase-locking against non–phase-locked and no-tone conditions to assess the net effect of phase-locking and tones; and (3) continuous 360° phase analysis to identify optimal timing locations beyond two broad phase categories.

Stimulation during HR-LF upstates and HR-HF downstates produced significantly larger SO amplitudes (up to 16% increase), more SO events (up to 22%), stronger SWA (up to 25%), and marked HR oscillatory responses (up to 56%) compared to opposite phases ($p < 0.05$). Relative to non–phase-locked stimulation, phase-locking to HR components enhanced SO amplitude by ~22 μV and SWA by 12%, while phase-locking exclusively to SO upstates increased SO amplitude by ~18 μV and SWA by 19%. Maximal effects were observed when optimal HR phases coincided with SO upstates, yielding 38 μV increases in SO amplitude and 32% increases in SWA. Continuous phase analysis further revealed that responses peaked just before the HR-LF up-peak and HR-HF down-peak.

These findings demonstrate that cortical and peripheral oscillatory phases provide robust timing cues for closed-loop auditory stimulation. Combining EEG and HR phase information enables more precise targeting, highlighting brain–heart coupling as a mechanism for refining adaptive stimulation strategies to enhance deep sleep and its associated physiological and cognitive benefits.

Keywords: brain–heart coupling, acoustic stimulation, slow oscillations, slow-wave activity, sleep enhancement, electroencephalogram, heart rate

TABLE OF CONTENTS

Page

LIST OF TABLES

LIST OF FIGURES

LIST OF ABBREVIATIONS

AASM	American Academy of Sleep Medicine
ANS	Autonomic nervous system
CLAS	Closed-loop auditory stimulation
CNS	Central nervous system
DOF	Degrees of freedom
ECG	Electrocardiography
EEG	Electroencephalography
EMG	Electromyography
EOG	Electrooculography
ERP	Event-related potential
FDR	False discovery rate
FFT	Fast Fourier transform
HR	Heart rate
HR-HF	High-frequency heart-rate oscillation (0.15–0.4 Hz)
HR-LF	Low-frequency heart-rate oscillation (0.04–0.15 Hz)
HRV	Heart-rate variability
MC	Monte Carlo
NCANDA	National Consortium on Alcohol and NeuroDevelopment in Adolescence
NREM	Non-rapid eye movement sleep

PNS	Parasympathetic nervous system
PSD	Power spectral density
PSG	Polysomnography
REM	Rapid eye movement sleep
RMS	Root mean square
SO	Slow oscillation
SS	Sleep spindles
SWA	Slow-wave activity
SWS	Slow-wave sleep

LIST OF SYMBOLS AND UNITS OF MEASUREMENTS

$x(t)$	Time-domain signal
$z(t)$	Analytic signal (complex representation of $x(t)$)
$\phi(t)$	Instantaneous phase of the analytic signal
$PSD(f)$	Power spectral density [μV^2/Hz]
μ	Mean value of a distribution
σ	Standard deviation of a distribution
p	p-value (probability of observing a result under H_0)
t	t-value (test statistic from a t-test)
z	Standardized test statistic (z-score approximation of W)
Hz	Hertz
s	Seconds
ms	Milliseconds
μV	Microvolt
bpm	Beats per minute
dB	Decibels

INTRODUCTION

Motivation

Sleep is an essential biological process involving complex physiological and neural mechanisms that are fundamental to health and well-being. Despite its importance, evidence suggests that the quantity and quality of sleep have been affected by modern lifestyles. Psychological disorders, lifestyle stressors, irregular schedules, and constant exposure to technology contribute to this disruption. These factors impair not only individual health but also broader societal domains, including reduced productivity (e.g., cognitive inefficiency in the workplace), increased accident risk (e.g., drowsy driving), and higher healthcare costs associated with chronic disease management (Grandner, 2018).

Sleep unfolds across distinct stages, each serving specific functions. Among them, slow-wave sleep (SWS), or deep sleep, represents the most restorative stage. SWS is closely linked to memory consolidation, emotional regulation, immune function, and physical recovery (Colrain, 2011; Purves *et al.*, 2018). Strengthening SWS could therefore improve personal well-being while benefiting public health and society.

A promising approach to enhancing deep sleep is acoustic stimulation. Studies show that auditory tones, when delivered at precise moments during SWS, can increase neural synchronization and enhance its restorative functions (Wilckens, Ferrarelli, Walker & Buysse, 2018; Cellini & Mednick, 2019; Ngo, Martinetz, Born & Mölle, 2013). However, effective implementation requires accurate timing, which remains a major barrier to real-world application (Esfahani *et al.*, 2023).

Consequently, this thesis is motivated by the need to better understand the mechanisms underlying sleep modulation and to develop data-driven, practical, and scalable tools for sleep enhancement. To this end, it applies statistical methods to a large polysomnography (PSG) dataset to identify new strategies for optimizing acoustic stimulation timing.

Problem statement

Understanding how the brain and body interact during sleep is essential for improving sleep enhancement methods. Research on auditory stimulation, however, has mainly focused on cortical activity, while interactions between brain and heart dynamics remain underexplored. This gap limits understanding of how heart–brain coordination influences the effects of auditory stimulation during sleep. Clarifying this relationship would improve our knowledge of how the brain and body work together to regulate sleep.

A key challenge in enhancing deep sleep through auditory stimulation lies in timing. Tones strengthen SWS only when delivered in synchrony with specific physiological rhythms. Yet, existing methods often struggle to achieve this alignment or rely on equipment for acquiring brain signals that is costly, intrusive, and largely impractical outside controlled laboratory environments (Esfahani *et al.*, 2023). These limitations hinder the translation of auditory stimulation techniques from experimental settings to real-world applications.

Although cardiac signals are routinely collected in sleep studies, their potential to inform stimulation timing has been largely overlooked. Cardiac rhythms reflect autonomic and physiological states that are closely coupled with cortical dynamics, particularly during non-rapid eye movement (NREM) sleep (de Zambotti *et al.*, 2016). Leveraging these signals alongside brain activity could offer a noninvasive and robust way to track the physiological phase, improving the precision and effectiveness of auditory stimulation. Integrating cardiac information into stimulation frameworks therefore represents a promising step toward more accessible and adaptive sleep enhancement approaches.

Limitations of current approaches

Current state-of-the-art closed-loop auditory stimulation (CLAS) systems are constrained by two key limitations that prevent them from achieving both precision and practicality.

1. **Limited understanding and utilization of heart–brain interaction under stimulation:** Although physiological interactions between the heart and brain during sleep are well established (Forouzanfar, Baker, Colrain & de Zambotti, 2019; de Zambotti *et al.*, 2016; Whitehurst, Chen, Naji & Mednick, 2020), their role in shaping responses to auditory stimulation remains poorly understood. Existing research, driven by its singular focus on brain rythms, has not incorporated heart–brain coupling into stimulation-control algorithms. As a result, the mechanisms by which bidirectional physiology modulates neural responsiveness to acoustic input remain critically unexamined. This omission leaves potentially synergistic timing information unused, limiting the performance of current closed-loop systems.
2. **Dependence on EEG-based systems:** Current CLAS methods depend heavily on electroencephalography (EEG), which requires specialized equipment and expert operation, limiting scalability (Rundo & Downey III, 2019). Peripheral measures such as electrocardiography (ECG) provide inexpensive, non-intrusive, and wearable-compatible signals (Swapna, Soman & Vinayakumar, 2019) that can not only complement EEG when available to improve timing precision, but also serve as the sole source of timing information for less intrusive and more cost-effective systems.

Taken together, these gaps highlight the need to integrate cardiac and cortical information to develop practical, scalable, and physiologically grounded approaches for deep-sleep enhancement.

Contributions

This thesis addresses the above challenges by making contributions at scientific, methodological, and technological levels.

1. **Characterization of stimulation effects and multimodal signal-processing pipeline:** It delivers a comprehensive analysis of the effects of acoustic stimulation during SWS using a large PSG dataset. Signal-processing pipelines and related algorithms were developed to derive instantaneous cortical and cardiac oscillations across relevant frequency bands, detect and quantify deep-sleep characteristics, and statistically compare tone-evoked neural and cardiac responses. By analyzing recordings from more than one hundred participants, the study demonstrates a bidirectional brain–heart interaction under stimulation and expands our understanding of physiological integration. It also shows that combining brain and heart signals yields more robust insights than analyzing either system alone.
2. **Continuous phase-analysis framework:** It introduces a continuous phase-analysis framework for identifying optimal timing windows for tone delivery. This methodological advancement uses EEG and ECG information and applies advanced statistical procedures, such as Monte-Carlo methods, to improve the reliability of timing estimates. The resulting improvement in precision lays the foundation for more accurate and deployable closed-loop stimulation technologies.
3. **ECG-guided timing for wearable CLAS:** It demonstrates the feasibility of using ECG as an alternative to EEG for guiding acoustic stimulation. ECG offers a less intrusive and more scalable tool for real-world and home-based sleep interventions. By leveraging cardiac phase information, the study shows that ECG-derived signals can effectively used for auditory stimulation timing, supporting the development of practical, cost-effective, and wearable CLAS systems.

Finally, the thesis synthesizes these findings into an optimized framework for stimulation timing that balances scientific precision with practical feasibility. This framework supports the development of non-pharmacological, sustainable interventions to improve sleep quality, cognitive performance, and long-term health outcomes.

Organization

This thesis is structured into three main chapters.

- Chapter 1 provides the scientific background and literature review. It introduces the physiology of sleep and its stages, describes PSG and its component signals, and discusses the importance of SWS and approaches to enhance it. The chapter also reviews previous acoustic stimulation and closed-loop methods, and identifies the research gaps that motivate this thesis. It concludes with an overview of the basic anatomy relevant to this work, along with the key preprocessing and statistical methods used.
- Chapter 2 presents the first research paper, which examines the feasibility of using peripheral rhythms—particularly heart-rate components—as alternative signals for guiding acoustic stimulation. This study evaluates whether cardiac dynamics can serve as reliable proxies for timing interventions.
- Chapter 3 contains the second research paper, which extends the analysis to more precise stimulation timing through continuous phase analysis. It introduces multidimensional approaches that combine cortical (EEG) and peripheral (ECG) features, and applies analytical methods to capture the complex interactions that shape optimal tone delivery.

The thesis concludes with a final section that summarizes the main contributions and outlines directions for future work.

Publication summary

The work conducted during my Master's studies has resulted in two papers: one peer-reviewed publication and one manuscript currently under review.

Accepted journal papers

• M. Forouzanfar, S. Sardooeinasab, F. C. Baker, I. M. Colrain, and M. de Zambotti. "Tone-evoked sleep electroencephalographic slow oscillations as a function of peripheral rhythms: new insights into the brain–heart integration." *Journal of Sleep Research*, 2025. (Impact Factor: 3.9)
Contribution: Joined the project after completion of the initial draft and experimental phase. Contributed to strengthening the analytical framework by introducing a pseudo-sham condition to better capture natural variability across physiological phases. Added slow-wave activity (SWA) as an outcome measure, whereas the original analysis reported only slow oscillation (SO) amplitude. Reviewed and validated the analysis code, implementing methodological improvements where appropriate, including modifying the SO detection criteria in response to reviewer comments. Improved the presentation of the results by revising sections of the Results and refining figures and plots to enhance clarity. Conducted additional targeted analyses requested during peer review, such as comparisons between up-peak and up-state dynamics. Contributed to improving the manuscript by adding relevant background and citations where needed, and participated substantially in manuscript revision and finalization for publication.

Manuscripts under review

• S. Sardooeinasab, M. de Zambotti, F. C. Baker and M. Forouzanfar. "Optimizing auditory stimulation timing in NREM sleep using peripheral rhythms: continuous phase analysis and multidimensional phase-locking." submitted to *SLEEP*, 2025. (Impact Factor: 4.9)
Contribution: Led the conceptualization and development of a multidimensional timing

framework integrating cortical and cardiac phase information. Designed and implemented continuous phase-analysis algorithms and conducted comprehensive data analyses to evaluate more accurate timing. Verified the robustness and correctness of the analytical pipeline. Drafted the initial manuscript and contributed to a subsequent revision by refining and clarifying methodological and conceptual aspects of the framework, as well as expanding the Discussion to address study limitations and provide reasoning for specific results. Participated actively in manuscript refinement to ensure clarity, coherence, and readiness for publication.

CHAPTER 1

BACKGROUND AND LITERATURE REVIEW

This chapter provides the scientific background for the thesis. It introduces sleep's role in health and cognition, describes the main tool for studying sleep, and reviews sleep stages with a focus on the neural dynamics of slow-wave sleep. The chapter then discusses acoustic stimulation as a promising non-pharmacological approach to enhance this stage. It also explains its key limitations, which motivate the analytic framework developed in this thesis. Finally, the chapter concludes by outlining the relevant anatomical background and the core preprocessing and statistical methods applied in this work.

1.1 Sleep

Sleep is a fundamental biological process essential for survival in mammals and present across most species. In humans, it occupies nearly one-third of life, with adults typically requiring about eight hours per night (Purves *et al.*, 2018). The need is even greater during development—infants may sleep up to 16 hours per day, while adolescents average around 9 hours. With age, sleep becomes shorter and more fragmented, though the overall requirement remains relatively stable (Colrain, 2011).

Once regarded as a passive state, sleep is now recognized as an active and tightly regulated process involving complex physiological and neural dynamics. It supports nearly every domain of health: learning and memory, emotional regulation, immune and metabolic balance, as well as cardiovascular and neurological stability. Insufficient sleep leads to the accumulation of sleep debt, which impairs attention, decision-making, and reaction speed, increasing accident risk. Chronic sleep loss has further been linked to immune suppression, cardiovascular disease, neurodegeneration, and reduced productivity (Colrain, 2011). Given sleep's importance, researchers typically study it using polysomnography, described in the following section.

1.2 Studying sleep: polysomnography

Polysomnography (PSG) is the gold standard for studying sleep. It records multiple physiological signals simultaneously, including electroencephalography (EEG), electro-oculography (EOG), electromyography (EMG), electrocardiography (ECG), airflow, respiratory effort, oxygen saturation, and body position (Rundo & Downey III, 2019). Combining these measures provides a comprehensive picture of brain, muscle, respiratory, and cardiac activity, allowing researchers to classify sleep stages and detect arousals, breathing irregularities, and other physiological events. After data acquisition, recordings are typically segmented into 30-second epochs and scored according to the American Academy of Sleep Medicine (AASM) guidelines (Iber, Ancoli-Israel, Chesson & Quan, 2007). PSG is usually conducted overnight in a sleep laboratory under the supervision of a trained technician.

1.2.1 Electroencephalography

Electroencephalography (EEG) is a non-invasive technique for measuring the brain's electrical activity through electrodes placed on the scalp. It captures the collective activity of large groups of neurons that fire in synchrony, providing a direct measure of brain dynamics with high temporal resolution (Light *et al.*, 2010). In sleep research, EEG is vital because it reveals the distinct oscillatory patterns that define different stages of sleep and wakefulness. For EEG acquisition, electrode placement typically follows standardized systems—most commonly the international 10–20 system, which is named for the 10% and 20% spacing intervals used to position electrodes along the skull's front–back and left–right axes (Figure 1.1). This configuration ensures consistent and reproducible coverage across cortical regions.

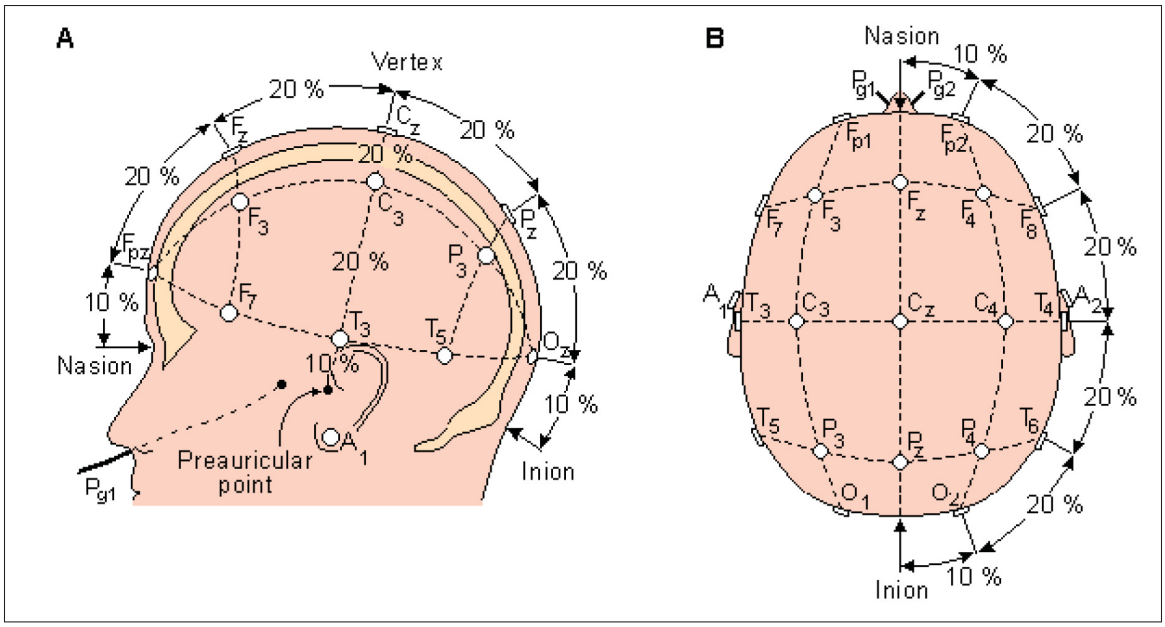

Figure 1.1 EEG electrode placement according to the international 10–20 system, shown from (A) the side and (B) the top view of the head.
Taken and adapted from Chenane *et al.* (2019)

1.2.2 Electrocardiography

Electrocardiography (ECG) is a non-invasive method for recording the heart's electrical activity via electrodes placed on the chest or limbs. The heart relies on an internal electrical system to coordinate its contractions, and the resulting voltage changes can be measured at the body surface. The electrodes capture the summed effect of these activations, which form a characteristic waveform in the ECG, typically consisting of the P wave, QRS complex, and T wave (Hall & Hall, 2020). Figure 1.2 illustrates how these electrical events produce the ECG waveform and its main features.

In sleep research, ECG is primarily used to monitor heart rate (HR) and its variability (HRV), as well as to detect arrhythmias. Compared to EEG, ECG is less intrusive and easier to acquire. In addition, consumer-grade wearables now make large-scale or ambulatory ECG recordings feasible.

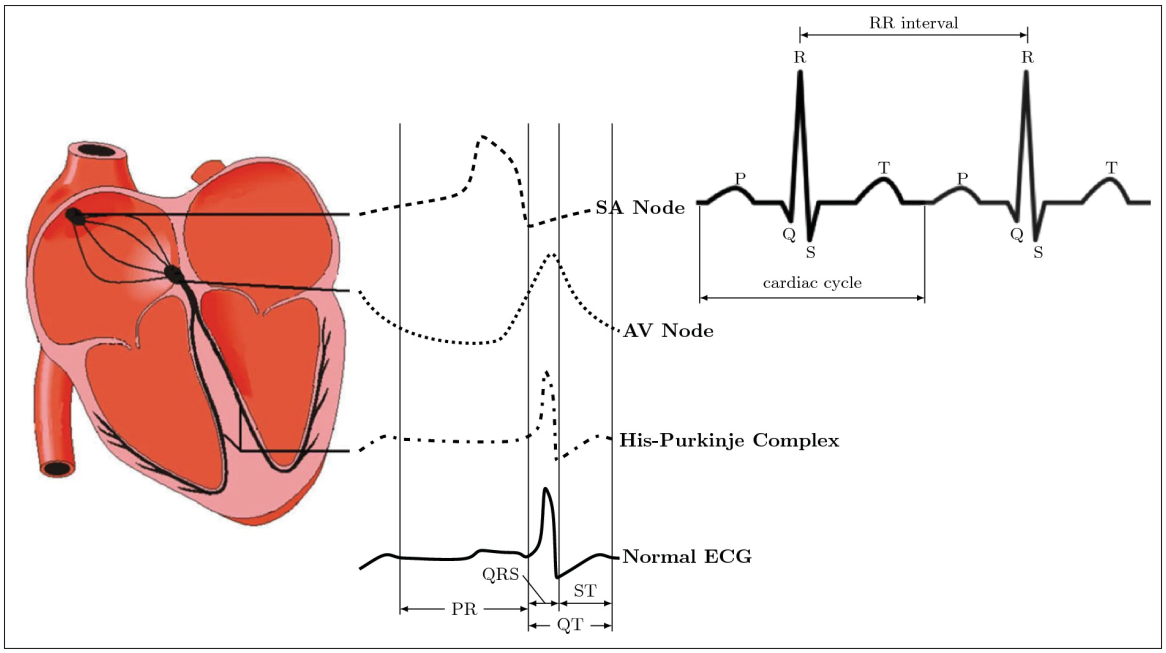

Figure 1.2 ECG signal representation, showing how cardiac electrical activity produces the characteristic PQRST components
Taken from Lima *et al.* (2023)

HR is commonly derived from the interval between successive R-peaks in the ECG signal, as expressed in Eq. 1.1

$$HR\ [\text{bpm}] = \frac{60\, f_s}{RR_{\text{samples}}}, \tag{1.1}$$

where f_s is the sampling rate (Hz) and RR_{samples} is the R–R interval in samples.

1.2.3 Other signals in PSG

EOG records voltage changes near the eyes to monitor eye movements. EMG, often measured at the chin or limb muscles, captures muscle tone and movement. Respiratory channels include airflow, chest and abdominal effort, and oxygen saturation, providing insight into breathing patterns. Together, these measures complement EEG and ECG, making PSG a comprehensive tool for sleep analysis.

1.3 Sleep stages and architecture

Human sleep is structured into repeating cycles lasting about 90–110 minutes. Each cycle includes non-rapid eye movement (NREM) sleep and rapid eye movement (REM) sleep, with their relative proportions shifting across the night. As the names suggest, REM involves rapid eye movements along with wake-like EEG activity, vivid dreaming, and near-complete muscle atonia, whereas NREM is defined by slower brain rhythms, reduced physiological activity, and the absence of such eye movements (Carskadon, Dement *et al.*, 2005). Early cycles are dominated by deep NREM sleep, while later cycles contain more REM sleep. A typical night consists of four to six such cycles, often illustrated with a hypnogram (Figure 1.3).

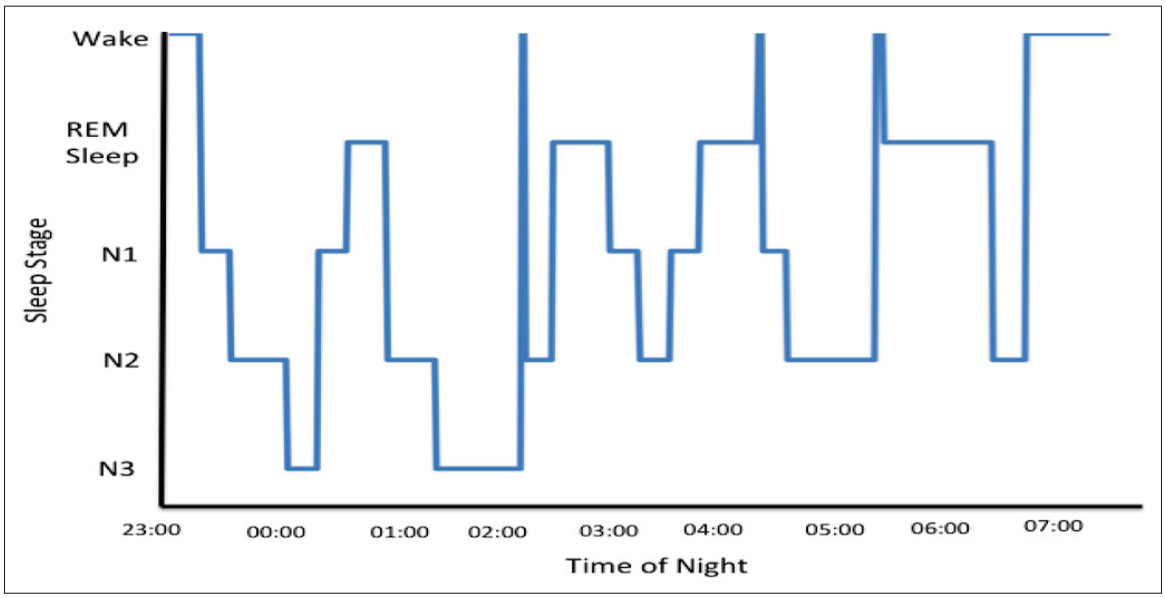

Figure 1.3 Example hypnogram showing the cycling of sleep stages (Wake, N1, N2, N3, and REM) across the night
Taken from Legault (2011)

NREM sleep itself is subdivided into three stages:

1. **Stage N1:** The lightest form of sleep, marking the transition from wakefulness to sleep. EEG shows reduced alpha activity (8–12 Hz) and mixed-frequency waves.
2. **Stage N2:** The most prevalent stage, defined by sleep spindles (11–16 Hz) and K-complexes, and associated with sensory gating and memory processing.

3. **Stage N3:** Also called slow-wave sleep (SWS), characterized by high-amplitude delta activity (0.5–4 Hz). It represents the deepest and most restorative stage of sleep.

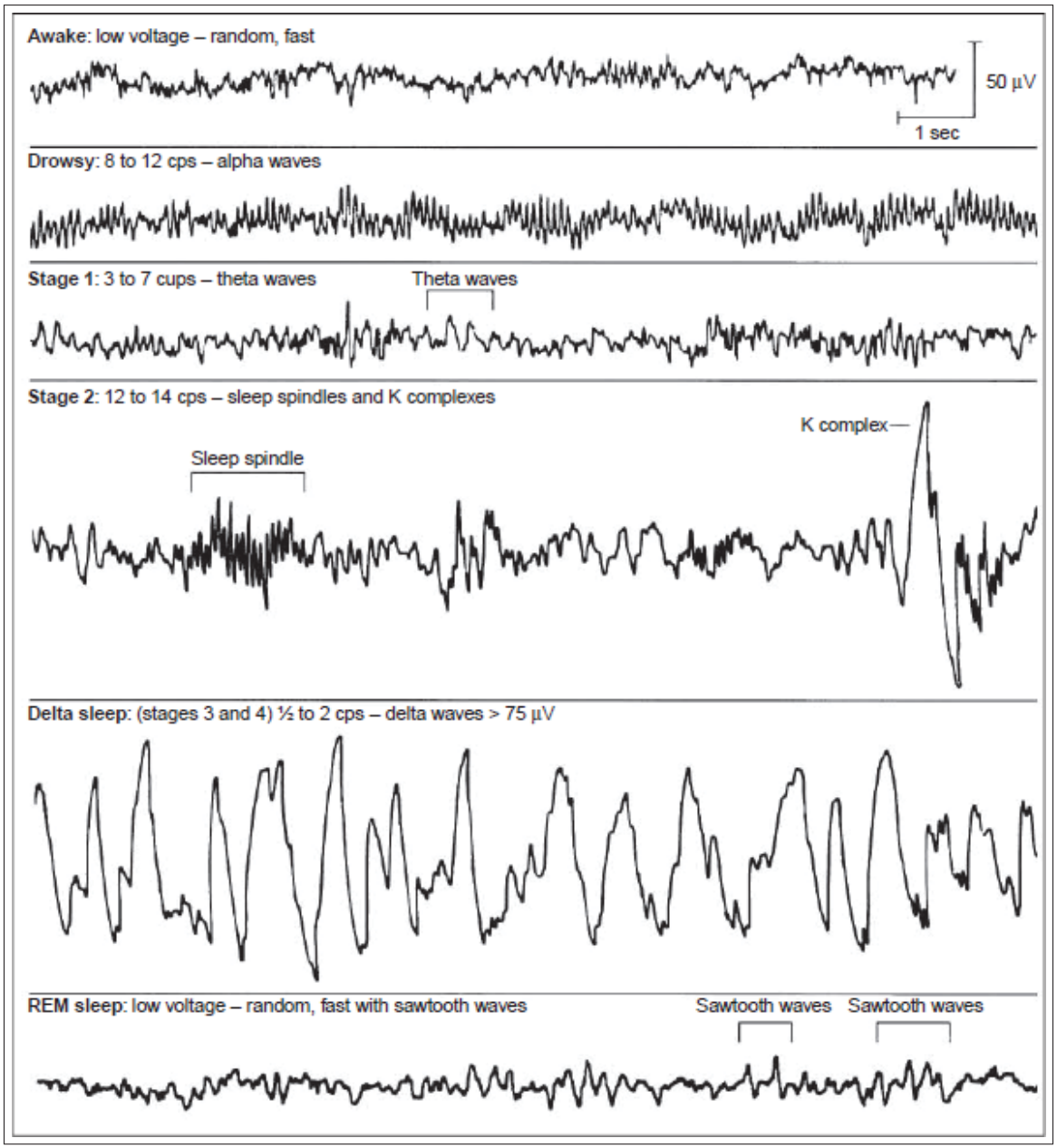

Figure 1.4 Example EEG traces illustrating the defining features of each sleep stage
Taken from Alhanoun *et al.* (2014)

The characteristics of each NREM stage, as well as REM sleep and wakefulness, are most evident in the EEG. However, signals such as the EOG and EMG also contribute to more accurate classification. Figure 1.4 illustrates the EEG features and defining characteristics of each stage.

1.4 Importance of slow-wave sleep and its EEG characteristics

SWS or N3 is the deepest stage of NREM sleep, defined by high-amplitude, low-frequency delta waves (0.5–4 Hz) in the EEG and accompanied by marked reductions in heart rate, blood pressure, and respiration. It is widely considered the most restorative sleep stage, with critical roles in both neural and physiological regulation.

At the neural level, SWS is strongly associated with memory consolidation. During this process, newly acquired information stored temporarily in the hippocampus is reactivated and gradually redistributed to long-term storage sites in the neocortex, the brain's outer layer. This hippocampal–cortical dialogue is thought to stabilize and integrate memories into broader networks. SWS is also linked to synaptic downscaling, a hypothesized mechanism by which the overall strength of synaptic connections built up during wakefulness is globally reduced. This renormalization prevents synaptic saturation, conserves metabolic resources, and maintains the brain's capacity for new learning on the following day (Staresina *et al.*, 2015).

Physiologically, SWS coincides with increased growth hormone secretion, reduced sympathetic activity, and enhanced parasympathetic dominance, supporting tissue repair, immune function, and cardiovascular recovery. Disruptions of SWS have been associated with impairments in memory, mood regulation, metabolic balance, and an increased risk of neurological disorders (Khan & Al-Jahdali, 2023).

1.4.1 Slow oscillations

A hallmark of SWS is the presence of slow oscillations (SOs), large EEG waves below 1 Hz that alternate between active (up) and silent (down) phases. During the up-phase, neurons in the cortex fire together, while the down-phase reflects a brief period of silence. These oscillations

provide a temporal framework for other brain rhythms. For instance, sleep spindles (11–16 Hz bursts) and hippocampal sharp-wave ripples are often coordinated with SOs, enabling memory transfer from hippocampus to neocortex for long-term storage.

1.4.2 Slow-wave activity

Slow-wave activity (SWA) refers to EEG power in the 0.5–4 Hz range during SWS and serves as a robust marker of sleep depth and restorative quality. Reduced SWA is associated with aging, sleep disorders, and neurological decline, whereas healthy levels are strongly linked to learning, memory consolidation, and brain plasticity.

Operationally, SWA is quantified as the total EEG power within the delta band, obtained by integrating the power spectral density (PSD, see Subsection 1.8.2) between 0.5 and 4 Hz

$$SWA = \int_{0.5}^{4} PSD(f)\, df, \tag{1.2}$$

where $PSD(f)$ denotes the power spectral density at frequency f.

1.5 Enhancing slow-wave sleep

Given the importance of deep sleep, and the fact that SOs and SWA amplitude serve as reliable markers of its quality, numerous strategies have been tested to enhance them. These can be grouped into two broad categories: lifestyle interventions and direct manipulations during sleep.

Lifestyle interventions act during wakefulness and aim to set the conditions for deeper sleep at night. For example, exercise, cognitive training, and other activities that increase brain activity raise the homeostatic drive for sleep, thereby promoting deeper subsequent sleep (Määttä *et al.*, 2010). In addition, pharmacological approaches have been developed to target neurotransmitter systems directly (Yamatsu *et al.*, 2015), while thermal regulation studies demonstrate that mild body warming can also facilitate deeper sleep (Kräuchi *et al.*, 2018).

In contrast, direct manipulations act on the brain during sleep itself. One approach uses weak electrical currents or magnetic pulses applied to the scalp to promote neural synchronization and strengthen slow waves (Saebipour *et al.*, 2015; De Gennaro *et al.*, 2008). Another approach relies on sensory stimulation, delivered through sound, odor, or vibration. Among sensory approaches, auditory stimulation has shown the greatest promise. Short tones, when timed to align with specific phases of ongoing SOs, can reliably enhance them and increase SWA (Wilckens *et al.*, 2018; Cellini & Mednick, 2019). However, the effectiveness of this method depends on accurate alignment with the brain's activity, making precise timing a critical requirement.

1.6 Literature review and gaps in acoustic stimulation

1.6.1 Mechanism

Acoustic stimulation leverages the fact that the auditory cortex remains responsive during sleep, even when consciousness is absent. External sounds can therefore interact with ongoing neural rhythms without fully waking the sleeper. To minimize the risk of arousal, most studies employ brief bursts of pink noise. These tones are broadband and relatively neutral, presented at an intensity that is clearly perceivable by the brain but low enough to avoid awakening the individual.

When delivered at the right phase of the SO cycle, these tones can amplify the ongoing oscillation, prolong trains of SOs, and enhance the synchronization of cortical networks. This effect is especially evident when tones are timed to delivered in phase with the SO up-state, a period of neuronal depolarization that provides a window of heightened cortical excitability. As a result, acoustic stimulation has been shown to boost SWA, facilitate SO–spindle coupling, and promote memory consolidation across sleep.

Early attempts, however, did not account for the timing of the endogenous SO. Studies using fixed-interval or random stimulation protocols reported mixed outcomes: in some cases, tones modestly increased slow-wave activity, but in others they disrupted sleep architecture or triggered

micro-arousals (Schade, Mathew, Roberts, Gartenberg & Buxton, 2020). These inconsistencies highlighted the crucial role of timing in determining whether stimulation enhances or impairs sleep, but they also revealed the limitations of open-loop designs, where tones are delivered independent of the ongoing brain state.

1.6.2 Closed-loop auditory stimulation

The recognition of timing as a critical factor in earlier studies directly motivated the development of closed-loop auditory stimulation (CLAS). In this approach, EEG is monitored in real time to detect the instantaneous phase of ongoing SOs, and auditory tones are delivered in synchrony with specific phases of the oscillation. Two main tone-delivery strategies are commonly used (Figure 1.5): (A) one or two tones delivered at the preferred phase, followed by a short pause; or (B) repeated tones within a stimulation window (5–10 s), followed by a no-tone interval of similar length.

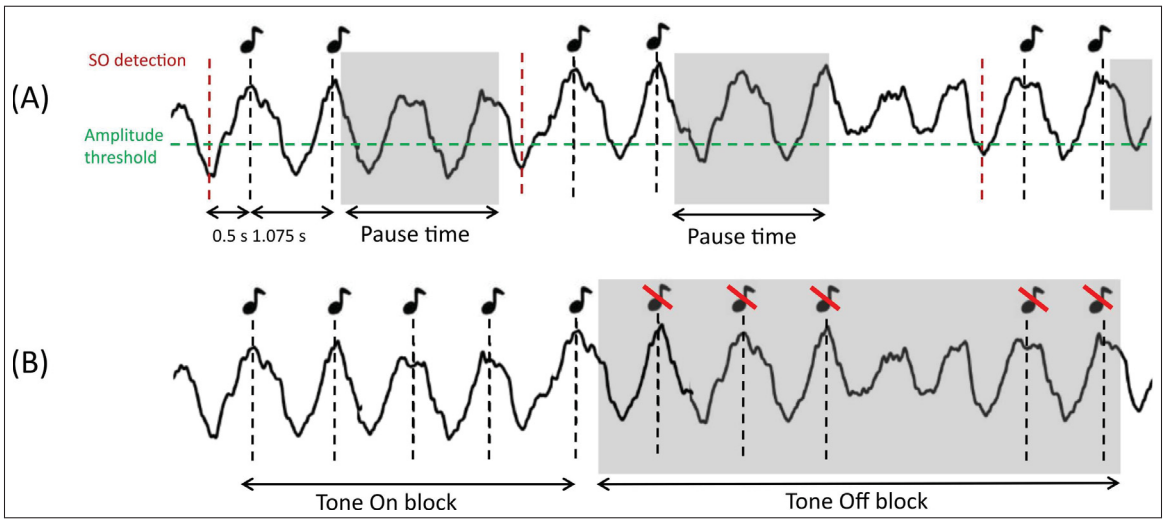

Figure 1.5 Two CLAS tone-application strategies: (A) single-tone stimulation with a short pause; (B) repeated tones within a stimulation window followed by a rest period Taken from Esfahani *et al.* (2023)

In a landmark study, Ngo *et al.* (2013) demonstrated that delivering auditory tones phase-locked to the SO up-state enhanced ongoing oscillations and improved memory consolidation. Their closed-loop system detected the negative half-wave peak of SOs in real time and triggered paired

pink-noise bursts (50 ms) to align with the predicted up-states of the current and subsequent cycles. This intervention reliably increased SO amplitude and strengthened the coupling of spindles to the SO cycle. Crucially, stimulation out of phase—during the down-state—failed to produce these effects and instead disrupted oscillatory activity.

The behavioral consequences were equally important. Participants performed a declarative word-pair learning task before sleep, in which they studied lists of semantically unrelated word pairs (e.g., "dog–lamp") and were later tested on their ability to recall the second word when cued with the first. Those who received in-phase stimulation during sleep showed significantly better recall the next day compared to both sham (control nights) and down-state stimulation conditions.

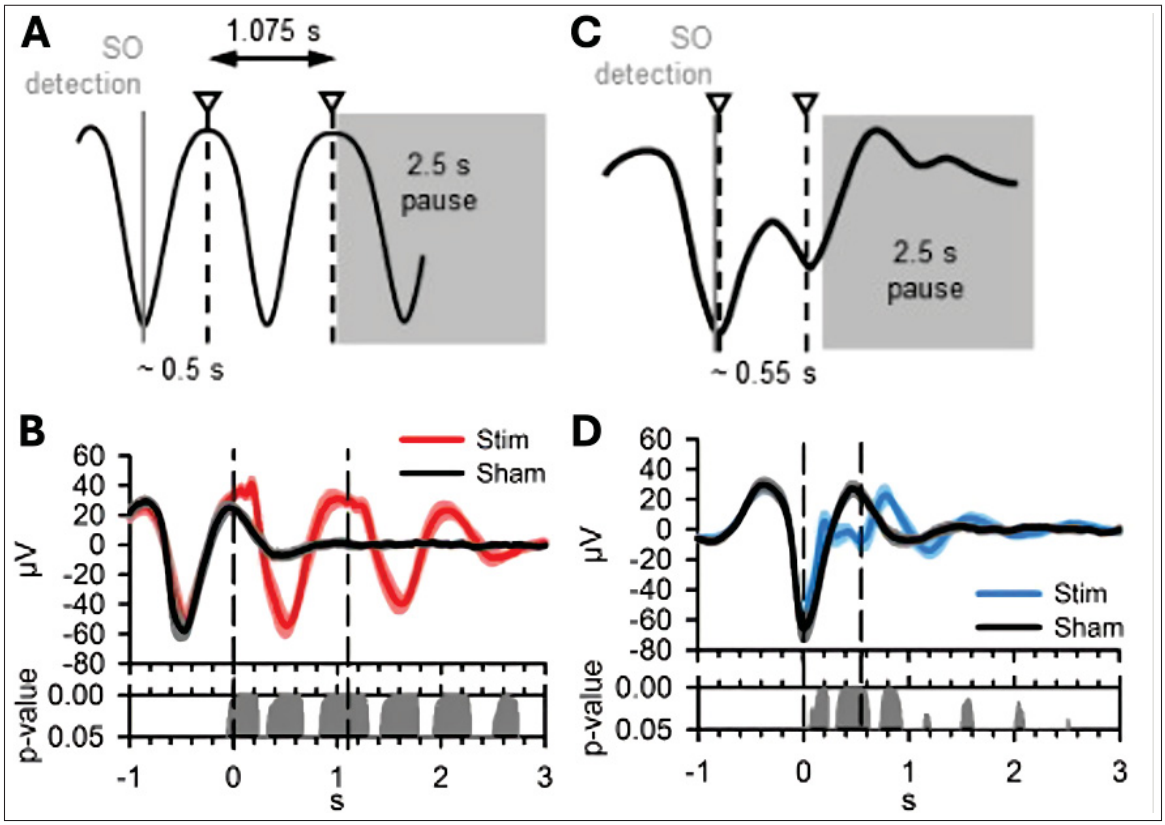

Figure 1.6 Closed-loop auditory stimulation effects phase-locked to EEG SO upstate vs. downstate. (A) EEG trace showing the timing of tones delivered during the SO up-state. (B) Averaged EEG responses of up-state stimulation. (C) EEG trace showing the timing of tones delivered during the SO down-state. (D) Averaged EEG responses of down-state stimulation Taken and adopted from Ngo *et al.* (2013)

Event-related potential (ERP, described in Section 1.8.1) analyses of this study are shown in Figure 1.6. These findings established that the efficacy of auditory stimulation depends critically on precise alignment with the brain's endogenous rhythms, providing strong motivation for closed-loop approaches.

1.6.3 Limitations of current methods

Despite these advances, fixed or random stimulation methods lack adaptability, and EEG-based CLAS remains limited by its reliance on electrodes, calibration, and specialized equipment, making it impractical for everyday use.

To address these limitations, alternative biosignals are being investigated. Among them, ECG is particularly promising: it is low-cost, non-intrusive, and already widely available through consumer wearables. Research has demonstrated bidirectional interactions between cardiac rhythms and brain activity during sleep, suggesting that heart-rate oscillations could provide a viable guide for stimulation. Moreover, combining ECG with EEG may further improve the precision and robustness of stimulation, potentially leading to stronger and more consistent enhancement effects.

1.7 Neuroanatomical basis

1.7.1 Sympathetic and parasympathetic systems

The central nervous system (CNS)—comprising the brain and spinal cord—plays the primary role in generating and coordinating sleep activity. The peripheral nervous system (PNS) connects the CNS with organs and muscles, allowing central signals to influence physiological processes throughout the body. Within the PNS, the autonomic nervous system (ANS) is particularly important, as it regulates essential functions such as heart rate, breathing, digestion, and thermoregulation.

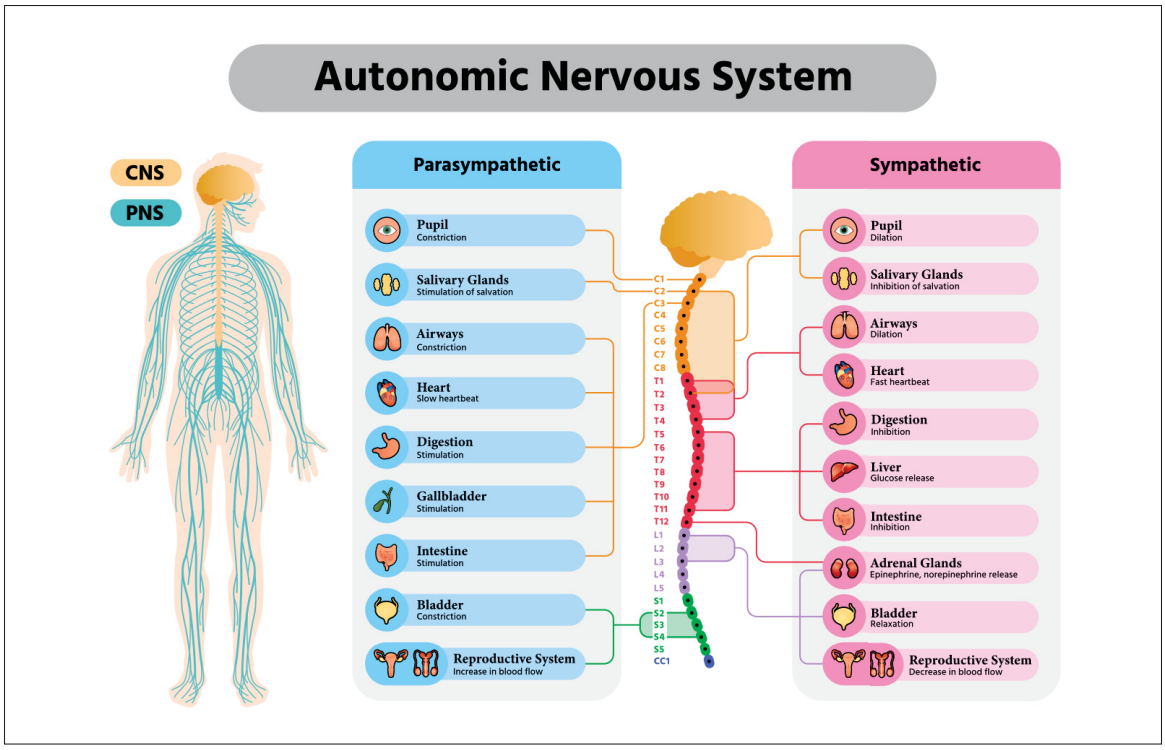

Figure 1.7 Illustration of the central and peripheral nervous systems, including autonomic components and their functions
Taken from Flores (2025)

The ANS consists of two complementary branches. The sympathetic nervous system, often described as the "fight-or-flight" branch, increases heart rate, blood pressure, and metabolic activity to prepare the body for action. By contrast, the parasympathetic nervous system, or "rest-and-digest" branch, slows the heart rate, supports digestion, and promotes restorative processes (Hall & Hall, 2020). Sleep is characterized by a dynamic interplay between these two systems. Parasympathetic activity dominates during NREM sleep, especially in deep stages, facilitating recovery and repair, whereas sympathetic activity becomes more pronounced during REM sleep or in response to stress and arousals.

The balance between sympathetic and parasympathetic activity not only underpins cardiovascular regulation but also reflects the degree of brain–body coordination during sleep. Importantly, this balance can be indexed through heart rate and heart rate variability (HRV), making the ANS a key link between neural and cardiac dynamics that can be measured non-invasively via ECG.

1.8 Signal processing techniques

1.8.1 Event-related measures

Event-related measures were used to assess how acoustic stimulation influenced neural and cardiac dynamics in the time domain. Event-related averaging involves aligning the signal to the onset of an external event (e.g., an auditory tone) and averaging across trials. This suppresses unrelated background activity and highlights stimulus-locked responses (See Fig 1.8).

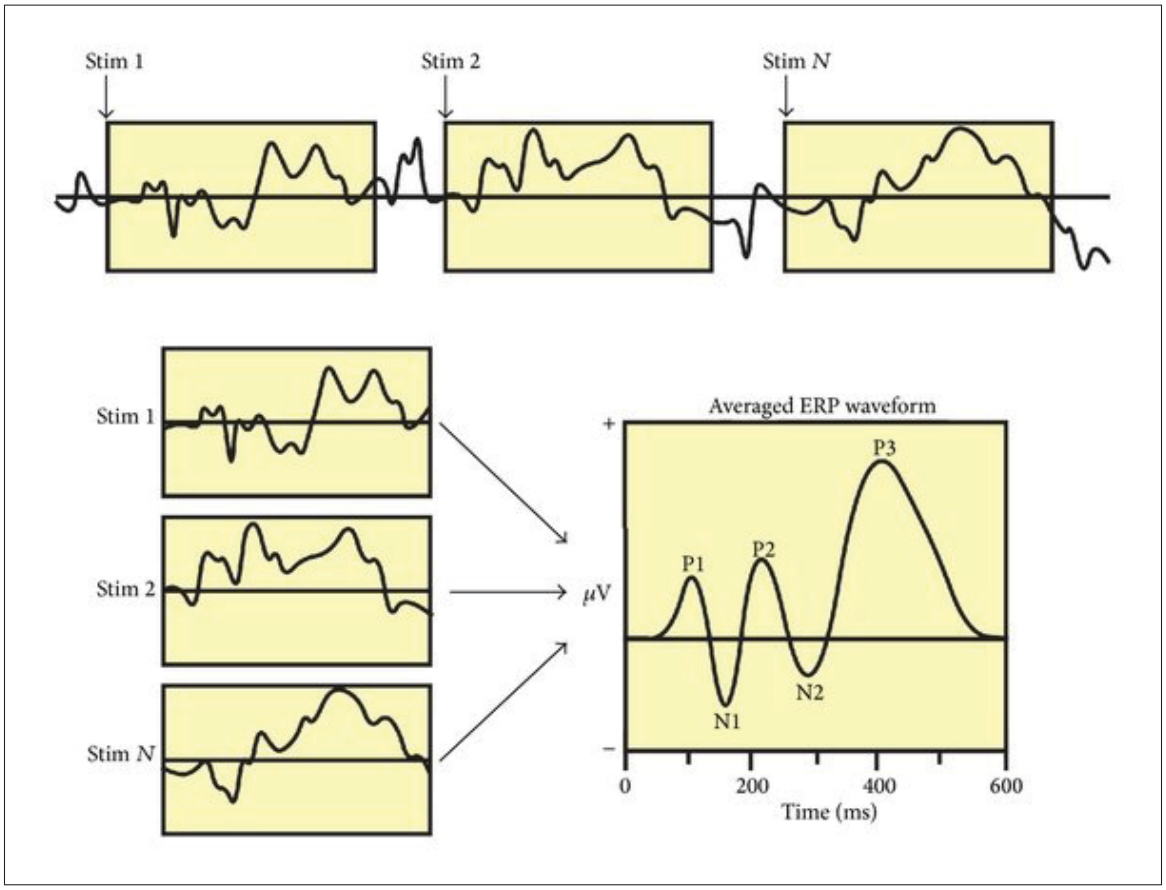

Figure 1.8 Event-related potential (ERP)
Taken from Tiriac & Blumberg (2016).

Mathematically, if $x_i(t)$ denotes the signal from the ith trial aligned to an event at $t = 0$, the event-related response is

$$\overline{x}(t) = \frac{1}{N} \sum_{i=1}^{N} x_i(t), \tag{1.3}$$

where N is the number of trials. This highlights consistent features across trials, such as amplitude or phase changes following stimulation.

1.8.2 Spectral analysis

Neural rhythms are often described in the frequency domain. The power spectral density (PSD) quantifies how signal power is distributed across frequencies, providing a compact description of oscillatory activity.

Formally, for a signal $x(t)$ the PSD is defined as

$$PSD(f) = \lim_{T \to \infty} \frac{1}{T} \mathbb{E}\left[|X_T(f)|^2 \right], \tag{1.4}$$

where $X_T(f)$ is the Fourier transform of $x(t)$ over a window of length T.

In practice, the PSD was estimated using Welch's method. The signal was divided into overlapping segments, each multiplied by a Hann window to reduce spectral leakage. After applying a fast Fourier transform (FFT) to each segment, the resulting periodograms were averaged to yield a stable estimate with reduced variance.

In this thesis, PSD analysis was used to quantify SWA, defined as the integrated power in the delta band (0.5–4 Hz).

1.8.3 Instantaneous phase estimation

Instantaneous phase estimation provides a continuous representation of an oscillatory signal's temporal evolution and is fundamental for phase-dependent analyses such as closed-loop stimulation. To estimate instantaneous phase, each signal was first preprocessed and bandpass-

filtered to isolate the frequency range of interest (e.g., HR-LF: 0.04–0.15 Hz; HR-HF: 0.15–0.4 Hz; EEG slow oscillations: 0.5–1 Hz).

The analytic signal $z(t)$ was then computed using the Hilbert transform:

$$z(t) = x(t) + j\,\mathcal{H}\{x(t)\}, \tag{1.5}$$

where $x(t)$ is the bandpass-filtered real-valued signal and $\mathcal{H}\{x(t)\}$ denotes its Hilbert transform, providing a 90° phase-shifted version of $x(t)$. The complex-valued analytic signal allows extraction of both instantaneous amplitude and phase.

The instantaneous phase $\phi(t)$ was obtained as the angle of $z(t)$:

$$\phi(t) = \tan^{-1}\left(\frac{\mathcal{H}\{x(t)\}}{x(t)}\right). \tag{1.6}$$

1.8.4 Morlet wavelet transform

Sleep spindles are short-lived oscillations in the sigma band (11–16 Hz) that require analysis methods capable of capturing both temporal and spectral dynamics. To this end, the Morlet wavelet transform was used, providing a localized representation of signal power as it evolves across time and frequency.

A Morlet wavelet can be viewed as a brief oscillatory wave tapered by a Gaussian envelope. Formally, it is expressed as

$$\psi(t, f) = \frac{1}{\sqrt{\sigma_t \sqrt{\pi}}} e^{j2\pi f t} e^{-t^2/(2\sigma_t^2)}, \tag{1.7}$$

where f is the center frequency and σ_t controls the temporal width of the Gaussian window.

By convolving this wavelet with the EEG signal and evaluating the resulting magnitude, one obtains a time–frequency representation showing how power within specific frequency bands changes dynamically. Increases in sigma-band power correspond to spindle events.

This approach is particularly suited for spindle detection because it balances temporal precision with frequency resolution, maintaining sensitivity to brief oscillatory bursts while avoiding the smearing typical of standard Fourier-based methods.

1.9 Statistical approaches

1.9.1 Monte Carlo methods

Monte Carlo (MC) methods were applied to improve statistical stability and construct empirical reference distributions, particularly when the number of available trials differed across conditions. Two complementary approaches were used: Monte Carlo simulation and Monte Carlo resampling.

1.9.1.1 Monte Carlo simulation

For continuous phase-dependent measures, each phase bin was modeled as a Gaussian random variable,

$$x \sim \mathcal{N}(\mu, \sigma^2), \tag{1.8}$$

where μ and σ^2 were estimated from the observed data. 200 random samples were drawn from this model to generate synthetic datasets, allowing the construction of an empirical null distribution for hypothesis testing. This simulation-based approach provides smooth, parametric estimates when data are limited but approximately normal.

1.9.1.2 Monte Carlo resampling

For analyses involving discrete events such as spindle likelihood, a data-driven resampling approach was used instead. In each iteration, two-thirds of the available no-tone trials were

randomly selected to form a surrogate dataset. This procedure was repeated 200 times, producing a distribution of spindle-likelihood estimates that served as a robust reference baseline.

1.9.2 False discovery rate

Statistical analyses in this work often involved repeated testing across multiple time bins, frequency bands, or phase conditions. Such multiple comparisons increase the probability of obtaining false positives, even when each individual test is evaluated at a conventional threshold (e.g., $\alpha = 0.05$). To address this problem, all reported p-values were corrected using the Benjamini–Hochberg false discovery rate (FDR) procedure.

The FDR procedure ranks all obtained p-values from smallest to largest and compares each against an adjusted significance level that increases with rank. This step-up approach controls the expected proportion of false discoveries among all rejected null hypotheses, while retaining higher statistical power than more conservative methods such as the Bonferroni correction.

In this thesis, the FDR threshold was set at $\alpha = 0.05$. This ensured that significant results reflect genuine effects with a controlled false discovery rate, rather than artifacts of multiple testing.

CHAPTER 2

TONE-EVOKED SLEEP ELECTROENCEPHALOGRAPHIC SLOW OSCILLATIONS AS A FUNCTION OF PERIPHERAL RHYTHMS: NEW INSIGHTS INTO THE BRAIN-HEART INTEGRATION

Mohamad Forouzanfar[1,2,3] , Sepehr Sardooeinasab[4] , Fiona C. Baker[1] , Ian M. Colrain[1] , Massimiliano de Zambotti[1]

[1] Center for Health Sciences, SRI International, Menlo Park, CA 94025, USA
[2] Department of Systems Engineering, École de technologie supérieure, Université du Québec, Montréal, QC H3C 1K3, Canada
[3] Centre de recherche de l'Institut universitaire de gériatrie de Montréal (CRIUGM), Montréal, QC H3W 1W5, Canada
[4] Department of Electrical Engineering, École de technologie supérieure, Université du Québec, Montréal, QC H3C 1K3, Canada

The article was published by *Journal of Sleep Research* in October 2025.

2.1 Presentation

This chapter presents the article "Tone-evoked sleep electroencephalographic slow oscillations as a function of peripheral rhythms: new insights into the brain–heart integration" by Forouzanfar, Sardooeinasab, Baker, Colrain, and de Zambotti, published in the *Journal of Sleep Research* in October 2025. This work investigates how the effectiveness of acoustic stimulation during sleep depends not only on the phase of cortical slow oscillations, but also on the timing of stimulation relative to peripheral cardiac rhythms. The results show that stimulation delivered at specific phases of heart rate high-frequency and low-frequency oscillations enhances slow oscillation amplitude, slow-wave activity, and heart rate responses, highlighting the role of brain–heart interactions in shaping sleep modulation.

2.2 Introduction

Sleep is a fundamental human need. Despite its outward appearance as a period of inactivity, it is a highly active and regulated physiological state during which numerous biological systems engage in restoration and reorganization. Sleep is characterized by a complex interplay of oscillatory

dynamics across the central nervous system (CNS) and peripheral nervous system, which interact continuously under the influence of homeostatic and circadian processes (de Zambotti, Trinder, Silvani, Colrain & Baker, 2018). The autonomic nervous system (ANS), a branch of the peripheral nervous system, regulates critical internal functions such as cardiovascular activity, respiration, digestion, and thermoregulation. The CNS orchestrates neural oscillations across different frequency bands, including cortical electroencephalographic (EEG) slow oscillations (SOs; ~0.8 Hz), a hallmark of non-rapid eye movement (NREM) sleep. These SOs—prominent over frontal cortical regions and characterized by large peak-to-peak amplitudes often exceeding 140 μV—are embedded within the broader spectrum of slow-wave activity (SWA; 0.5–4 Hz) and reflect the highest level of neuronal synchronization during sleep (Esser, Hill & Tononi, 2007; Massimini, Huber, Ferrarelli, Hill & Tononi, 2004).

SWA is of particular interest due to its crucial role in health and disease. Among the various aspects of sleep, EEG-measured SWA is recognized for its restorative functions and cognitive benefits (Irwin, 2015a; Rasch & Born, 2013). Diminished SWA has been associated with several clinical conditions, including mild cognitive impairment, schizophrenia, and Parkinson's disease (Papalambros *et al.*, 2019; Schreiner *et al.*, 2021a). At a mechanistic level, SWA is linked to synaptic homeostasis and plasticity, processes essential for learning and memory (Tononi & Cirelli, 2006).

Given its importance, numerous approaches have been explored to enhance SWA, ranging from daytime behavioral interventions that increase brain metabolism (Määttä *et al.*, 2010) to nighttime strategies including pharmacology (e.g., GABAergic agents) (Yamatsu *et al.*, 2015), thermoregulatory manipulations (Kräuchi *et al.*, 2018), and noninvasive neurostimulation (e.g., transcranial direct current or magnetic stimulation) (Saebipour *et al.*, 2015; De Gennaro *et al.*, 2008; Massimini *et al.*, 2007). Among neurostimulation techniques, sensory stimulation has emerged as particularly promising due to its noninvasive nature, ease of implementation, and high temporal precision. Within sensory modalities (vestibular, olfactory, acoustic, tactile), rhythmic acoustic stimulation with brief, low-intensity tones (~50 ms; 40–60 dB) has yielded strong effects in humans—improving cognition (Diep *et al.*, 2019, 2021; Wilckens *et al.*, 2018),

supporting sleep-dependent memory consolidation (Cellini & Mednick, 2019; Leminen *et al.*, 2017; Ngo *et al.*, 2013; Ngo *et al.*, 2015; Ong *et al.*, 2016, 2018a; Papalambros *et al.*, 2017; Stanyer *et al.*, 2021; Wunderlin, Zeller, Wicki, Nissen & Züst, 2024), enhancing immune-related markers (Besedovsky *et al.*, 2017a), and modulating autonomic function (Diep, Ftouni, Drummond, Garcia-Molina & Anderson, 2022; Grimaldi *et al.*, 2019; Huwiler *et al.*, 2022, 2023; Lustenberger, 2025). The effectiveness of acoustic stimulation depends on tone properties and intensity (Bellesi, Riedner, Garcia-Molina, Cirelli & Tononi, 2014), and critically on precise timing relative to the ongoing SO phase (Fattinger *et al.*, 2017a). Most closed-loop paradigms have optimized stimulation based on cortical phase alone (Cellini & Mednick, 2019; Santostasi *et al.*, 2016; Esfahani *et al.*, 2023).

However, the sleeping brain communicates bidirectionally with peripheral systems, producing coordinated cascades of central and autonomic events, with cortico-cardiac coupling being especially well studied (de Zambotti *et al.*, 2018). Such coupling is relevant not only to sleep physiology but also to cognition: measures that capture central–autonomic interactions can better predict sleep-dependent memory outcomes than central or autonomic measures alone (Whitehurst *et al.*, 2020; Naji, Krishnan, McDevitt, Bazhenov & Mednick, 2019). The integration of exteroceptive sensory input and interoceptive bodily signals—mediated by CNS–ANS dynamics—shapes sensory processing (Critchley & Harrison, 2013). During slow-wave sleep (SWS), parasympathetic predominance and reduced sympathetic tone (Baharav *et al.*, 1995) alter arousal state and may modify neural gain applied to sensory inputs; simultaneously, cortical excitability fluctuates with SO phase, with tones presented in the SO upstate eliciting larger SOs (Ngo *et al.*, 2013). Together, these findings suggest that brain responsiveness to auditory stimuli during sleep is jointly shaped by cortical phase and sleep-stage-dependent autonomic regulation (de Zambotti *et al.*, 2018; Helfrich, Mander, Jagust, Knight & Walker, 2018; Niizeki & Saitoh, 2018).

Auditory tones during sleep do not merely evoke cortical responses. Spontaneous and tone-evoked SOs are accompanied by transient increases in heart rate (HR) and blood pressure, increased muscle sympathetic nerve activity, and a subsequent return to or below baseline

(de Zambotti *et al.*, 2018; de Zambotti *et al.*, 2016). These autonomic oscillations manifest specifically in the presence of SOs, indicating tight interdependence between central and autonomic events (de Zambotti *et al.*, 2016). Conversely, phases of peripheral rhythms are associated with the incidence and magnitude of spontaneous and evoked SOs—for example, isolated spontaneous SOs occur preferentially on the descending phase of slow blood pressure oscillations (Forouzanfar *et al.*, 2019; Monstad & Guilleminault, 1999), and SOs are more likely to be evoked when pre-tone cardiac activity is low (de Zambotti *et al.*, 2016). Overall, these results point to (1) specific windows in which acoustic stimuli are most likely to maximize SOs and (2) cascades of peripheral oscillations temporally aligned to SOs. Of particular interest are cortical SOs (~0.8 Hz) and associated spindles (12–15 Hz) (Helfrich *et al.*, 2018), cardiorespiratory slow oscillations and phases of slow blood pressure rhythms (< 2 Hz) (Forouzanfar *et al.*, 2019), and dynamics of the cardiac cycle (Stefanovska, Lotric, Strle & Haken, 2001; Stankovski, Pereira, McClintock & Stefanovska, 2017b).

In this exploratory study, we investigated how the phase of ongoing physiological rhythms influences the effects of acoustic stimulation during sleep. Specifically, we examined tones delivered at the upstate and downstate phases of three oscillations: EEG SOs (0.5–4 Hz) (Papalambros *et al.*, 2017; Sharon & Nir, 2018), heart-rate low-frequency (HR-LF; 0.04–0.15 Hz), and heart-rate high-frequency (HR-HF; 0.15–0.4 Hz) components (Shaffer & Ginsberg, 2017). We assessed tone-evoked responses across four coupling domains: cortical–cortical, cardiac–cortical, cortical–cardiac, and cardiac–cardiac interactions. HR-LF reflects mixed sympathetic/parasympathetic influences (often more strongly sympathetic), whereas HR-HF (respiratory band) primarily indexes parasympathetic (vagal) activity and tracks respiratory-coupled HR fluctuations. During inhalation, vagal withdrawal accelerates HR (HR-HF upstate), whereas exhalation restores vagal activity and slows HR (HR-HF downstate). Based on these principles, we hypothesized maximal SO enhancement when tones are delivered during the EEG SO upstate, HR-LF upstate, and HR-HF downstate—aligning stimulation with periods of higher cortical excitability or vagal dominance. We tested these hypotheses using overnight in-lab

polysomnography (PSG) from 133 healthy sleepers with tones randomly delivered throughout the night.

2.3 Methods

2.3.1 Participants

Included in the analyses were 133 adolescents, aged between 12–21 years (Age, mean ± SD 15.6 ± 2.4y; 60 females; body mass index, mean ± SD: 21.6 ± 4.7 kg m^{-2}; 93 Caucasian) of the National Consortium on Alcohol and NeuroDevelopment in Adolescence (NCANDA) special sleep study conducted at SRI International and University of Pittsburgh (baseline NCANDA cohort, sleep special project; sample characteristics were obtained from data release version: `NCANDA_DATA_00010_V2`). For a description of the NCANDA sleep study methodology, sample characteristic and sleep outcomes at the baseline assessment please refer to Baker *et al.* (2016). None of the participants had severe mental (e.g., bipolar disorder, schizophrenia) and/or medical (e.g., heart diseases) conditions. None of the participants showed evidence of sleep disorders (e.g., sleep disordered breathing, periodic limb movement disorder) as confirmed by a clinical PSG evaluation. The study was approved by the Institutional Review Boards at SRI International and University of Pittsburgh. Adult participants consented to participate, and minors provided written assent along with consent from a parent/legal guardian. Participants and parents were compensated for participation.

2.3.2 Laboratory procedure

As part of the NCANDA sleep special project protocol, all participants underwent an event-related potential (ERP) PSG night at SRI International (N = 104) or Pittsburgh University (N = 29), in which acoustic tones were randomly presented throughout the night during NREM sleep (de Zambotti *et al.*, 2016). All participants self-selected their bedtime. At SRI, participants woke up at their typical weekday times but at the University of Pittsburgh, participants were allowed to wake up when they chose. All participants tested negative at lab-entry on a breath

alcohol test (S75 Pro, BACtrack Breathalyzers, San Francisco, CA, USA) and urine drug test (10 Panel iCup drug test kit, Instant Technologies, Inc.), confirming the absence of recent alcohol or drug use.

2.3.3 Polysomnographic sleep assessment

Recordings were performed using the Compumedics Grael® HD-PSG system (Compumedics, Abbotsford, Victoria, Australia). The standard PSG montage included several EEG (1024 Hz sampled) leads (FP1, FP2, F3, F4, FC3, FC4, C3, C4, CP3, CP4, P3, P4, O1, O2 referenced to the contralateral mastoids), submental electromyogram and bipolar electrooculogram, following the American Academy of Sleep Medicine (AASM) rules (Iber *et al.*, 2007). In addition, electrocardiographic (ECG) recordings were also made using 1 cm diameter Ag/AgCl surface spot electrodes placed in a modified Lead II Einthoven configuration. Raw ECG waveforms (512 Hz sampled) were acquired via dedicate channels in the Compumedics Grael® HD-PSG system. PSG sleep records were manually single-scored in 30-s epochs, and sleep (wake, N1, N2, N3, REM) classified following the AASM rules. Arousals were also scored, as abrupt shifting in EEG frequency ($\geq$ 3 s, $<$ 30 s), following the AASM rules.

2.3.4 Acoustic stimulation

Acoustic tones (80 dB at 1000 Hz for 50 msec) were randomly binaurally played overnight (during NREM sleep) after 30 min of stable NREM sleep with a random 15–30-sec inter-stimulus interval using Compumedics NeuroScan Stim software (Compumedics Ltd, Abbotsford, Victoria, Australia) or Eprime (Psychology Software Tools, Inc, Pittsburgh, PA) through E-A-RTONE 3A insert earphones (3M Auditory Systems, Indianapolis, IN, USA). The program for playing the tones was manually started and stopped by a trained staff member; tones were halted during major awakenings and REM sleep and restarted once stable NREM sleep returned. All participants were confirmed as being able to hear the tones when they were played to them before going to bed.

2.3.5 Selection of the trials

Only tones occurring in arousal and artifact free intervals in N2 and N3 sleep were considered in the analysis. Arousal-free tones were defined as those tones with no arousal happening within 15 s around them. Artifact-free tones were defined as those tones with no signal outlier within 15 s around them. In addition, the analysis was only limited to the tones that induced an EEG SO.

2.3.6 Characterization and analysis of ECG and EEG rhythms

To study the effect of played tones on cortical and cardiac functions, the EEG SO (within the SWA frequency range: 0.5–4 Hz), HR LF oscillation (0.04–0.15 Hz), and HR HF oscillation (0.15–0.4 Hz) were extracted. The ECG signal was digitally filtered with a 4th-order Butterworth bandpass filter with lower and upper cut-off frequencies of 0.5 Hz and 35 Hz, respectively. The filter was applied in both forward and backward directions to avoid any phase shift. Customized algorithms were applied to detect ECG R peaks (de Zambotti *et al.*, 2019) and calculate R–R intervals. Those ECG cycles that happened to have an out-of-range (10 standard deviations away from the mean) ECG signal level or R–R value were identified as invalid beats (corrupted by noise and artifacts or ectopic beats). The instantaneous HR was derived from R–R intervals and interpolated at 10 Hz. The EEG signal was recorded from the F3 electrode referenced to the average of the contralateral mastoid electrodes. To process the EEG data, we applied a 4th-order Butterworth bandpass filter with cut-off frequencies of 0.1 Hz and 30 Hz. This filter was applied bidirectionally to prevent phase shift. Specifically, the high-pass component (0.1 Hz) mitigated DC and baseline drift, while the low-pass component (30 Hz) reduced high-frequency noise and power line interference. Finally, any EEG samples that happened to have an out-of-range level (10 standard deviations away from the mean, $> 1500\,\mu$V, or $< -1500\,\mu$V) were identified as invalid (corrupted by noise and artifacts).

2.3.6.1 Extraction and characterization of EEG SOs

A digital 4th-order Butterworth bandpass filter was designed to extract the low frequency component of the EEG signal by bandpass filtering it between 0.5 Hz to 4 Hz (Papalambros *et al.*, 2017; Sharon & Nir, 2018). Fig. 2.1(a) shows an example of the EEG signal and Fig. 2.1(b) shows the signal after bandpass filtering with a selected SO. EEG SO were detected as those oscillations with peak-to-peak amplitude $> 140\,\mu$V, a negative peak $< -80\,\mu$V (Massimini *et al.*, 2004) and duration of < 2.5 s, > 0.25 s. To detect peak-to-peak amplitude of oscillations, signal zero-crossings were calculated, and the oscillations' peaks and troughs were detected as the signal maximums and minimums between two consecutive zero-crossings. The peak-to-peak amplitude was calculated as the amplitude difference between peaks and troughs. The SO duration was calculated as the time difference between consecutive downward zero-crossings.

2.3.6.2 Extraction and characterization of cardiac oscillations

Digital 4th-order Butterworth bandpass filters were designed to extract the LF (0.04–0.15 Hz) and HF (0.15–0.4 Hz) components of the HR signal (Shaffer & Ginsberg, 2017) (see Figure 1). Fig. 2.1(d) shows an example of the HR signal with its LF and HF components plotted in Figs. 2.1(e) and 2.1(f), respectively.

2.3.6.3 Phase characterization

To study the acoustic tone effect with respect to different phases of the central and peripheral oscillations, cardiac oscillations (HR SO) and central oscillations (EEG SO) were decomposed into two phase regions representing the downstate and upstate of the systems as follows:

Downstate	$-\pi \leq \varphi(t) < 0$
Upstate	$0 \leq \varphi(t) < \pi$

To estimate the instantaneous phases and frequencies of the peripheral oscillations, the Hilbert transform was applied, and an analytic signal was formed on the complex plane. Instantaneous

phases were calculated as the angle of the analytic signal's complex representation (Forouzanfar *et al.*, 2019). Since the Hilbert transform inherently introduces a 90-degree phase shift, we have accounted for this adjustment throughout our analysis to ensure that the reported phases align with their conventional interpretation. Figure 2.1(b) illustrates the downstate (blue) and upstate (red) phases of a sample EEG signal bandpass-filtered within the SWA frequency range. Similarly, Figures 2.1(e) and 2.1(f) illustrate the downstate (blue) and upstate (red) phases of HR LF and HF oscillations, respectively.

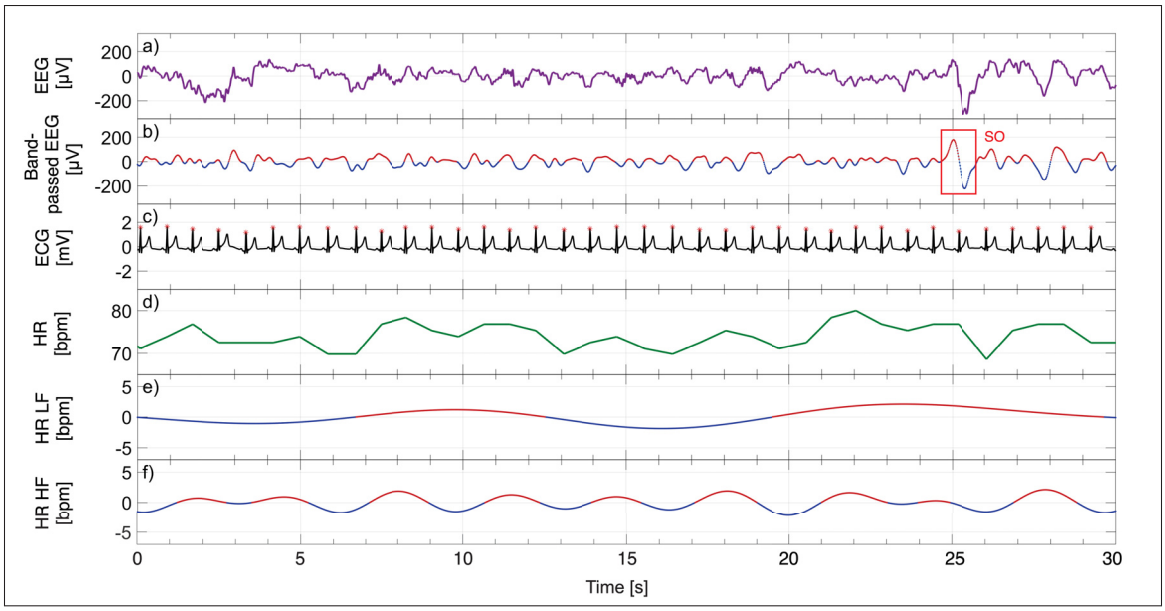

Figure 2.1 Examples of synchronous physiological signals during N3 (deep) sleep in a 12-year-old male: (a) raw EEG, (b) bandpass-filtered EEG and detected slow oscillation (SO), (c) ECG, (d) ECG-derived heart rate (HR), (e) extracted HR low-frequency (LF) oscillation, and (f) extracted HR high-frequency (HF) oscillation. Downstate and upstate phases are indicated in blue and red, respectively. Red stars mark detected ECG R-peaks

2.3.6.4 Spectral power analysis

To quantify EEG power within specific frequency bands, we employed a multi-step spectral analysis procedure. First, continuous EEG data were segmented into 8-second epochs. Power spectral density (PSD) estimates for each epoch were calculated using Welch's method. We utilized a 4-second Hanning window with 50% overlap to optimize spectral resolution while

minimizing edge artifacts. The resulting PSDs were then linearly interpolated to a 10 Hz frequency resolution. To assess tone-evoked spectral changes, PSDs were averaged across epochs corresponding to tone presentation for each subject. Subsequently, to normalize inter- and intra-subject variability in baseline power, each subject's PSDs were normalized by their mean cumulative power up to 20 Hz across all epochs. We focused on the SWA band, specifically analyzing power within the slow oscillatory (SO; 0.5–1 Hz) and high-SWA (1–4 Hz) sub-bands, as well as the combined SWA (0.5–4 Hz) band. The results of this analysis are depicted in Supplementary Figure I-1 and further discussed in the Results Section.

2.3.6.5 Time-resolved SWA analysis

To examine the temporal dynamics of SWA following tone presentation, we performed a time-resolved spectral analysis. A periodogram estimation with 1-second Hanning windows and 1-second shifts was employed, providing a 1-second resolution of SWA power changes after tone onset. The results of this analysis are depicted in Supplementary Figure I-2.

2.3.6.6 Characterizing tone-evoked cortical and cardiac interactions

Cortical and cardiac tone evoked responses were calculated by grand averaging the EEG and HR signals for each individual according to the time points at which the tones were played as follows:

Cortical–Cortical Effect: The effect of acoustic tones played according to the phases of EEG SOs on inducing tone evoked EEG oscillations was studied by calculating the induced EEG SO peak-to-peak amplitude.

Cortical–Cardiac Effect: The effect of acoustic tones played according to the phases of EEG SOs on inducing tone evoked HR oscillations was studied by calculating the induced HR oscillation peak-to-peak amplitude.

Cardiac–Cortical Effect: The effect of acoustic tones played according to the phases of HR LF and HF oscillations on inducing tone evoked EEG oscillations was studied by calculating the induced EEG SO peak-to-peak amplitude.

Cardiac–Cardiac Effect: The effect of acoustic tones played according to the phases of HR LF and HF oscillations on inducing tone evoked HR oscillations was studied by calculating the induced HR oscillation peak-to-peak amplitude.

2.3.7 Data analysis

Averaged EEG and HR tone-evoked oscillations were calculated for each individual. Each oscillation was characterized with different distinctive points characterizing the minimums, maximums, baseline, and recovery values. EEG tone-evoked activity was characterized by averaging EEG segments aligned with respect to the time at which the tones were played. Baseline and the recovery levels were calculated as the average of the EEG signal for 8 to 10 seconds before and after the tone. HR tone-evoked activity was characterized by averaging HR segments aligned with respect to the time at which the tones were played. Baseline and recovery levels were calculated as the average of the HR signal 13 to 15 seconds before and after the tone. The differing approaches to establishing baseline and recovery for EEG and ECG are driven by the temporal characteristics of each signal and the need to avoid stimulus-evoked activity. EEG's rapid responses allow for a baseline period closer to the tone. In contrast, the slower, more sustained changes in heart rate necessitate a baseline and recovery period positioned further away in time from the tone presentation to avoid contamination from the cardiac response itself. To account for intra-subject variability, heart rate responses were baseline-normalized per subject and per phase. This procedure also aimed to correct for inter-individual differences in baseline heart rate and did not alter the peak-to-peak amplitude of the evoked heart rate oscillations. Following normality assessment via the Shapiro-Wilk test ($\alpha = 0.05$), we compared peak-to-peak amplitudes of induced oscillations as well as SWA in cortical-cortical and cardiac-cortical experiments using paired t-tests (for normally distributed data) or paired two-sided Wilcoxon signed-rank tests (for non-normal data), both at a 5% significance level. Corresponding t-values (for t-tests) and z-scores (for Wilcoxon tests) are reported. For each paired t-test, the degrees of freedom (DOF) can be calculated as the number of participants in the given experiment minus one ($n - 1$). Although the full sample included 133 participants, the exact number used in each

analysis is specified when fewer subjects were available. Although our hypothesis suggested a specific direction of effect, we employed a more conservative two-sided test to minimize bias and ensure robust detection of significant differences in either direction. All processing was performed in MATLAB R2023a (MathWorks, Inc., Natick, MA) via customized algorithms.

2.4 Results

2.4.1 Cortical-Cortical tone-enhanced oscillations

The effect of acoustic tones on enhancing EEG SO when played in the downstate and upstate phases of the EEG SO is shown in Figure 2.2(a). In total, 152±64 tones were played in the downstate phase of EEG and 336±128 tones were played in the upstate phase of EEG per individual out of which 64±38 (~42%) and 216±108 (~64%) induced a SO, respectively. It was observed that three main oscillations exist in the EEG that are marked by A-B-C oscillation, C-D-E oscillation, and E-F-recovery oscillation (Figure 2.2.a). When tones were played in the upstate phase of the EEG SO, no clear B point was observable. The main characteristics of the tone-enhanced EEG are summarized in Table 2.1. The amplitude of the maximum induced SO, when tones were played in the downstate phases (B-C difference), was observed to be 95.3±39.2 μV, compared to 199.7±52.4 μV when tones were played in the upstate phases (A-C difference) which shows a significant difference (~110%, $p<0.001$, $Z=-10.0$). The SWA was approximately 3% ($p<0.05$, $Z=-2.2$) higher when tones were played in the upstate phases compared to when tones were played in the downstate phases. This increase in SWA was driven by increased power in the SO frequency range, which was ~23% higher ($p<0.001$, $Z=-8.4$), despite the power in the high-SWA being ~12% lower ($p<0.001$, $t=8.6$). (Figure I-1.a). Notably, inducing SO and presenting tones during either the downstate or upstate phase increased the ratio of SWA to total power relative to baseline, with a larger increase during the upstate phase. Most of this increase occurred within the first second after tone presentation (Figure I-2.a).

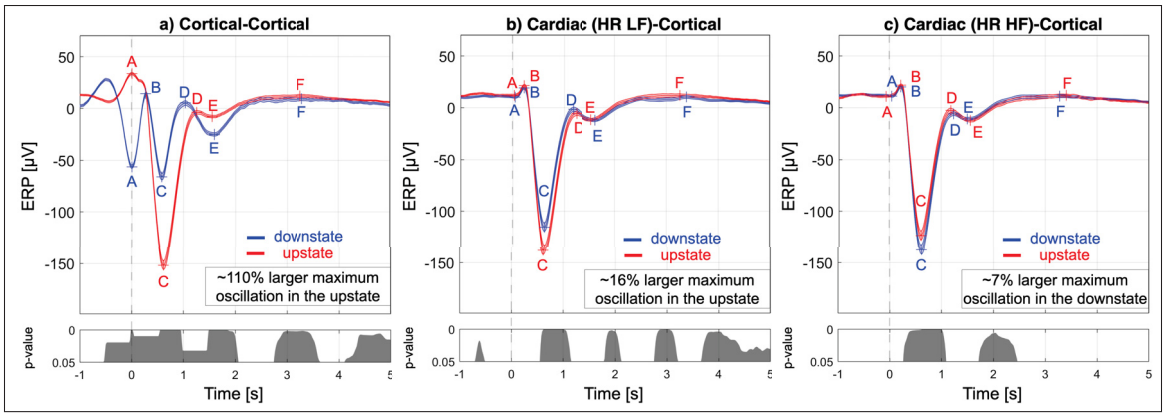

Figure 2.2 Effect of acoustic tones played in the downstate (blue) and upstate (red) phases of (a) EEG SO, (b) HR LF oscillations, and (c) HR HF oscillations on EEG. The main characteristic points are shown by letters A to F. The plots display the standard error of means, the percentage increase in the amplitude of the induced oscillation, and the p-value for comparison

Table 2.1 Characterization of tone-evoked EEG oscillations when tones are played at the downstate and upstate phases of the EEG SOs (Figure 2.2.a)

Cortical-Cortical	Downstate		Upstate	
	Time [msec]	Amplitude [μV]	Time [msec]	Amplitude [μV]
Baseline	[-10000, -8000]	-2.1±6.1	[-10000, -8000]	-2.7±2.3
Point A	0±36.5	-58.3±18.3	83.5±111	37±12.3
Point B	272.1±46.8	20.7±18.8	—	—
Point C	575.1±106.3	-74.7±35.4	612.8±71.2	-162.7±48.7
Point D	882±127.7	4.3±32.9	1194.9±204.9	5.3±26.5
Point E	1442.9±316.3	-39.5±17.7	1811±292.5	-9.4±18.7
Point F	3912.2±1490.1	20.5±18.5	3720.3±1283.2	16.9±7.9
Recovery	[8000, 10000]	-1.7±4.3	[8000, 10000]	-2.2±3.6

2.4.2 Cardiac-Cortical tone-enhanced oscillations

Next, we investigated the effect of tones played in the upstate and downstate phases of the HR LF (0.04-0.15 Hz) and HF (0.15-0.4 Hz) oscillations on enhancing EEG SO.

2.4.2.1 HR LF oscillations

In total, 156±66 tones were played in the downstate and 325±130 tones were played in the upstate phases of HR LF oscillations per individual out of which 78±41 (~50%) and 202±98 (~62%) induced an EEG SO, respectively. A similar induced ERP pattern was observed in both cases (see Fig. 2.2.b) where the EEG level from a local minimum around the tone (A-point) was slightly increased to a maximum (B-point) followed by a deep decrease to a minimum (C-point), and a recovery to a maximum (D-point). This was followed by another slight decrease to a minimum (E-point), a slight increase to a maximum (F point), and a recovery toward baseline. The main characteristics of the tone-enhanced EEG activities based on the phase of HR LF oscillations are summarized in Table 2.2. The amplitude of the induced oscillation (B-C difference) was 150.7±51.1 μV and 174.3±56.5 μV when tones were played in the downstate and upstate phases of the HR LF oscillations, respectively, which showed a significant higher amplitude oscillation when tones were played in the upstate phases of HR LF oscillations (~16%, p<0.001, Z=-8.2). The SWA was about 14% (p<0.001, Z=-9.1) higher when tones were played during the upstate phases compared to when tones were played during the downstate phases. This was due to a higher power in the SO frequency range (~20%, p<0.001, t=-13.0) and higher high-SWA power (~10%, p<0.001, t=-9.1) (Figure I-1.b).

Table 2.2 Characterization of tone-evoked EEG oscillations when tones are played at the downstate and upstate phases of the HR LF oscillations (Figure 2.2.b)

Cardiac-Cortical (LF)	Downstate		Upstate	
	Time [msec]	Amplitude [μV]	Time [msec]	Amplitude [μV]
Baseline	[-10000, -8000]	-3.1±5.6	[-10000, -8000]	-2.5±2.8
Point A	64.5±125.3	10.1±11.7	73.2±97.7	12.1±11.4
Point B	211.8±85.5	23.9±12.1	228±54.0	26.2±12.8
Point C	608.2±99.5	-126.8±44.9	612.1±70.2	-148.1±49.8
Point D	1070.3±153.0	4.2±26.5	1168.6±210.5	4.1±25.7
Point E	1133.8±166.8	-3.3±24.5	1262.5±239.6	-5.0±25.4
Point F	3204.5±1448.7	26.3±15.5	3243.4±1302.5	23.3±18.3
Recovery	[8000, 10000]	-1.2±4.7	[8000, 10000]	-2.4±3.3

2.4.2.2 HR HF oscillations

In total, 266±98 tones were played in the downstate and 222±77 tones were played in the upstate phases of HR HF oscillations per individual out of which 158±64 (~59%) and 122±58 (~54%) induced an EEG SO, respectively. A similar induced ERP pattern was observed as those of the HR LF oscillations. The main characteristics of the tone-enhanced EEG activities based on the phase of HR HF oscillations are summarized in Table 2.3. The amplitude of the induced oscillation was 172.7±56 μV and 161.2±54 μV when tones were played in the downstate and upstate phases of the HR HF oscillations, respectively, showing a significantly higher oscillation amplitude when tones were played in the downstate phases of HR HF oscillations (~7%, $p<0.001$, $Z=5.8$). The SWA was about 3% higher ($p<0.01$, $Z=3.0$) when tones were played during the downstate phases compared to when tones were played during the upstate phases. This difference was due to a higher power of the SO frequency range (~6%, $p<0.001$, $t=5.2$), while the high-SWA power was similar ($p=0.7$, $t=0.4$) (Figure I-1.c).

Table 2.3 Characterization of tone-evoked EEG oscillations when tones are played at the downstate and upstate phases of the HR HF oscillations (Figure 2.2.c)

Cardiac-Cortical (HF)	Downstate		Upstate	
	Time [msec]	Amplitude [μV]	Time [msec]	Amplitude [μV]
Baseline	[-10000, -8000]	-3.0±3.2	[-10000, -8000]	-2.1±3.3
Point A	76.8±99.2	10.8±11.8	79.3±90.0	11.4±12.6
Point B	227.7±59.4	24.6±12.7	227.4±58.1	27.1±12.5
Point C	609.8±72.0	-148.1±49.2	622.3±154.3	-134.1±48.1
Point D	1139.3±152.0	0.7±21.5	1123.4±200.1	2.9±24.8
Point E	1215.6±175.8	-5.8±21.2	1209.9±228.0	-5.8±23.3
Point F	3243.5±1215.6	23.9±17.7	3164.2±1370.5	25.8±18.4
Recovery	[8000, 10000]	-2.2±3.4	[8000, 10000]	-1.7±4.5

2.4.3 Cortical-Cardiac tone-enhanced oscillations

We further investigated the effect of acoustic tones played in upstate and downstate phases of EEG SO on the HR profile (see Figure 2.3.a). In both cases, an oscillation in HR is induced where HR increases from a minimum baseline value (A-point) to a maximum (B-point) and then

decreased to a minimum value (C-point) followed by a recovery pattern. Given that tones were played with a random time interval of 15-30 seconds, our analysis was limited to ±15s around the tones. The main characteristics of the baseline-normalized tone-induced HR oscillations are summarized in Table 2.4. The amplitude of the induced oscillations was 5.1±3.1 bpm when tones were played in the downstate phase of the EEG SOs, while it was 5.9±2.9 bpm when tones were played in the upstate phase which was significantly higher (~16%, p<0.001, Z=-6.4).

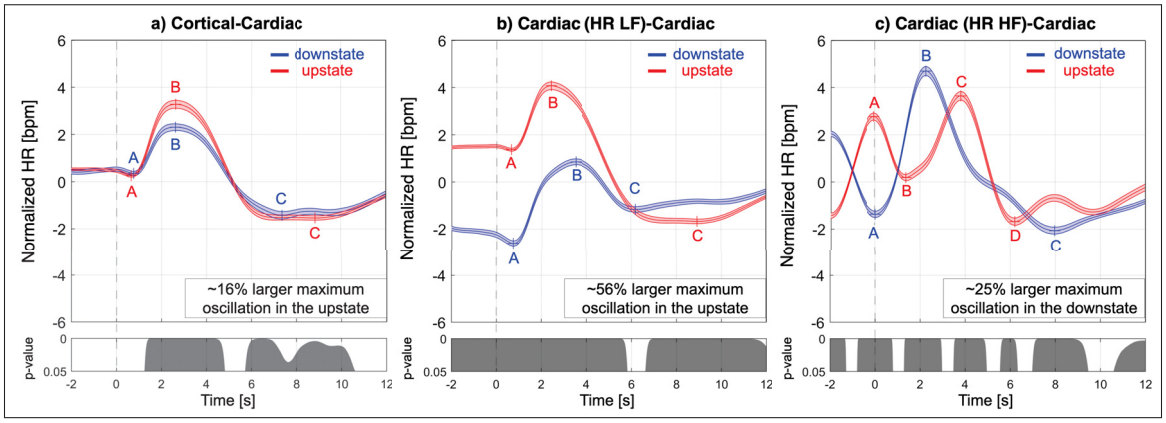

Figure 2.3 Effect on normalized HR of acoustic tones played in the downstate (blue) and upstate (red) phases of (a) EEG SO, (b) HR LF oscillations, and (c) HR HF oscillations. The main characteristic points are shown by letters A to D. The figures also display the continuous standard error of the means and the p-value for comparing the effects

Table 2.4 Characterization of normalized tone-evoked HR oscillations when tones are played at the downstate and upstate phases of the EEG SOs (Figure 2.3.a)

Cortical-Cardiac	Downstate		Upstate	
	Time [msec]	Amplitude [bpm]	Time [msec]	Amplitude [bpm]
Baseline	[-15000, -13000]	0.0±0.0	[-15000, -13000]	0.0±0.0
Point A	462.3±658.4	-0.1±0.9	447.4±542.8	0.1±0.7
Point B	3045.3±1211.9	2.9±1.7	2922.2±925.0	3.7±1.9
Point C	8770.2±1845.7	-2.2±1.9	8440.1±1785.8	-2.2±1.3
Recovery	[13000, 15000]	-0.1±1.0	[13000, 15000]	0.0±0.6

2.4.4 Cardiac-Cardiac tone-enhanced oscillations

We further investigated the effect of acoustic tones played in upstate and downstate phases of HR LF and HF oscillations on the HR profile.

2.4.4.1 HR LF oscillations

A similar pattern was observed when tones were played in the upstate and downstate phases of HR LF oscillations where HR increased from a minimum baseline value (A-point) to a maximum (B-point) and then decreased to a minimum value (C-point) followed by a recovery pattern (see Fig. 2.3.b). The main characteristics of the tone-induced HR oscillations based on the phase of HR LF oscillations are summarized in Table 2.5. Given that our tones were played with a random time interval of 15-30 seconds, our analysis was limited to ±15s around the tones. The amplitude of the induced oscillations was 4.3±2.2 bpm when toned were played in the downstate phase of the EEG SOs, while it was 6.7±2.9 bpm when tones were played in the upstate phase, which was significantly higher (~56%, $p<0.001$, $Z=-9.6$).

Table 2.5 Characterization of normalized tone-evoked HR oscillations when tones are played at the downstate and upstate phases of the HR LF oscillations (Figure 2.3.b)

Cardiac-Cardiac (LF)	Downstate		Upstate	
	Time [msec]	Amplitude [bpm]	Time [msec]	Amplitude [bpm]
Baseline	[-15000, -13000]	0.0±0.0	[-15000, -13000]	0.0±0.0
Point A	98.0±1081.5	-2.9±1.3	179.9±768.3	1.1±0.7
Point B	3471.8±733.0	1.3±1.5	2646.9±632.0	4.4±1.9
Point C	7441.4±1672.3	-1.9±1.3	8297.0±1301.7	-2.3±1.3
Recovery	[13000, 15000]	0.0±1.0	[13000, 15000]	0.0±0.5

2.4.4.2 HR HF oscillations

When tones were played in the downstate phase of HR HF oscillations, HR increased from a minimum baseline value (A-point) to a maximum (B-point) and then decreased to a minimum value (C-point) followed by a recovery pattern (See Fig. 2.3.c, blue). When tones were played in the upstate phase of HR HF oscillations, HR decreased from a maximum baseline value (A-point) to a minimum (B-point) followed by another oscillation with a maximum at C-point and a minimum at D-point (See Fig. 2.3.c, red). The main characteristics of the tone-induced HR oscillations based on the phase of HR HF oscillations are summarized in Table 2.6. The amplitude of the induced oscillations was 7.5±3.4 bpm when tones were played in the downstate

phase of the HR HF oscillations, which was significantly higher (~25%, p<0.001, Z=5.8) than when tones were played in the upstate phase (6.0±3.3 bpm).

Table 2.6 Characterization of normalized tone-evoked HR oscillations when tones are played at the downstate and upstate phases of the HR HF oscillations (Figure 2.3.c)

Cardiac-Cardiac (HF)	Downstate		Upstate	
	Time [msec]	Amplitude [bpm]	Time [msec]	Amplitude [bpm]
Baseline	[-15000, -13000]	0.0±0.0	[-15000, -13000]	0.0±0.0
Point A	-29.6±564.0	-1.4±1.5	-51.2±147.0	2.8±1.7
Point B	2325.7±287.1	4.8±2.2	2482.3±1541.6	-0.6±1.5
Point C	7986.0±1270.0	-2.7±1.5	4678.5±1467.5	3.2±2.4
Point D	—	—	8239.4±1648.1	-2.8±1.6
Recovery	[13000, 15000]	0.0±0.7	[13000, 15000]	0.0±0.7

2.4.5 Pseudo-sham experiment

To determine whether the observed effects were due to auditory stimulation or merely differences in the ongoing signal phases, we conducted a secondary analysis using tone-free intervals of at least 30 seconds within the N2 and N3 sleep stages. The midpoints of these intervals served as hypothetical tone-onset time points. Using the same methodology as in the main analysis, we aligned and averaged EEG and HR segments across the phases of SO, and the LF and HF components of HR. This analysis, limited to 79 participants due to data constraints, enabled an assessment of baseline cortical and cardiac dynamics in the absence of tones (Figures I-3– I-6) and comparisons to the results from these same 79 participants during tone application. Regarding the cortical-cortical baseline comparison, neither SWA nor the maximum EEG peak-to-peak amplitude significantly differed between the downstate and upstate phases (SWA: p=0.6, Z=-0.5; amplitude: p>0.05, Z=1.4). In the context of cardiac-cortical interactions, a difference in EEG response was evident between the downstate and upstate phases of HR LF, specifically in amplitude (~2μV, p<0.01, Z=-2.6) and SWA (~12%, p<0.001, Z=-6.5). The amplitude difference was substantially smaller than that observed during tone presentation (~28μV, p<0.001, Z=-6.9), and the SWA difference between phases was also slightly lower than the tone-related phase difference (~16%, p<0.001, Z=-7.2). It is worth noting

that, when normalized to baseline, the SWA increase during tone presentation in the upstate phase was approximately 14% greater than that observed in the downstate phase. Conversely, no significant differences in amplitude or SWA were detected between the HR HF downstate and upstate phases (amplitude: p=0.4, Z=0.8; SWA: p=0.9, Z=0.1). Regarding cortical-cardiac interaction, no significant baseline difference was observed in heart rate peak-to-peak amplitude between upstate and downstate phases (p=0.9, Z=-0.1). In the cardiac-cardiac comparisons, tone application increased the amplitude difference between upstate and downstate phases from ~1.14 bpm (p<0.001, Z=-6.5) to ~2.42 bpm (p<0.001, Z=-7.4) and altered the signal shape of HR LF oscillations. Similarly, in HR HF oscillations, this difference increased from ~0.98 bpm (p<0.001, Z=7.3) to ~1.64 bpm (p<0.001, Z=4.8).

2.4.6 Fine-tuning of optimal phase

To further examine the optimal time for of phase targeting, we defined two EEG phase windows: the up-peak (π/4 to 3π/4) and the broader upstate (0 to π). Data from 72 participants with sufficient tone presentations in both conditions were analyzed, including matched no-tone segments. Both up-peak and general upstate stimulation resulted in significant SWA enhancement, with no statistically significant difference in SWA increase between them (p=0.7, Z=0.4). However, tones delivered at the up-peak phase elicited significantly higher EEG peak amplitudes (~7 μV; p<0.01, Z=3.2) and deeper troughs (~7 μV; p<0.001, Z=4.3), as shown in Figure I-7 (c). Additionally, event detection analysis revealed that tones at the up-peak triggered SOs in 73% of trials, compared to 68% for general upstate stimulation (Figure I-8).

2.5 Discussion

EEG SOs represent the most prominent marker of neuronal synchronization during non-REM sleep. Within the framework of CNS-ANS interplay, the biphasic HR fluctuation associated with isolated SOs constitutes the most substantial cardiac oscillation linked to undisturbed, synchronized EEG events—excluding arousals or awakenings, which are inherently desynchronizing events (de Zambotti *et al.*, 2018; de Zambotti *et al.*, 2016). Our findings strongly

support this CNS-ANS coupling, illustrating that auditory stimulation can either amplify or disrupt ongoing cortical and cardiac oscillations depending on the phase of the oscillatory cycle during which stimuli are delivered.

Our results align with a growing body of literature demonstrating that auditory stimulation timed to the upstate of EEG SOs can enhance SWA during sleep. For instance, consistent with studies such as (Diep *et al.*, 2019; Papalambros *et al.*, 2017), we observed increased SWA during periods of stimulation when tones were presented in the upstate phase of EEG SOs. However, in contrast to earlier findings by (Ngo *et al.*, 2013), who employed a specific paired-tone protocol where the second tone followed the first after a fixed 1.075s inter-tone interval and reported no significant difference in SWA relative to this protocol, we observed an increase in SWA across all phases of stimulation when comparing to baseline, with a significantly greater effect during the up-phase. This discrepancy may arise from methodological differences, including our continuous phase-locked stimulation approach, tone intensity, stimulus timing accuracy, and individual variability in SO morphology. Importantly, our results reinforce prior findings (Ngo *et al.*, 2013, 2015; Santostasi *et al.*, 2016) indicating that stimulation during the upstate phase of SOs can enhance their amplitude. This strategic augmentation of SOs holds promise for future applications aimed at improving downstream sleep-dependent processes, such as memory consolidation, given that prior research suggests this may occur through the enhancement of spindle activity phase-locked to the SO upstate (Ngo *et al.*, 2013, 2015; Santostasi *et al.*, 2016; Tononi & Cirelli, 2006). Indeed, our findings show that SOs evoked in the upstate phase are accompanied by larger troughs, a feature previously associated with improved memory performance (Heib *et al.*, 2013). Conversely, tones delivered outside of optimal timing—particularly just after the SO—may disrupt sleep architecture, as evidenced by spindle suppression and interference with ongoing oscillatory processes (Antony, Schonauer, Staresina & Cairney, 2019; Cellini & Mednick, 2019).

These insights have informed the development of closed-loop auditory stimulation systems aimed at enhancing deep sleep. While previous studies have focused primarily on the phase timing of cortical oscillations, our current study is the first, to our knowledge, to investigate the

effects of delivering auditory tones at specific phases of both central (EEG SO) and peripheral (HR LF and HF) oscillations. We systematically examined stimulation effects during the upstate and downstate phases of EEG SOs, as well as during the upstate and downstate of HR LF and HF oscillations. We found that auditory stimulation delivered in the EEG SO upstate, HR LF upstate, and HR HF downstate resulted in significantly greater enhancement of both the amplitude and the number of induced SOs, along with stronger HR oscillatory responses. These findings demonstrate that the timing of auditory stimulation relative to both cortical and autonomic rhythms is critical: optimal stimulation appears to require phase alignment with EEG SO upstate, HR LF upstate, and HR HF downstate to effectively enhance deep sleep and modulate cardiovascular dynamics.

Coupling between cortical and autonomic rhythms is a central topic in sleep research, with some of the most well-characterized interactions occurring between EEG SWA and cardiac function—particularly through measures like R-R intervals and high-frequency HRV, which reflect parasympathetic (vagal) activity (de Zambotti *et al.*, 2018; Niizeki & Saitoh, 2018). These dynamics represent a core aspect of CNS-ANS communication during sleep. Recent analytic frameworks have conceptualized the human body as a complex physiological network, where distinct biorhythms serve as interconnected nodes (Bartsch, Liu, Bashan & Ivanov, 2015; Porta & Faes, 2015; Ivanov, Liu & Bartsch, 2016). Through this lens, studies have demonstrated that sleep and its stages are accompanied by significant reorganization of network structure, driven by both unidirectional and bidirectional interactions between systems (de Zambotti *et al.*, 2018; Ivanov *et al.*, 2016; Stankovski *et al.*, 2017b). Thus, cortical and cardiac measures not only covary across the night but actively influence each other through precise temporal dynamics, leading to changes in overall network complexity and integration (de Zambotti *et al.*, 2018). Despite these advances, there remains a need to understand how central and peripheral systems respond and synchronize in reaction to external stimuli, particularly in the context of sleep neurostimulation. Determining whether coupling strength can guide optimal timing for intervention—and whether it influences the efficacy of stimulation—remains an open and important question. Furthermore, while enhancing deep sleep is often the primary

goal of auditory stimulation paradigms, it is essential to also consider potential impacts on the peripheral nervous system (Huwiler *et al.*, 2023; Lustenberger, 2025; Huwiler *et al.*, 2025). A comprehensive evaluation must weigh both the benefits and possible costs of modulating these systems during sleep. In our study, while the primary focus was on cortical effects of acoustic stimulation, we also examined cardiac dynamics—specifically HR oscillations peak-to-peak amplitude—to probe this CNS-ANS interplay. Our findings show that auditory stimulation can modulate both brain and heart rhythms, and that the phase of stimulation relative to ongoing oscillatory activity is a critical factor for maximizing these effects. Notably, a rapid increase in HR oscillations peak-to-peak amplitude may be associated with a rise in HR HF oscillations, which could indicate enhanced HRV, a recognized marker of autonomic flexibility and resilience. Higher HRV has been associated with improved cardiovascular health, better stress regulation, and cognitive performance (Thayer, Åhs, Fredrikson, Sollers III & Wager, 2012). These findings suggest that auditory stimulation might not only support sleep depth but also promote parasympathetic activation and physiological recovery during sleep (Grimaldi *et al.*, 2019). While HR oscillations alone are not sufficient to claim definitive health outcomes, their inclusion provides valuable insight into the systemic effects of sleep stimulation. Future research should continue to investigate the joint behavior of central and peripheral systems during stimulation and explore how enhancing HR oscillations peak-to-peak amplitude may contribute to broader markers of well-being and health.

Our findings align with those of (Navarrete *et al.*, 2020), suggesting that while stimulation during any point within the upstate enhances SO amplitude, targeting the up-peak phase may yield slightly stronger oscillatory responses. However, the relative magnitude of this difference was modest (~14%) compared to the much larger enhancement observed between upstate and downstate stimulation (~110%). This indicates that although up-peak targeting may optimize outcomes, stimulation during the broader upstate window remains a reliable and practical approach—particularly in real-world closed-loop systems where precise phase detection may be limited.

A key limitation of this study is the absence of a dedicated control night, which limits our ability to fully disentangle the effects of auditory stimulation from spontaneous fluctuations in ongoing neural activity. We attempted to address this by analyzing tone-free intervals as a pseudo-sham condition; however, future studies should incorporate formal control nights to more rigorously isolate tone-specific effects. Nevertheless, our findings suggest that the differences between upstate and downstate phases are due to tone application—either entirely or significantly in some interactions.

Future work should explore tone-enhanced SO in relation to additional HR frequency components, such as ultralow frequency (ULF; <0.003 Hz) and very low frequency (VLF; 0.003–0.04 Hz), as well as different phases of the ECG waveform. Beyond single-frequency-phase analysis, investigating optimal combinations of HR phase components may yield a more complete understanding of tone timing strategies. Importantly, phase-to-phase coupling is only one form of central–peripheral interaction; other types, such as amplitude-to-amplitude coupling, may also play critical roles in modulating sleep physiology and should be examined. Moreover, future studies should assess the effects of acoustic stimulation relative to other peripheral rhythms, including blood pressure, pulse pressure, and respiration. For instance, (Forouzanfar *et al.*, 2019) showed that NREM EEG delta power is higher during the down phases of slow and respiratory-frequency blood pressure oscillations, and during the up phases of respiration, suggesting meaningful CNS–ANS coupling during sleep that could guide stimulation timing. Improving timing precision may also benefit from analyzing instantaneous phase rather than classifying tones into broad up/down phases. This would require ensuring even tone distribution across all phases, allowing robust statistical comparison. Additionally, alternative phase classifications—such as ascending vs. descending phases, as studied by (Huwiler *et al.*, 2022)—could be considered. However, that study found no significant difference between ascending and descending EEG SO effects on SWA, suggesting that not all sub-phase distinctions yield differential outcomes.

This study utilized data collected using the standard sleep ERP protocol, as described by (Colrain, Crowley, Nicholas, Padilla & Baker, 2009). However, as noted in the introduction, brief acoustic tones—typically around 50 msec in duration and delivered at low intensities

(40–60 dB)—have shown more promising results in human studies, particularly in the context of auditory stimulation for cognitive enhancement (Diep *et al.*, 2019) and sleep-dependent memory consolidation (Cellini & Mednick, 2019; Ngo *et al.*, 2015). Most research in this area has focused on these brief, low-intensity tones. As such, further investigation into their effects is warranted. While similar optimal timing patterns for tone delivery are expected, the magnitude of enhancement in outcomes may differ. Additionally, evaluating arousal levels and sleep stage transitions in response to different tone types will be important for identifying the most effective and least disruptive acoustic stimuli for sleep-based interventions.

Another direction for future research is to investigate the influence of age on SWA, potentially through topographical comparisons. Our results consistently demonstrated that for all individuals, the proposed optimal timing of stimulation led to better outcomes compared to non-optimal timing. Despite this uniform direction of effect across our sample, exploring how age modulates these findings would be valuable. Furthermore, given our focus on the F3 channel, future studies could examine different brain regions to identify potential topographical variations in these effects.

The use of peripheral information in sleep enhancing technology within the context of neuromodulation provides a promising avenue toward the development of sleep enhancement wearables (Yoon & Baek, 2022; Henao *et al.*, 2022). Rather than relying on EEG measurements alone, stimulation based on peripheral information, or a combination of central and peripheral information can provide better opportunities toward sleep enhancement. Particularly, neuro-stimulation is growing in popularity within the boom of consumer wearable sleep devices. Closed-loop acoustic stimulation based on the phases of EEG signal has been implemented in several novel sleep enhancing tools. However, whether such acoustic stimulation could be delivered based on peripheral information is still an open question. This study suggests new avenues toward understanding the coupling between central and peripheral measurements and shows that peripheral measurements (here, HR) can be used to find an optimal timing for the application of external stimuli.

CHAPTER 3

OPTIMIZING AUDITORY STIMULATION TIMING IN NREM SLEEP USING BRAIN–HEART RHYTHMS: CONTINUOUS PHASE ANALYSIS AND MULTIDIMENSIONAL PHASE-LOCKING

Sepehr Sardooeinasab[1] , Massimiliano de Zambotti[2] , Fiona C. Baker[2] , Mohamad Forouzanfar[2,3,4]

[1] Department of Electrical Engineering, École de technologie supérieure, Université du Québec, Montréal, QC H3C 1K3, Canada
[2] Center for Health Sciences, SRI International, Menlo Park, CA 94025, USA
[3] Department of Systems Engineering, École de technologie supérieure, Université du Québec, Montréal, QC H3C 1K3, Canada
[4] Centre de recherche de l'Institut universitaire de gériatrie de Montréal (CRIUGM), Montréal, QC H3W 1W5, Canada

The article was submitted to *SLEEP* in October 2025.

3.1 Presentation

This chapter presents the article "Optimizing Auditory Stimulation Timing in NREM Sleep Using Brain–Heart Rhythms: Continuous Phase Analysis and Multidimensional Phase-Locking" by Sardooeinasab, de Zambotti, Baker, and Forouzanfar, submitted to the journal *SLEEP* in October 2025. The objective of this research is to develop a framework for optimizing the timing of auditory stimulation during non-rapid eye movement (NREM) sleep by first introducing continuous phase-analysis methods to identify more precise tone delivery timing, and subsequently extending the framework to a multidimensional approach that jointly considers cortical and cardiac rhythms.

3.2 Introduction

Non-rapid eye movement (NREM) sleep contributes to neural stability, supports psychological well-being, and maintains physiological homeostasis (Rasch & Born, 2013). The deeper stages of NREM sleep are characterized by prominent neural synchronization, with slow oscillations (SOs; ~0.5–1 Hz) representing the dominant synchronized EEG activity in NREM sleep (Steriade,

2006). Slow-wave activity (SWA; 0.5–4 Hz), which encompasses SOs, is closely linked to memory consolidation (Ong *et al.*, 2018b), synaptic homeostasis (Tononi & Cirelli, 2006), immune function (Besedovsky *et al.*, 2017b), and also serves as a physiological marker of sleep's restorative quality (Vyazovskiy & Harris, 2013).

SWA naturally declines with age (Mander, Winer & Walker, 2017) and can also be reduced in individuals with physical or psychological health conditions (Schreiner *et al.*, 2021b). Consequently, the enhancement of SOs and SWA has become a central focus of research aimed at improving sleep quality and associated cognitive and physiological outcomes.

A range of interventions have been explored, including invasive approaches such as pharmacological agents (Benedict, Scheller, Rose-John, Born & Marshall, 2009), non-invasive brain stimulation techniques such as transcranial direct current stimulation (tDCS) Prehn-Kristensen *et al.* (2014) and transcranial alternating current stimulation (tACS) (Ketz, Jones, Bryant, Clark & Pilly, 2018), and behavioral strategies (Määttä *et al.*, 2010). Other approaches include sensory stimulation modalities such as auditory or olfactory cues (Tononi, Riedner, Hulse, Ferrarelli & Sarasso, 2010) delivered during sleep, with closed-loop auditory stimulation (CLAS)—in which brief tones are delivered in synchrony with specific neural activity phases—emerging as particularly promising due to its temporal precision, and ease of implementation (Grimaldi, Papalambros, Zee & Malkani, 2020; Ngo *et al.*, 2015).

Multiple studies have shown that auditory tone stimulation, when delivered during the SO upstate, maximize SO amplitude and increases the likelihood of phase-locked spindle generation (Ngo *et al.*, 2013; Navarrete *et al.*, 2020). These stimulation-evoked dynamics have been linked to improved hippocampal–cortical communication and better performance on memory tasks, especially in declarative memory domains (Ong *et al.*, 2016). Experimental findings suggest that the peak of the SO upstate represents the most effective time for stimulation due to heightened cortical excitability at that phase (Navarrete *et al.*, 2020). Most CLAS systems, however, rely solely on EEG-based SO phase to determine stimulation timing and largely ignore the influence

of peripheral physiological dynamics—despite well-established evidence of central–autonomic coupling during sleep (de Zambotti *et al.*, 2018).

Auditory stimulation during sleep engages both cortical and autonomic systems. Tones that elicit SOs are accompanied by transient increases in heart rate, blood pressure, and sympathetic activity, followed by compensatory rebounds toward or below baseline levels (de Zambotti *et al.*, 2018; de Zambotti *et al.*, 2016). Conversely, the likelihood of SO occurrence depends on autonomic state: they are more frequent during parasympathetic dominance, such as when blood pressure decreases (Forouzanfar *et al.*, 2019), and when pre-tone cardiac activity is low (de Zambotti *et al.*, 2016). These findings highlight a bidirectional coupling between central and autonomic events. HR low-frequency (LF; 0.04–0.15 Hz) and high-frequency (HF; 0.15–0.4 Hz) oscillations provide accessible indices of autonomic state, with HF power reflecting parasympathetic activity and LF power capturing a mix of sympathetic, parasympathetic and baroreflex influences (Shaffer & Ginsberg, 2017).

Based on prior work (Forouzanfar, Sardooeinasab, Baker, Colrain & de Zambotti, 2025) showing that both cortical excitability and autonomic state shape the brain's responsiveness to auditory input—and that specific autonomic phases, particularly the HR-LF upstate and HR-HF downstate, modulate this responsiveness—we formulated two directional hypotheses. First, extending earlier findings from binary upstate/downstate comparisons, we expected that tones occurring near the peaks of the HR-LF and HR-HF oscillations (i.e., the HR-LF up-peak and HR-HF down-peak) would be associated with stronger enhancement of SO amplitude and SWA than tones occurring at other phases, as these peaks correspond to moments when autonomic oscillatory activity is most strongly expressed. Second, we hypothesized that combining EEG SO timing with HR-derived timing cues could show the largest enhancement effects, reflecting the additive contributions of cortical excitability and autonomic phase alignment in shaping tone-evoked slow-wave dynamics. To test these hypotheses, we investigated the optimal timing for auditory stimulation by examining which phases were associated with stronger responses based on continuous phase representations of EEG SOs, HR-LF, and HR-HF components. We also compared cortical responses evoked by tones occurred at the upstate and downstate phases of

each oscillation, both individually and in combination. Specifically, we aimed to determine whether auditory stimulation occurring at specific HR component phases enhances SO amplitude and SWA more effectively than random delivery, and whether combining HR component phases with SO phase provides greater enhancement than EEG-based timing alone.

3.3 Methods

3.3.1 Participants and dataset

The research examined data from 133 adolescents (12–21 years old; mean ± SD: 15.6 ± 2.4 years; 60 females) from the National Consortium on Alcohol and NeuroDevelopment in Adolescence (NCANDA) (Brown *et al.*, 2015) sleep substudy conducted at SRI International and the University of Pittsburgh. Previous studies (Forouzanfar *et al.*, 2025; Baker *et al.*, 2016) provide complete details on participant demographics, enrollment procedures, IRB approval, site-specific sample sizes, and technical specifications of the PSG setup. In summary, participants were healthy, drug-free, and without psychiatric, medical, or sleep disorders.

3.3.2 Auditory stimulation and trial selection

Auditory tones (80 dB, 1000 Hz, 50 ms) were delivered binaurally during NREM sleep at random intervals of 15–30 s, as detailed in (Forouzanfar *et al.*, 2025). Analyses included only tones in N2 and N3 epochs free of artifacts (no EEG/ECG outliers within ±10 s) and arousals (none within ±10 s). Analyses were further restricted to trials that successfully evoked a SO; these 20-s segments were defined as the stimulated windows (STIM). Table 3.1 reports tones per individual per condition and the subset followed by a SO.

To serve as comparison trials, tone-free intervals of at least 20 s during N2 and N3 sleep were identified using the same artifact- and arousal-free criteria. Intervals whose midpoints were followed by a spontaneous SO were used as matched unstimulated windows (UNSTIM). These midpoints were treated as hypothetical tone-onset time points, enabling the assessment of

spontaneous EEG activity under equivalent, non-stimulated conditions. Across participants, an average of 283.3 ± 127.2 STIM events were available, alongside 239.8 ± 177.5 UNSTIM windows.

Table 3.1 Number of tones presented in each condition and number of tones followed by a SO (mean ± SD per individual)

Condition	**Tones Played**	**Tones → SO**
——	493.50±163.58	324.62±105.91
U—	339.81±128.39	242.31±97.57
–U–	331.94±124.06	226.21±84.98
—D	269.51±98.90	180.66±68.97
UU–	235.93±104.70	172.21±78.91
U–D	189.81±82.36	137.77±65.10
–UD	185.67±78.27	129.36±56.68
UUD	134.81±67.98	100.36±53.34

Conditions are defined by phase-locking based on EEG SO, HR-LF, and HR-HF phases in order: U = upstate, D = downstate, – = no phase-locking.

3.3.3 ECG and EEG preprocessing

3.3.3.1 EEG preprocessing

EEG from the F3 electrode (referenced to the contralateral mastoid) was band-pass filtered between 0.1–30 Hz using a 4th-order Butterworth filter. The filter was applied in both directions to avoid phase shifts. Segments with amplitudes exceeding ±1500 μV or standard deviations exceeding 10 from the mean were classified as artifacts and excluded (Forouzanfar *et al.*, 2025). SOs were extracted by filtering the EEG between 0.5–4 Hz (Papalambros *et al.*, 2017) using a 4th-order Butterworth filter. The SOs were defined as waves that had a negative peak less than -80 μV, a peak-to-peak amplitude greater than 140 μV (Massimini *et al.*, 2004), and durations between 0.25 and 2.5 seconds. Peaks and troughs were identified between successive zero-crossings, and the duration of the signal was the interval between two downward zero-crossings (see 3.1b).

To examine power alterations in specific frequency bands, EEG data were segmented into 8-second segments. Welch's method was used to calculate power spectral density (PSD) with a 4-second Hanning window and 50% overlap. The PSDs were then interpolated to a resolution of 0.1 Hz. In order to reduce inter-individual variability, PSDs for each individual were normalized to the mean total spectral power in the 0–20 Hz range across all stimulated windows. For SWA, the power within the range of 0.5–4 Hz was extracted (Forouzanfar *et al.*, 2025).

Sleep spindle (SS) detection followed prior work criteria (Clemens *et al.*, 2007; Purcell *et al.*, 2017). EEG was band-pass filtered between 11 and 16 Hz, and the root mean square (RMS) envelope was computed with a 0.2-s sliding window. Candidate spindles were identified when the RMS envelope exceeded the 88.86th percentile of spindle activity during N2 and N3. Then, SS were identified as events with a duration between 0.3 and 3 seconds, exhibiting at least five oscillations, a unimodal peak in the spindle frequency band (11–16 Hz), and decreasing power for higher frequencies, as computed by the Morlet wavelet. SS duration was defined as interval during which the RMS signal remained above threshold. Stimuli-dependent SS were those initiating after the trough of a detected SO following tone presentation (or its hypothetical timing in unstimulated windows). Finally, SS likelihood was defined as the proportion of stimuli-dependent spindles (Navarrete *et al.*, 2020).

3.3.3.2 ECG preprocessing

ECG signals were filtered using a 4th-order Butterworth bandpass filter (0.5–35 Hz). R-peaks were detected using custom algorithms (de Zambotti *et al.*, 2020), and R–R intervals were used to derive instantaneous HR, interpolated at 10 Hz. ECG segments with out-of-range signals or R–R intervals exceeding 10 standard deviations from the mean were excluded as artifacts or ectopic beats. HR signals were decomposed into low-frequency (LF; 0.04–0.15 Hz) and high-frequency (HF; 0.15–0.4 Hz) components (Shaffer & Ginsberg, 2017) using separate 4th-order Butterworth filters.

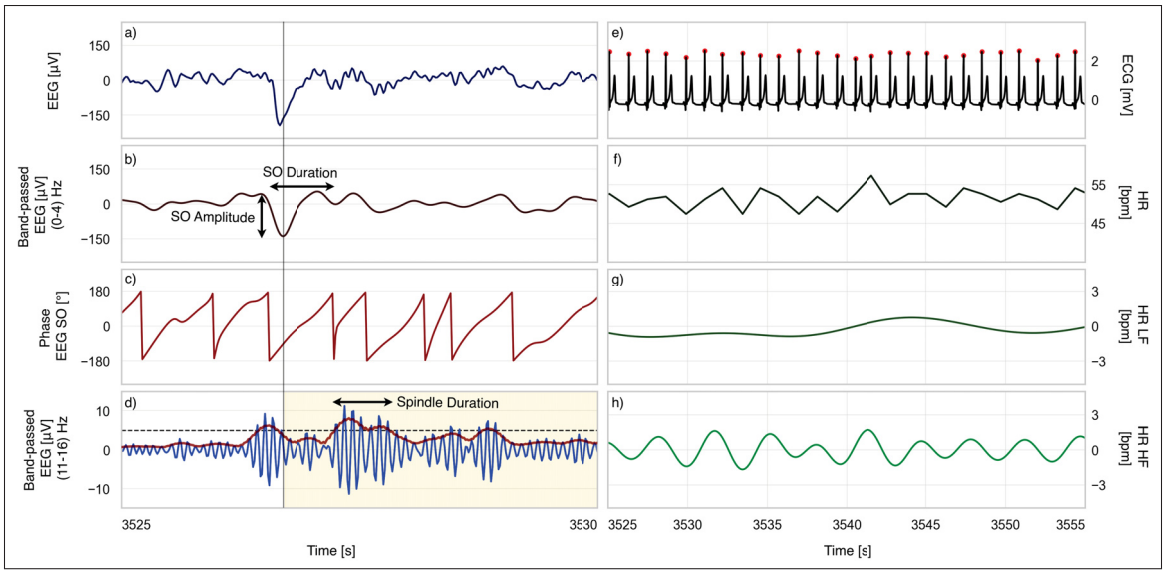

Figure 3.1 EEG and ECG signals with extracted oscillations. EEG-related panels: (a) raw EEG, (b) EEG filtered in the SO band with a sample SO showing its peak-to-peak amplitude and duration, (c) instantaneous phase of the EEG filtered in the SO band, and (d) EEG filtered in the spindle band with RMS envelope and spindle duration illustrated for a sample spindle. The shaded yellow area shows the search interval for SOlocked spindles. ECG-related panels: (e) raw ECG with detected R-peaks, (f) derived HR, (g) low-frequency (HR-LF) component, and (h) high-frequency (HR-HF) component. Each EEG panel shows a 5-s segment and each ECG panel a 30-second segment, both recorded during N3 sleep in a representative individual

3.3.4 Phase-locking analysis

Instantaneous phases of EEG SOs and HR components (HR-LF and HR-HF) were computed using the Hilbert transform (Forouzanfar *et al.*, 2019). A 90° phase shift was applied to account for the quadrature offset, such that –90° corresponded to the trough, 90° to the peak, and 0° to the negative-to-positive zero crossing (see Fig. 3.2a).

3.3.4.1 Continuous phase analysis

To examine fine-grained phase effects, tones were grouped according to the instantaneous phase of EEG SO, HR-LF, and HR-HF at the time of tone onset. Phases were binned into 60° windows shifted by 15° across the full 360° cycle. Using overlapping bins helped reduce edge artifacts

and assumed that responses vary smoothly across neighboring phases. This design also ensured that each bin contained a sufficient number of tones, while the small shift preserved resolution.

For each tone trial in STIM and each hypothetical tone in UNSTIM, SO peak-to-peak amplitude, normalized SWA, and stimulus-dependent spindle occurrence were quantified. Monte Carlo (MC) baselines were estimated per phase bin (details in the Statistics section). SO amplitude and SWA were averaged within each phase bin, and spindle likelihood was defined as the proportion of SO-coupled spindles following tone presentation. These analyses yielded continuous indices describing how SO amplitude, SWA, and spindle likelihood varied across EEG SO, HR-LF, and HR-HF phases.

3.3.4.2 Multidimensional phase analysis

EEG–HR phase-locking was analyzed using binary 180° bins. For each signal (EEG SO, HRLF, HR-HF), the downstate was defined as –180° to 0° and the upstate as 0° to 180°. Phaselocking conditions were constructed either unimodally (based on one signal) or multidimensionally (combining EEG and/or HR components phases, for example EEG upstate with HR-HF downstate).

For each condition, event-related potentials (ERPs) and power spectral densities (PSDs) were computed separately for STIM and UNSTIM by averaging tone-locked EEG segments. Difference signals were obtained by subtracting UNSTIM from STIM, producing difference waveforms and spectra. In the ERP domain, extrema were identified, and peak-to-peak amplitudes were quantified. In the spectral domain, PSDs were estimated from tone-locked segments, averaged within conditions, and compared to derive difference spectra. Mean SWA power (0.5–4 Hz) was extracted from all spectra.

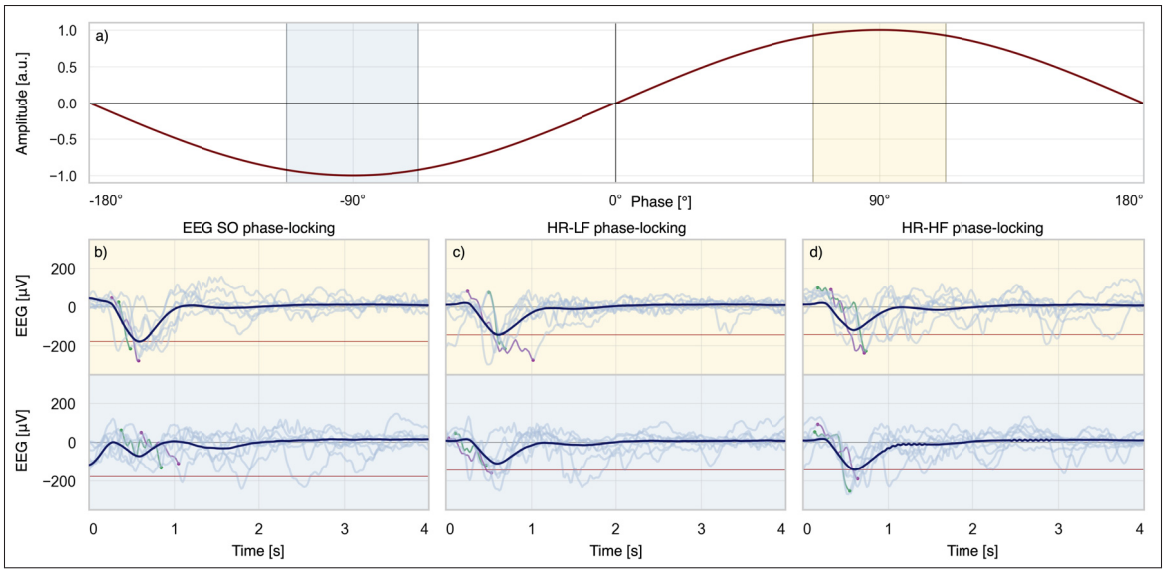

Figure 3.2 Sinusoidal signal and EEG responses to phase-locked tones. (a) Example sinusoidal signal with up-peak (yellow) and down-peak (blue) highlighted. (b–d) EEG averages time-locked to tones delivered at phases of (b) EEG SO, (c) HR-LF, and (d) HR-HF. Yellow shading marks up-peak locking, blue shading marks down-peak locking, and the red horizontal line indicates the minimum SO amplitude at each peak

3.3.5 Statistics

3.3.5.1 Continuous phase analysis

Responses were mean-centered within individuals to isolate phase-dependent effects. For SO amplitude and SWA, individual STIM and UNSTIM values were extracted for each phase bin. Because tone delivery was not uniformly distributed across phases, UNSTIM values were modeled by Gaussian approximations of empirical mean and variance. From this distribution, 200 Monte Carlo samples were generated to form phase-specific surrogate baselines. This approach allowed us to normalize each subject–bin by a common UNSTIM-derived reference without discarding data and ensured that STIM and UNSTIM differences reflected phase structure rather than unequal sampling. These provided STIM–MC and UNSTIM-MC contrasts at the individual level (Navarrete *et al.*, 2020). At the group level, one-sample t-tests compared STIM

and UNSTIM across phase bins, with false discovery rate (FDR) correction applied using the Benjamini–Hochberg procedure ($\alpha = 0.05$).

Spindle likelihood analysis used a Monte Carlo resampling approach to define a baseline. For each phase bin, UNSTIM events were resampled 200 times, drawing two-thirds of events per iteration. The geometric mean of these resamples likelihood provided a null reference value for that bin. For each participant, spindle likelihood was then calculated as the percentage of SO-coupled spindle occurrences in STIM and UNSTIM conditions, expressed relative to this baseline. Differences between STIM and UNSTIM were tested per bin using Welch's unequal-variance t-tests, and p-values were corrected for multiple comparisons using the FDR method.

In addition, we computed a Pairwise Response Index (PRI) to quantify phase preference at the individual level. For each subject, we considered the distribution of STIM–MC contrasts in each phase bin, obtained from the Monte Carlo procedure described above. For every pair of bins, we compared the corresponding STIM–MC distributions using Welch's unequal-variance t-test and noted whether the t-statistic was positive or negative. The PRI for a given bin was defined as the average sign of these pairwise t-statistics across all comparisons with other bins, yielding values between 1 (consistently weaker than other bins) and +1 (consistently stronger than other bins). Group-level PRI values were then tested against zero using one-sample t-tests per bin, and p-values were corrected for multiple comparisons using FDR ($\alpha = 0.05$).

3.3.5.2 Multidimensional phase analysis

For binary phase comparisons (upstate versus downstate; EEG–HR phase combinations), individual-level averages from the STIM and UNSTIM conditions, as well as their difference (STIM – UNSTIM), were compared across phase-locking strategies. Normality was assessed with the Shapiro–Wilk test ($\alpha = 0.05$), and paired-samples t-tests were used when this assumption held, while Wilcoxon signed-rank tests were applied otherwise.

3.3.5.3 Software

Preprocessing was performed in MATLAB R2023a (MathWorks, Natick, MA). Statistical analysis and visualization were conducted in Python 3.9.

3.4 Results

3.4.1 Tone presentation is optimal at SO up-peak, HR-LF up-peak, and HR-HF down-peak

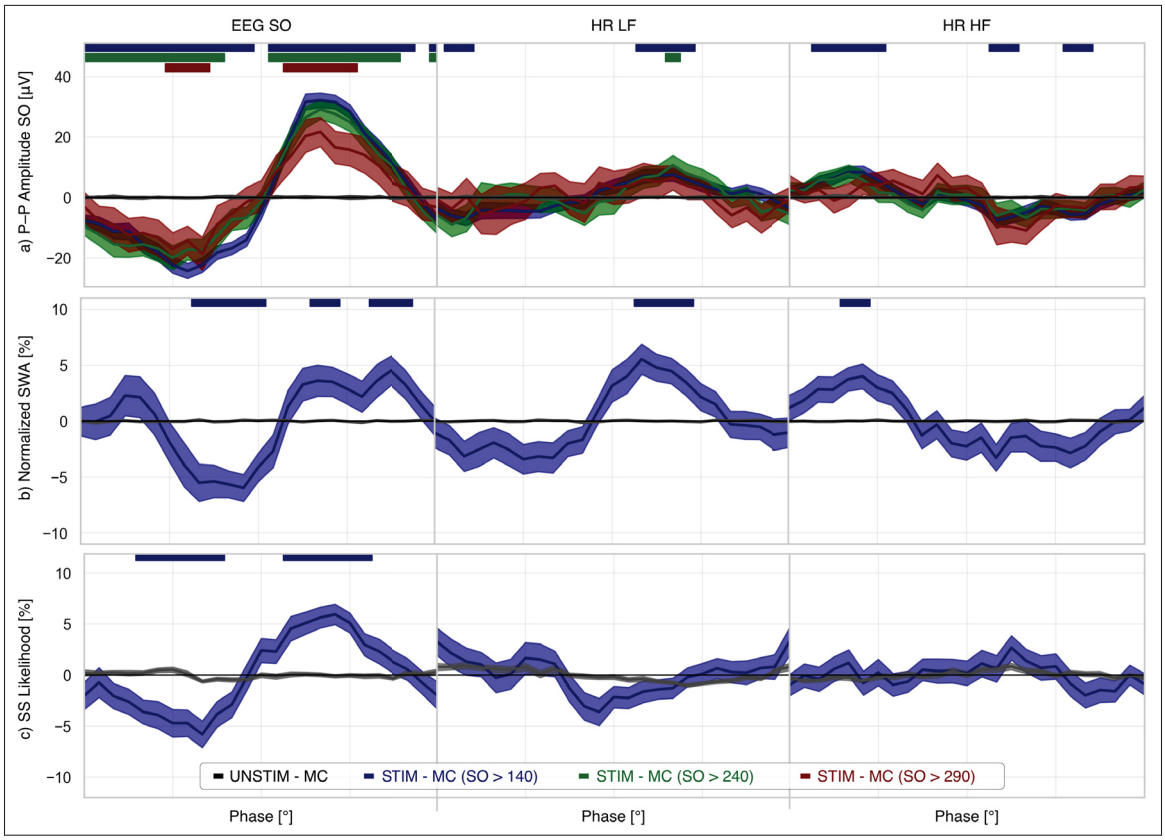

Figure 3.3 Continuous SO amplitude, SWA, and spindle likelihood as functions of SO and HR component phases. (a) SO peak-to-peak amplitude across EEG SO, HR-LF, and HR-HF phases. (b) Continuous SWA and (c) continuous spindle likelihood across phases. Phases range from –180° to 180°, with shaded ribbons marking intervals where tone-evoked responses differ significantly from unstimulated intervals

Continuous phase analysis (Fig. 3.3) revealed phase-dependent differences in EEG SO, HR-LF, and HR-HF, with peak-to-peak amplitudes were largest when tones were delivered at the SO up-peak, the HR-LF up-peak, and the HR-HF down-peak, and smallest during the SO down-peak, the HR-LF down-peak, and the HR-HF up-peak. The windows of significant differences in the PRI comparison were similar to those found in the STIM-MC vs. SHAM-MC analysis.

As shown in Fig. 3.3a, The maximum effect on SO amplitude occurred at 75° ($p < 0.001$), 60° ($p < 0.05$), and –120° ($p < 0.001$) for SO, HR-LF, and HR-HF phases, respectively. In contrast, minimal responses were observed at –75° ($p < 0.05$), –150° (n.s.), and 30° ($p < 0.01$). The differences between extreme bins reached 55.6 μV for SO ($p < 0.001$), 14.5 μV for HR-LF ($p < 0.01$), and 15.9 μV for HR-HF ($p < 0.001$). The window of significant effects extended over 225° and 195° for SO (optimal and non-optimal phases, respectively), 105° and 75° for HR-LF, and 120° and 75° for HR-HF. Larger SOs were less easily enhanced, and their response depended only on SO phase. Medium-sized SOs were affected both by SO and HR-HF timing. Small SOs were the most sensitive, showing phase-dependent changes across all oscillatory components.

SWA showed similar patterns (Fig. 3.3b). The largest increases were detected at 135° ($p = 0.01$), 30° ($p < 0.01$), and –120° ($p < 0.01$), with minimal values at 0° ($p < 0.01$), –90° (n.s.), and 30° (n.s.) for SO, HR-LF, and HR-HF, respectively. Window sizes of significance covered 60° (optimal) and 120° (non-optimal) for SO, 105° for HR-LF, and 75° for HR-HF (optimal). The magnitude of SWA modulation, quantified as the difference between extreme bins relative to mean SWA across individuals, reached 10.6% for SO, 8.9% for HR-LF, and 6.9% for HR-HF (Fig. 3.3b).

Spindle likelihood (Fig. 3.3c) exhibited significant phase-dependence for SO but not for HR-related components. Relative to the average spindle likelihood across bins, likelihood of spindles was enhanced near 75° ($p < 0.001$) and suppressed near –60° ($p < 0.001$). The associated windows measured 135° and 135°, and the difference between extremes reached 11.2% ($p < 0.001$).

3.4.2 Peak HR response occurs at the SO up-peak

In cortical–cardiac continuous phase analysis (Fig. 3.4), HR responses were phase-dependent on EEG SO activity. HR increased most prominently during the ascending positive SO phase at 45° ($p < 0.001$) and decreased during the descending negative phase at –105° ($p < 0.001$). These responses covered window sizes of 150° and 180°, respectively. The difference between extreme bins corresponded to 1.8 bpm ($p < 0.001$), confirming that HR changes were phase-dependent and peaked at the SO up-peak.

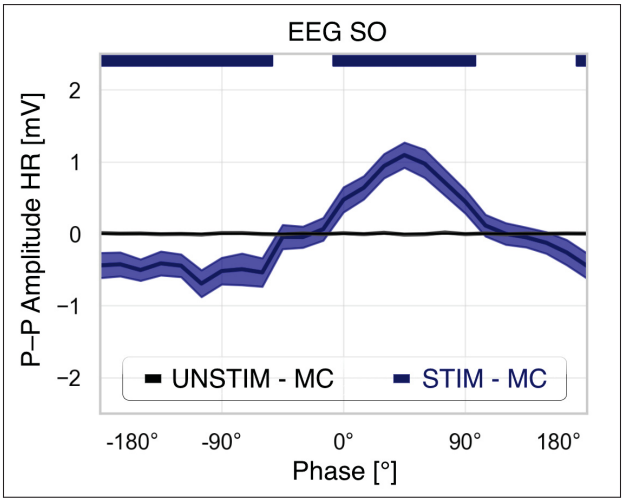

Figure 3.4 Continuous HR peak-to-peak amplitude as a function of SO phase. Phases range from –180° to 180°, with shaded ribbons marking intervals where tone-evoked responses differ significantly from unstimulated intervals

3.4.3 SO and SWA are enhanced by HR component phase-locking alone

In the multidimensional phase analysis, cardiac contributions were assessed by comparing EEG responses between open-loop stimulation (across all phases) and stimulation phase-locked to the HR-LF upstate and/or HR-HF downstate (Fig. 3.5; Table 3.2). Data from 104 participants with sufficient tone counts across conditions were analyzed.

Relative to random stimulation, tones presented during the HR-LF upstate, HR-HF downstate, or the combined HR-LF+HR-HF condition increased SO amplitude by 11.2 μV ($p < 0.001$),

10.1 μV ($p < 0.001$), and 21.8 μV ($p < 0.001$), respectively. SWA was likewise enhanced by 4% ($p < 0.01$), 7% ($p < 0.001$), and 12% ($p < 0.001$). Pairwise comparisons showed significant differences between HR-LF and the combined condition (SO $p < 0.001$; SWA $p < 0.01$) and between HR-HF and the combined condition (SO $p < 0.01$; SWA $p < 0.05$), whereas no significant differences were observed between HR-LF and HR-HF phase-locking alone (SO n.s.; SWA n.s.).

Table 3.2 SO amplitude and SWA for stimulated and unstimulated conditions across different phase-locking strategies

Condition	EEG SO	HR-LF	HR-HF	Stimulated Metrics		Unstimulated Metrics	
				SO Amp.	SWA[1]	SO Amp.	SWA
Open-loop	✗	✗	✗	170.80	123.22	12.06	100.00
HR Phase-locking 1	✗	✓[2]	✗	180.47	127.82	24.84	103.86
HR Phase-locking 2	✗	✗	✓	177.87	124.61	24.78	99.59
HR Phase-locking 3	✗	✓	✓	187.58	129.24	35.46	103.07
SO Phase-locking 1	✓	✗	✗	208.63	124.12	80.256	99.42
SO Phase-locking 2	✓	✓	✗	218.59	128.60	87.77	103.50
SO Phase-locking 3	✓	✗	✓	215.72	124.97	88.38	98.17
SO Phase-locking 4	✓	✓	✓	226.20	129.15	98.55	101.92

[1] Expressed as % of average SWA in unstimulated windows without phase-locking.

[2] Tick mark indicates stimulation phase-locked to optimal state of the oscillation.

3.4.4 EEG–HR phase-locking enhances SO and SWA beyond EEG alone

The multidimensional phase analysis was further extended to EEG–HR combinations by comparing stimulation effects when tones were phase-locked to the SO upstate alone versus when combined with the HR-LF upstate and/or HR-HF downstate (Fig. 3.6). Relative to random stimulation, phase-locking to SO upstate alone increased SO amplitude by 17.8 μV ($p < 0.001$) and SWA by 19% ($p < 0.001$). When combined with HR-LF upstate, responses increased further to 27.3 μV for SO amplitude ($p < 0.001$) and 23% for SWA ($p < 0.001$). While, combination with HR-HF downstate yielded increases of 25.7 μV for SO ($p < 0.001$) and 28% for SWA ($p < 0.001$). The strongest increase in SO amplitude and SWA occurred when tones were delivered

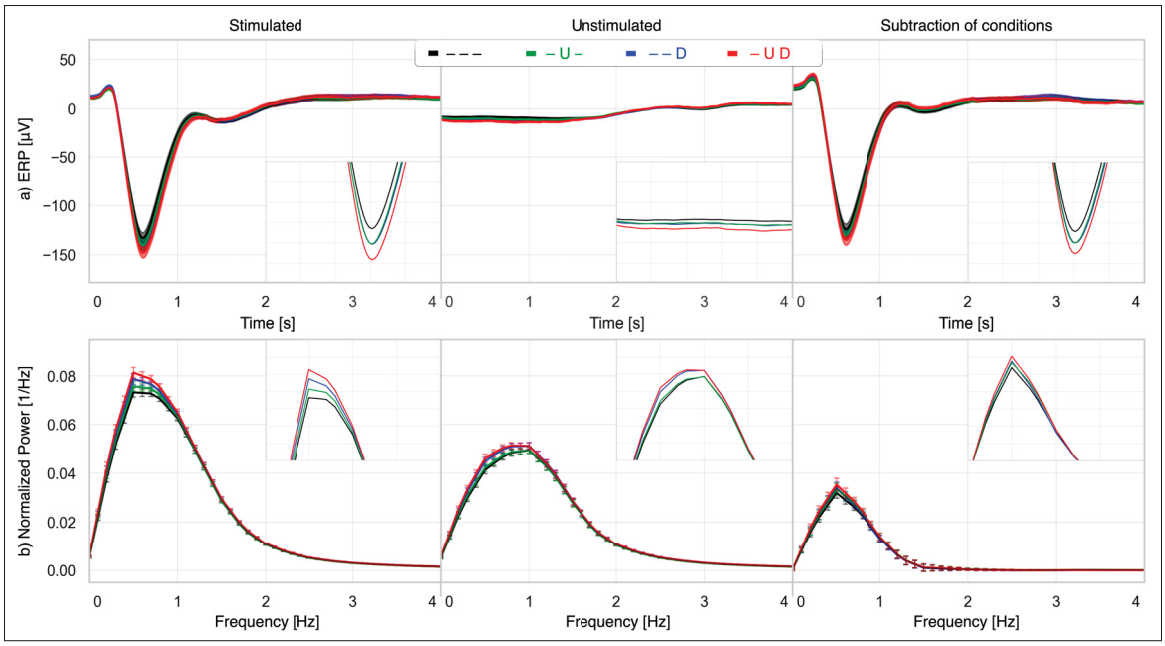

Figure 3.5 Average EEG and PSD for HR component phase-locking and their combinations. Columns show stimulated, unstimulated, and difference. (a) EEG time-locked to tones. (b) PSD up to 4 Hz. Legend: "–" = no phase-locking, "U" = upstate, "D" = downstate; e.g., "—D" means no phase-locking to EEG SO or HR-LF, with tones phase-locked to the HR-HF downstate

at SO upstate, HR-LF upstate, and HR-HF downstate simultaneously, resulting in a 38.1 μV increase in SO amplitude ($p < 0.001$) and a 32% increase in SWA ($p < 0.001$).

Comparisons across combined conditions showed no significant differences between SO + HR-LF or SO + HR-HF relative to SO alone (SO n.s.; SWA n.s.). However, the full triple-locking condition produced significantly greater SO/SWA enhancement than SO combined with either HR component alone. Specifically, SO+HR-LF versus SO+HR-LF+HR-HF differed significantly ($p < 0.001$ for SO; $p < 0.05$ for SWA), and SO+HR-HF versus SO+HR-LF+HR-HF also differed ($p < 0.001$ for SO; SWA n.s.).

3.5 Discussion

This study demonstrates that peripheral oscillatory phases, particularly HR-LF and HR-HF dynamics, carry timing information that may be useful for optimizing closed-loop auditory

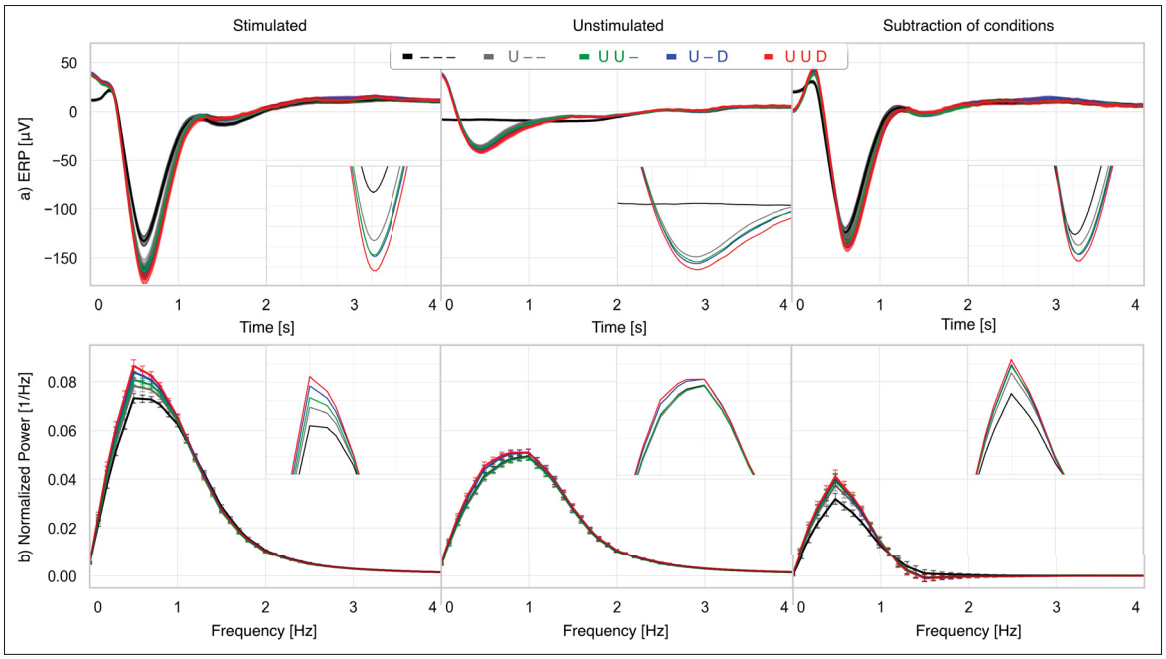

Figure 3.6 Average EEG and PSD for EEG SO phase-locking and multidimensional EEG–HR component combinations. Columns show stimulated, unstimulated, and difference. (a) EEG time-locked to tones. (b) PSD up to 4 Hz. Legend: "–" = no phase-locking, "U" = upstate, "D" = downstate; e.g., "U–D" means phase-locking to the SO upstate and HR-HF downstate, with no phase-locking to HR-LF

stimulation. By evaluating the full phase continuum and comparing unimodal and combined EEG–HR strategies, we found that tones that occurred near specific HR phases were associated with larger enhancements in SO amplitude and SWA, and that the strongest effects emerged when SO up-states coincided with these autonomic optima. These findings extend prior CLAS work, which has predominantly relied on EEG-only cues, by highlighting a potential role for brain–heart coupling in shaping the timing-related effectiveness of stimulation.

Consistent with prior research, our results show that the timing of auditory stimulation critically determines the extent of SO and SWA enhancement (Papalambros *et al.*, 2017; Fattinger *et al.*, 2017b). While SO-based phase-locking is well established, our study introduces novelty by identifying precise HR-HF and HR-LF phases that also modulate SO amplitude and SWA. These findings indicate that auditory stimulation systems can leverage HR component phases either

independently or in combination with EEG SO, providing a multidimensional approach to phase-locked stimulation.

We observed that SO amplitude increased when tones were delivered during the rising phase of SOs, particularly near the up-peak, consistent with (Navarrete *et al.*, 2020). Spindle likelihood and SWA also increased at nearly the same phases, indicating that this SO timing represents a general optimal target. Beyond EEG SOs, phase-locking tones to the up-peak of HR-LF and the down-peak of HR-HF also enhanced responses. These findings extend earlier work by pinpointing narrower windows of optimal stimulation compared to broader upstate/downstate segmentation.

Similar to earlier studies (Navarrete *et al.*, 2020), the effective windows were narrower (by 75° at peak) for large SOs (>290 μV) compared to smaller SOs (>140 μV) when phase-locking was based on EEG SOs. In our study, this was also accompanied by a reduced amplitude of post-stimulus increases for large SOs. Moreover, we observed that large SOs could not be enhanced using peripheral rhythms. This pattern suggests that once SOs reach higher amplitudes, their dynamics approach a physiological ceiling, limiting the extent to which external stimulation—whether timed using cortical or autonomic rhythms—can further modulate them. Consequently, effective enhancement of large SOs may require exceptionally precise timing, and autonomic rhythms alone may not provide sufficient modulatory influence.

Spindle likelihood showed clear phase dependence with EEG SOs but not with HR components. Because memory consolidation depends in part on SO–spindle coupling (Staresina *et al.*, 2015), the lack of spindle enhancement suggests that HR-based timing may be less predictive of memory outcomes. However, SO amplitude alone has been shown to predict next-day memory improvements (Heib *et al.*, 2013). Thus, experiments implementing HR-based timing of SO stimulation with pre- and post-sleep memory testing are needed to evaluate memory benefits explicitly and to determine how they compare with EEG-based timing.

Importantly, the results demonstrate that SO amplitude and SWA enhancement can be achieved through HR component phase-locking, either independently or in combination with EEG SO.

Effects scaled systematically: modest increases with HR-LF or HR-HF alone ($\leq$ 11.2 μV in SO amplitude; $\leq$ 7% in SWA), moderate with both HR components combined (21.8 μV; 12%), stronger when pairing one HR component with EEG SO ($\leq$ 25.7μV; $\leq$ 28%), and maximal when integrating both HR components with EEG SO ($\leq$ 38.1μV; 32%). These findings highlight the potential of HR-guided closed-loop stimulation strategies for wearable systems where EEG recordings are challenging but ECG is readily available. They also demonstrate the value of hybrid strategies, which yield maximal enhancement when both EEG and ECG can be acquired.

Theoretically, our findings show that cardiac oscillations influence sleep dynamics alongside cortical activity (de Zambotti *et al.*, 2018). This supports the view that the autonomic system actively participates in processing external inputs (Stankovski, Pereira, McClintock & Stefanovska, 2017a), which aligns with network-based models in which brain and body oscillations interact as components of a dynamic system (Bartsch *et al.*, 2015). From this perspective, auditory stimulation not only modifies local brain rhythms but also transiently reorganizes large-scale cortico–autonomic coupling (Grimaldi *et al.*, 2019).

Prior work has shown interactions between cardiac activity and sigma oscillations—for example, increases in sigma power following autonomic events and transient autonomic changes accompanying spindle occurrences (Mikutta *et al.*, 2022). However, these findings describe event-related co-modulation rather than a stable, cycle-by-cycle alignment between spindles and the ongoing phase of HR-LF or HR-HF rhythms, and thus do not imply that timing stimulation to HR-component phases should enhance SO-coupled spindle expression. Consistent with this distinction, we did not observe modulation of SO-coupled spindle likelihood across HR-LF or HR-HF phases. Nonetheless, other ECG-derived features may contain more precise autonomic signatures associated with spindle generation and could provide more effective timing cues for closed-loop stimulation. Therefore, future work should explore alternative ECG-based indicators—beyond the phase of HR-LF and HR-HF—to identify the most effective peripheral timing cues for modulating SO-coupled spindle activity.

A limitation of the present approach is the absence of a separate control night. Although tone-free segments within each night (UNSTIM windows) provided closely matched comparison periods, this approach cannot fully exclude the possibility of longer-lasting effects of acoustic stimulation. In addition, UNSTIM windows were not explicitly balanced across sleep cycles. Future studies incorporating dedicated sham-control nights and ensuring cycle-matched sampling of STIM and UNSTIM events will be important for isolating stimulation effects and refining phase-specific comparisons.

An important limitation of this study relates to the distribution of tones across conditions. Random delivery of tones every 15–30 seconds created uneven distributions across bins. This imbalance was worsened by the lower SO induction rates in non-optimal phases, which reduces available events for comparison. Future studies should adopt shorter or structured intervals, ideally combined with control nights, so that no tone-free interval is needed and more balanced tone distributions can be achieved.

Stimulus characteristics also play a critical role. In this study, we used a dataset that employed brief auditory tones (50 ms, 1000 Hz) at 80 dB, following a standard ERP-style parameters described by Colorin et al. (Colrain *et al.*, 2009). In contrast, many CLAS studies employ brief ($\approx$50 ms), low-intensity (40–60 dB) pink noise bursts, which may more effectively increase SOs while minimizing arousal. Comparative studies are needed to test how different stimulus parameters influence both cortical and autonomic outcomes.

Additionally, although SO amplitude, SWA, and spindle likelihood are strongly linked to memory consolidation, direct cognitive testing is necessary to confirm functional benefits. This is particularly relevant because HR component phase-locking increased SO amplitude and SWA but did not enhance spindle likelihood. Future studies should therefore incorporate declarative and procedural memory tasks as well as measures of attention and executive function to determine whether the observed physiological changes translate into cognitive gains.

Multidimensional phase-locking raises another challenge. While combining HR and EEG SO phases produced stronger enhancements, it also reduced the number of tones per condition. This

raises the question of whether stimulation is more effective when delivering more frequent but weaker effects, or when delivering fewer tones with stronger effects. A practical solution is to develop predictive algorithms that adaptively select the best available phase-locking option in real time, ensuring tone counts remain high while exploiting multidimensional phase information. In addition, including nights without tone application would help identify how often such optimal opportunities occur naturally and how they differ from stimulated nights.

For future work, it will be essential to deliver stimulation at specific EEG and HR phases rather than relying on post-hoc analyses. Prospective phase-targeting would not only allow causal testing of the effects observed here, but also provide an opportunity to evaluate the practical challenges and yield of targeting these oscillations in real time. Although methods for predicting ECG R-peaks exist, algorithms capable of accurately predicting HR-derived phases remain limited, and the feasibility of real-time LF- and HF-phase estimation has yet to be demonstrated. Because HF-HR oscillations typically have cycle durations of approximately 2–7 seconds and LF-HR oscillations evolve even more slowly (around 7–25 seconds per cycle), these autonomic rhythms may be easier to target once an instantaneous phase is identified. However, systematic testing will be required to determine how reliably these phases can be predicted and applied in closed-loop stimulation.

Beyond these limitations, these results suggest that integrating peripheral signals into closed-loop algorithms offers a promising direction. Wearable devices that combine EEG with HR components could use the optimal phases to enhance SO and SWA through cumulative effects. Such multimodal strategies may reduce inter-individual variability and facilitate the translation of stimulation protocols into practical sleep-enhancement technologies.

3.6 Conclusions

Auditory stimulation was associated with increases in SO amplitude and SWA, and these effects varied systematically with oscillatory phase. The largest responses occurred when tones happened to fall near the SO up-peak, the HR-LF up-peak, and the HR-HF down-peak.

Multidimensional phase analyses further showed that cardiac timing carried informative structure, with the strongest enhancements observed when EEG and HR phase optima coincided. These results highlight coordinated CNS–ANS dynamics in sleep neurostimulation and suggest that future closed-loop systems may benefit from multidimensional phase-targeting to optimize sleep physiology and support wearable applications for enhancing memory and resilience.

CONCLUSION AND RECOMMENDATIONS

The Introduction and Background chapters of this thesis highlighted the importance of deep sleep and the benefits of its enhancement. They emphasized the need to understand brain–heart interactions during sleep, particularly in relation to non-invasive neuromodulation methods such as acoustic stimulation. The Background chapter also provided an overview of fundamental aspects of human physiology and sleep mechanisms, reviewed common approaches for enhancing SWS, and summarized key literature. It also described the analytical tools used throughout the thesis to support the presented contributions.

Contribution 1: Demonstrating that the effects of acoustic stimulation depend on the phases of HR components

In Chapter 2, we established that the efficacy of acoustic stimulation in enhancing SOs is phase-dependent, not only on cortical SOs (~0.8 Hz) but also on peripheral oscillations, specifically HR low-frequency and high-frequency rhythms. This contribution extends existing closed-loop stimulation approaches by demonstrating that phase-locking to HR-LF upstates and HR-HF downstates produces greater increases in SO amplitude and SWA than stimulation delivered at other phases. These findings suggest that the interaction between brain and heart rhythms may provide a more reliable window for intervention than considering the cortex alone. They also open the possibility of using ECG-based signals in wearable closed-loop systems that aim to enhance deep sleep outside the laboratory.

Contribution 2: Cortico–cardiac phase alignment maximizes the effect of acoustic stimulation

In Chapter 3, we demonstrated that SO enhancement and SWA increase are maximized when acoustic stimulation is delivered at the optimal alignment of both cortical and cardiac phases. This finding highlights the importance of considering both central and autonomic systems

together when designing sleep neuromodulation strategies. The results provide strong evidence that brain–heart coupling plays a critical role in determining how the sleeping brain responds to external stimulation. This joint optimization framework can serve as a template for future closed-loop algorithms that integrate multiple physiological signals to maximize intervention outcomes.

Contribution 3: Identifying more precise timing for auditory stimulation

Also in Chapter 3, we showed that stimulation timing can be defined with greater precision. It is not only a matter of targeting the general upstate or downstate, but of aligning stimulation more closely with the peaks of these oscillations. This continuous phase analysis enables more accurate targeting, which may be particularly relevant for populations requiring precise timing for enhancement, such as older adults or neurodivergent individuals. The methodology underscores the importance of moving beyond binary phase categories and instead modeling the full temporal dynamics of oscillatory activity. With more precise temporal alignment, future interventions may achieve stronger and more consistent effects on sleep quality and recovery.

Limitations and Future work

In this section, we summarize the main limitations of the present study and outline directions for future research that could address these issues and extend the current findings.

1. This study examined only EEG and ECG measures, such as slow oscillation amplitude, SWA, and HR, to identify optimal phase-locking timing and strategies. While these markers reflect sleep depth and physiological engagement, further research should determine whether stimulation translates into functional outcomes, such as improvements in memory or cognition. Including simple behavioral tasks (e.g., paired-associate word learning) would help establish the link between physiological enhancement and real-world benefits.

2. We used 1000 Hz, 80 dB, 50 ms tones. Although these tones were effective, many prior studies have used pink noise bursts that may engage broader cortical networks and produce different responses. Systematically comparing stimulus types (e.g., pure tones, pink noise) could reveal which type of tones most effectively enhance sleep quality, oscillatory activity, and memory consolidation.
3. The data were collected from adolescents in a controlled laboratory setting, which limits the generalizability of the findings. Other populations—such as older adults, who show reduced SWA, or clinical groups with sleep or cardiac dysfunction—may respond differently. Moreover, responses in home or ambulatory environments may vary due to noise, comfort, and adherence factors. Extending this research across age groups, health conditions, and real-world contexts would clarify the robustness and scalability of the proposed approach.
4. The random inter-stimulus interval of 15–30 seconds resulted in an unequal number of tones across phases, reducing statistical power for certain comparisons. This imbalance may bias phase-specific results or obscure smaller effects. Future studies could adopt balanced phase-targeting protocols and adaptive timing algorithms to improve reliability.
5. For future work, machine learning and deep learning methods could be leveraged to predict stimulation outcomes and identify more precise timing locations. For example, EEG and ECG segments preceding tone delivery could serve as inputs, while changes in SWA or SO amplitude following stimulation could serve as prediction targets. Sequential deep learning architectures (such as LSTMs or transformer-based models) are promising candidates, as they can learn temporal dependencies within physiological signals. Preliminary attempts using simpler deep learning models with raw input data (e.g., multilayer perceptrons and convolutional neural networks), as well as regression-based machine learning approaches (e.g., linear and polynomial regression, random forest regression, and support vector regression) incorporating features such as instantaneous SO phase, cardiac phase at the time of stimulation, and subject characteristics (e.g., age, sex), did not yield satisfactory results

(MAPE > 58% for SWA). However, continued exploration of such approaches could enable more precise and subject-specific timing for closed-loop auditory stimulation systems.

APPENDIX I

SUPPLEMENTARY FIGURES FOR CHAPTER 2

1. Presentation

This appendix presents supplementary figures associated with Chapter 2, based on the article "Tone-evoked sleep electroencephalographic slow oscillations as a function of peripheral rhythms: new insights into the brain–heart integration" by Forouzanfar, Sardooeinasab, Baker, Colrain, and de Zambotti, published in the Journal of Sleep Research in October 2025. The supplementary figures provide additional analyses and visualizations that support and extend the results presented in the main chapter.

2. Figures

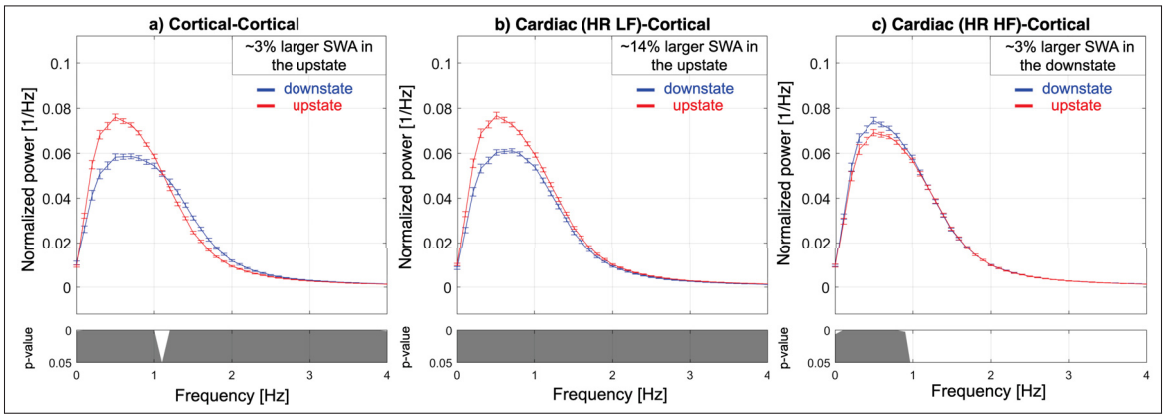

Figure-A I-1 Normalized EEG power (0–4 Hz) during tone presentation in the downstate (blue) and upstate (red) phases of: (a) EEG slow oscillations (SO), (b) heart rate (HR) low-frequency (LF) oscillations, and (c) HR high-frequency (HF) oscillations

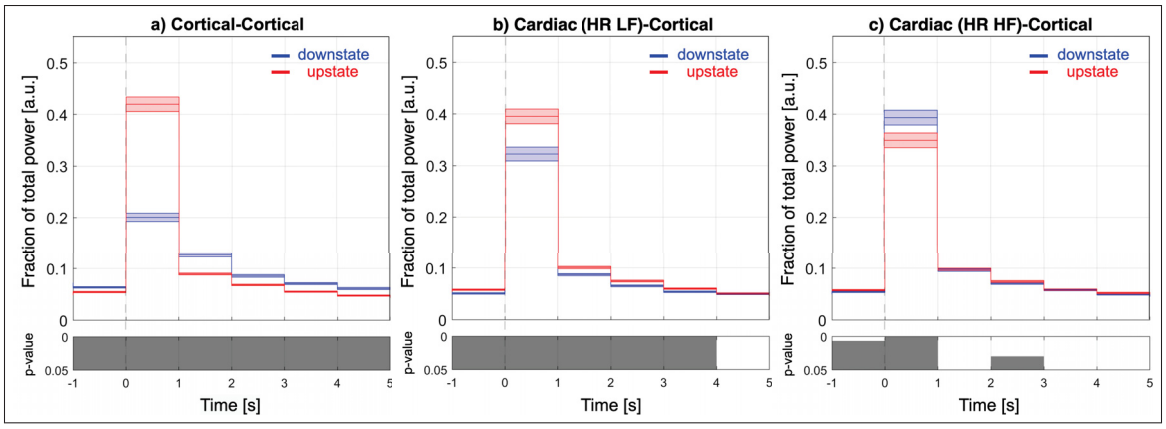

Figure-A I-2 Normalized slow-wave activity (SWA) per second before and after tone presentation, when tones occurred during the downstate (blue) and upstate (red) phases of: (a) EEG slow oscillations (SO), (b) HR low-frequency (LF) oscillations, and (c) HR high-frequency (HF) oscillations

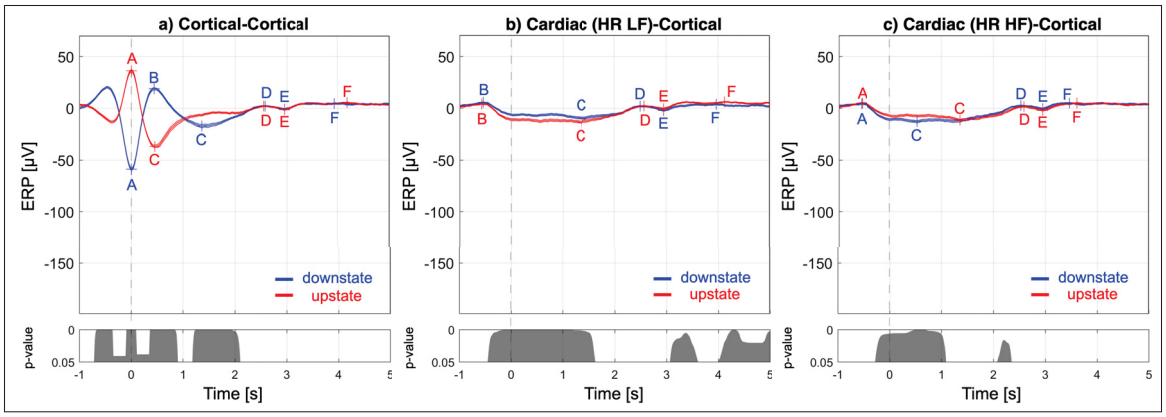

Figure-A I-3 Average EEG activity (without tone application) time-locked to random points in the downstate (blue) and upstate (red) phases of: (a) EEG slow oscillations (SO), (b) HR low-frequency (LF) oscillations, and (c) HR high-frequency (HF) oscillations. Letters A–F indicate key characteristic points. Shaded areas represent standard error of the mean, and p-values are shown for comparisons

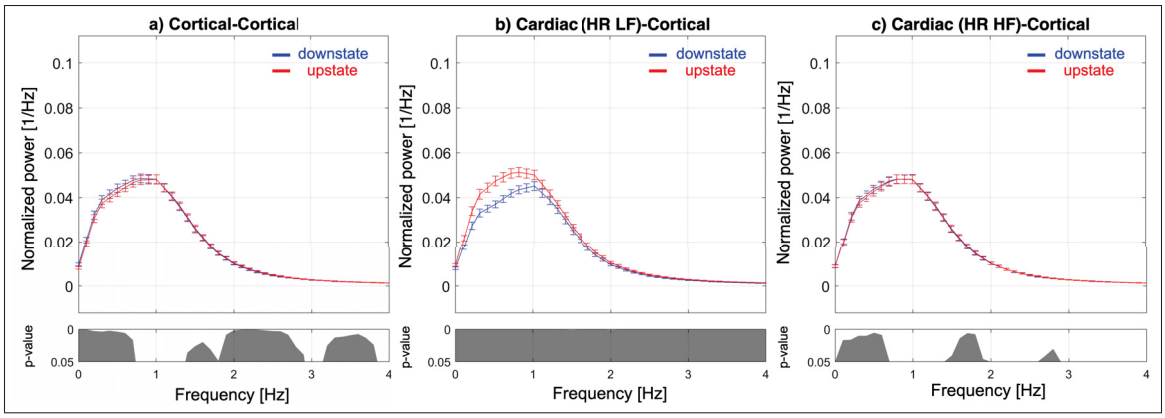

Figure-A I-4 Normalized EEG power (0–4 Hz) during no-tone periods, aligned to downstate (blue) and upstate (red) phases of: (a) EEG slow oscillations (SO), (b) heart rate (HR) low-frequency (LF) oscillations, and (c) HR high-frequency (HF) oscillations

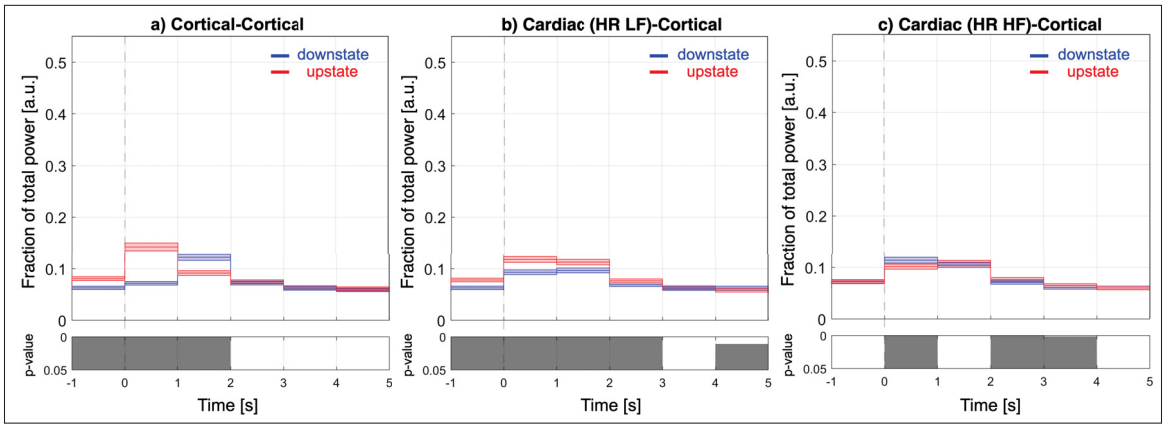

Figure-A I-5 Normalized slow-wave activity (SWA) (per second, no tones) time-locked to random points in the downstate (blue) and upstate (red) phases of: (a) EEG slow oscillations (SO), (b) heart rate (HR) low-frequency (LF) oscillations, and (c) HR high-frequency (HF) oscillations

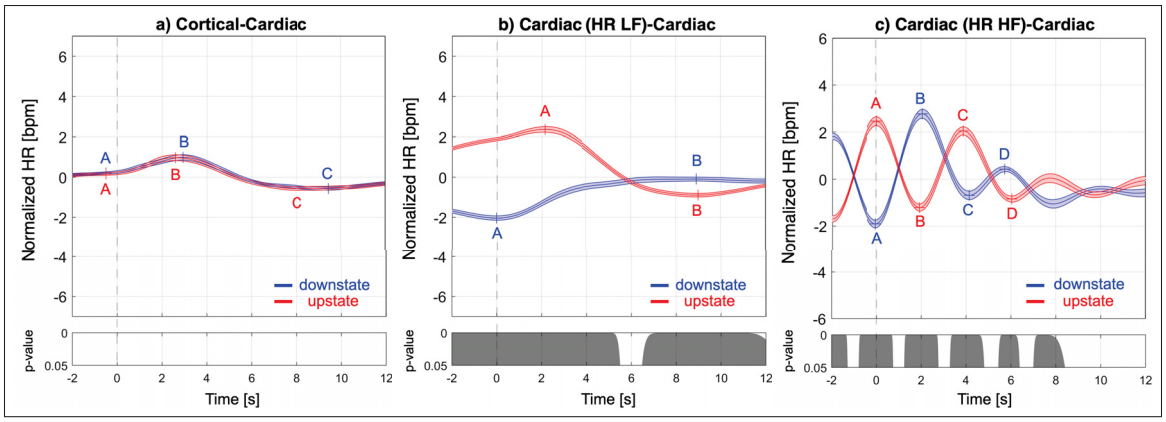

Figure-A I-6 Average normalized heart rate (HR) (no tone applied) time-locked to random points in the downstate (blue) and upstate (red) phases of: (a) EEG slow oscillations (SO), (b) heart rate (HR) low-frequency (LF) oscillations, and (c) HR high-frequency (HF) oscillations. Letters A–D indicate key characteristic points. Shaded areas represent standard error of the mean, and p-values are shown for comparisons

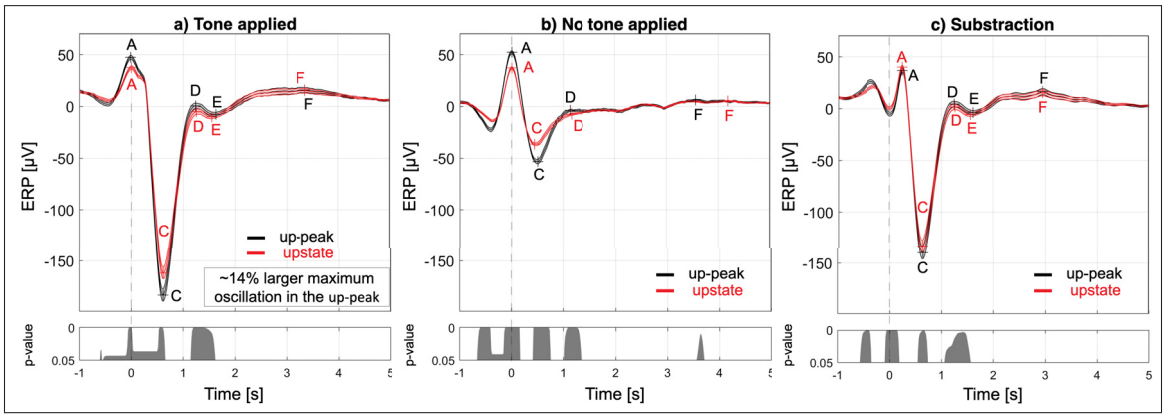

Figure-A I-7 Average EEG activity during (a) tone application and (b) no tone application, time-locked to the up-peak (black) and upstate (red) phases of EEG slow oscillations (SO), and (c) the subtraction of these two conditions. Letters A–F indicate key characteristic points. Shaded areas represent standard error of the mean, percentage increase in induced oscillation amplitude, and p-values for comparisons are shown

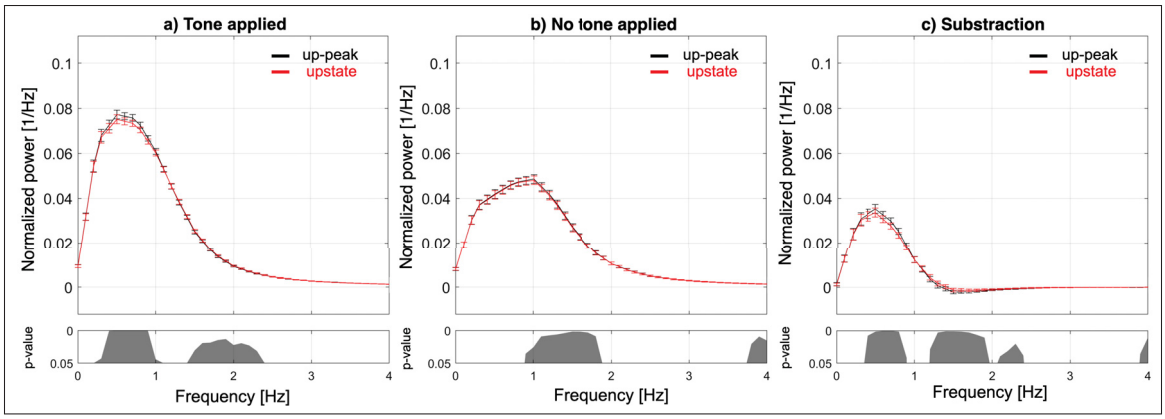

Figure-A I-8 Normalized EEG power during (a) tone application and (b) no tone application, aligned to the up-peak (black) and upstate (red) phases of EEG slow oscillations (SO), and (c) the subtraction of these two conditions

BIBLIOGRAPHY

Alhanoun, E., Rosenberg, C. & Strohl, K. (2014). Atlas of Clinical Sleep Medicine, second edition, by Meir H. Kryger, Alon Y. Avidan, and Richard B. Berry, 511 pages, ISBN: 978-0-323-18727-5; Elsevier, Saunders. *Sleep and Breathing*, 19, 749-750. doi: 10.1007/s11325-014-1064-z.

Antony, J. W., Schonauer, M., Staresina, B. P. & Cairney, S. A. (2019). Sleep Spindles and Memory Reprocessing. *Trends Neurosci*, 42(1), 1-3. doi: 10.1016/j.tins.2018.09.012.

Baharav, A., Kotagal, S., Gibbons, V., Rubin, B. K., Pratt, G., Karin, J. & Akselrod, S. (1995). Fluctuations in autonomic nervous activity during sleep displayed by power spectrum analysis of heart rate variability. *Neurology*, 45(6), 1183-1187. doi: doi:10.1212/WNL.45.6.1183.

Baker, F. C., Willoughby, A. R., Massimiliano, d. Z., Franzen, P. L., Prouty, D., Javitz, H., Hasler, B., Clark, D. B. & Colrain, I. M. (2016). Age-related differences in sleep architecture and electroencephalogram in adolescents in the national consortium on alcohol and neurodevelopment in adolescence sample. *Sleep*, 39(7), 1429-1439.

Bartsch, R. P., Liu, K. K. L., Bashan, A. & Ivanov, P. C. (2015). Network Physiology: How Organ Systems Dynamically Interact. *PLOS ONE*, 10(11), 1-36. doi: 10.1371/journal.pone.0142143.

Bellesi, M., Riedner, B. A., Garcia-Molina, G. N., Cirelli, C. & Tononi, G. (2014). Enhancement of sleep slow waves: underlying mechanisms and practical consequences. *Frontiers in systems neuroscience*, 8, 208.

Benedict, C., Scheller, J., Rose-John, S., Born, J. & Marshall, L. (2009). Enhancing influence of intranasal interleukin-6 on slowwave activity and memory consolidation during sleep. *The FASEB Journal*, 23(10), 3629–3636.

Besedovsky, L., Ngo, H.-V. V., Dimitrov, S., Gassenmaier, C., Lehmann, R. & Born, J. (2017a). Auditory closed-loop stimulation of EEG slow oscillations strengthens sleep and signs of its immune-supportive function. *Nature Communications*, 8.

Besedovsky, L., Ngo, H.-V. V., Dimitrov, S., Gassenmaier, C., Lehmann, R. & Born, J. (2017b). Auditory closed-loop stimulation of EEG slow oscillations strengthens sleep and signs of its immune-supportive function. *Nature Communications*, 8(1), 1984. doi: 10.1038/s41467-017-02170-3.

Brown, S. A., Brumback, T., Tomlinson, K., Cummins, K., Thompson, W. K., Nagel, B. J., De Bellis, M. D., Hooper, S. R., Clark, D. B., Chung, T. et al. (2015). The National Consortium on Alcohol and NeuroDevelopment in Adolescence (NCANDA): a multisite study of adolescent development and substance use. *Journal of studies on alcohol and drugs*, 76(6), 895–908.

Carskadon, M. A., Dement, W. C. et al. (2005). Normal human sleep: an overview. *Principles and practice of sleep medicine*, 4(1), 13–23.

Cellini, N. & Mednick, S. C. (2019). Stimulating the sleeping brain: Current approaches to modulating memory-related sleep physiology. *J Neurosci Methods*, 316, 125-136. doi: 10.1016/j.jneumeth.2018.11.011.

Chenane, K., Touati, Y., Boubchir, L. & Daachi, B. (2019). Neural net-based approach to EEG signal acquisition and classification in BCI applications. *Computers*, 8(4), 87.

Clemens, Z., Mölle, M., Erőss, L., Barsi, P., Halász, P. & Born, J. (2007). Temporal coupling of parahippocampal ripples, sleep spindles and slow oscillations in humans. *Brain*, 130(11), 2868–2878.

Colrain, I. M. (2011). Sleep and the Brain. *Neuropsychology Review*, 21(1), 1-4. doi: 10.1007/s11065-011-9156-z.

Colrain, I. M., Crowley, K. E., Nicholas, C. L., Padilla, M. & Baker, F. C. (2009). The Impact of Alcoholism on Sleep Evoked Delta Frequency Responses. *Biological Psychiatry*, 66(2), 177-184. doi: 10.1016/j.biopsych.2008.10.010. doi: 10.1016/j.biopsych.2008.10.010.

Critchley, H. D. & Harrison, N. A. (2013). Visceral Influences on Brain and Behavior. *Neuron*, 77(4), 624-638. doi: 10.1016/j.neuron.2013.02.008.

De Gennaro, L., Fratello, F., Marzano, C., Moroni, F., Curcio, G., Tempesta, D., Pellicciari, M. C., Pirulli, C., Ferrara, M. & Rossini, P. M. (2008). Cortical plasticity induced by transcranial magnetic stimulation during wakefulness affects electroencephalogram activity during sleep. *PloS one*, 3(6), e2483.

de Zambotti, M., Willoughby, A., Franzen, P., Clark, D., Baker, F. & Colrain, I. (2016). K-Complexes: Interaction between the Central and Autonomic Nervous Systems during Sleep. *Sleep*, 39(5), 1129-1137.

de Zambotti, M., Trinder, J., Silvani, A., Colrain, I. M. & Baker, F. C. (2018). Dynamic coupling between the central and autonomic nervous systems during sleep: A review. *Neuroscience & Biobehavioral Reviews*, 90, 84-103. doi: https://doi.org/10.1016/j.neubiorev.2018.03.027.

de Zambotti, M., Goldstone, A., Forouzanfar, M., Javitz, H., Claudatos, S., Colrain, I. M. & Baker, F. C. (2019). The falling asleep process in adolescents. *Sleep*. doi: 10.1093/sleep/zsz312.

de Zambotti, M., Goldstone, A., Forouzanfar, M., Javitz, H., Claudatos, S., Colrain, I. M. & Baker, F. C. (2020). The falling asleep process in adolescents. *Sleep*, 43(6), zsz312.

Diep, C., Ftouni, S., Manousakis, J. E., Nicholas, C. L., Drummond, S. P. A. & Anderson, C. (2019). Acoustic slow wave sleep enhancement via a novel, automated device improves executive function in middle-aged men. *Sleep*, 43(1). doi: 10.1093/sleep/zsz197.

Diep, C., Garcia-Molina, G., Jasko, J., Manousakis, J., Ostrowski, L., White, D. & Anderson, C. (2021). Acoustic enhancement of slow wave sleep on consecutive nights improves alertness and attention in chronically short sleepers. *Sleep Medicine*, 81, 69-79.

Diep, C., Ftouni, S., Drummond, S. P., Garcia-Molina, G. & Anderson, C. (2022). Heart rate variability increases following automated acoustic slow wave sleep enhancement. *Journal of Sleep Research*, e13545.

Esfahani, M. J., Farboud, S., Ngo, H.-V. V., Schneider, J., Weber, F. D., Talamini, L. M. & Dresler, M. (2023). Closed-loop auditory stimulation of sleep slow oscillations: Basic principles and best practices. *Neuroscience & Biobehavioral Reviews*, 153, 105379.

Esser, S. K., Hill, S. L. & Tononi, G. (2007). Sleep Homeostasis and Cortical Synchronization: I. Modeling the Effects of Synaptic Strength on Sleep Slow Waves. *Sleep*, 30(12), 1617-1630. doi: 10.1093/sleep/30.12.1617.

Fattinger, S., de Beukelaar, T. T., Ruddy, K. L., Volk, C., Heyse, N. C., Herbst, J. A., Hahnloser, R. H. R., Wenderoth, N. & Huber, R. (2017a). Deep sleep maintains learning efficiency of the human brain. *Nature Communications*, 8(1), 15405. doi: 10.1038/ncomms15405.

Fattinger, S., de Beukelaar, T. T., Ruddy, K. L., Volk, C., Heyse, N. C., Herbst, J. A., Hahnloser, R. H., Wenderoth, N. & Huber, R. (2017b). Deep sleep maintains learning efficiency of the human brain. *Nature communications*, 8(1), 15405.

Flores, J. (2025). Basic Principles in Neuroanatomy. Retrieved from: https://pressbooks.online.ucf.edu/neuroplasticityofhumanmovements/chapter/chapter-1-basic-principles-in-neuroanatomy/.

Forouzanfar, M., Baker, F., Colrain, I. & de Zambotti, M. (2019, 07). Electroencephalographic Slow-Wave Activity During Sleep in Different Phases of Blood Pressure and Respiration Oscillations. 2019, 2564-2567. doi: 10.1109/EMBC.2019.8857490.

Forouzanfar, M., Sardooeinasab, S., Baker, F. C., Colrain, I. M. & de Zambotti, M. (2025). Tone-Evoked Sleep Electroencephalographic Slow Oscillations as a Function of Peripheral Rhythms: New Insights Into the Brain–Heart Integration. *Journal of Sleep Research*, n/a(n/a), e70212. doi: https://doi.org/10.1111/jsr.70212. e70212 JOSR-23-171.R2.

Grandner, M. A. *(2018)*. The cost of sleep lost: Implications for health, performance, and the bottom line. Sage Publications Sage CA: Los Angeles, CA.

Grimaldi, D., Papalambros, N. A., Reid, K. J., Abbott, S. M., Malkani, R. G., Gendy, M., Iwanaszko, M., Braun, R. I., Sanchez, D. J., Paller, K. A. et al. (2019). Strengthening sleep-autonomic interaction via acoustic enhancement of slow oscillations. *Sleep*, 42(5), zsz036.

Grimaldi, D., Papalambros, N. A., Zee, P. C. & Malkani, R. G. (2020). Neurostimulation techniques to enhance sleep and improve cognition in aging. *Neurobiology of Disease*, 141, 104865. doi: https://doi.org/10.1016/j.nbd.2020.104865.

Hall, J. E. & Hall, M. E. (2020). *Guyton and Hall Textbook of Medical Physiology E-Book: Guyton and Hall Textbook of Medical Physiology E-Book*. Elsevier Health Sciences.

Heib, D. P. J., Hoedlmoser, K., Anderer, P., Zeitlhofer, J., Gruber, G., Klimesch, W. & Schabus, M. (2013). Slow Oscillation Amplitudes and Up-State Lengths Relate to Memory Improvement. *PLOS ONE*, 8(12), null. doi: 10.1371/journal.pone.0082049.

Helfrich, R. F., Mander, B. A., Jagust, W. J., Knight, R. T. & Walker, M. P. (2018). Old Brains Come Uncoupled in Sleep: Slow Wave-Spindle Synchrony, Brain Atrophy, and Forgetting. *Neuron*, 97(1), 221-230 e4. doi: 10.1016/j.neuron.2017.11.020.

Henao, D., Navarrete, M., Juez, J. Y., Dinh, H., Gómez, R., Valderrama, M. & Le Van Quyen, M. (2022). Auditory closed-loop stimulation on sleep slow oscillations using in-ear EEG sensors. *Journal of Sleep Research*, 31(6), e13555.

Huwiler, S., Carro Dominguez, M., Huwyler, S., Kiener, L., Stich, F. M., Sala, R., Aziri, F., Trippel, A., Schmied, C., Huber, R., Wenderoth, N. & Lustenberger, C. (2022). Effects of auditory sleep modulation approaches on brain oscillatory and cardiovascular dynamics. *Sleep*, 45(9). doi: 10.1093/sleep/zsac155.

Huwiler, S., Carro-Domínguez, M., Stich, F. M., Sala, R., Aziri, F., Trippel, A., Ryf, T., Markendorf, S., Niederseer, D., Bohm, P., Stoll, G., Laubscher, L., Thevan, J., Spengler, C. M., Gawinecka, J., Osto, E., Huber, R., Wenderoth, N., Schmied, C. & Lustenberger, C. (2023). Auditory stimulation of sleep slow waves enhances left ventricular function in humans. *European Heart Journal*, 44(40), 4288-4291. doi: 10.1093/eurheartj/ehad630.

Huwiler, S., Ferster, M. L., Brogli, L., Huber, R., Karlen, W. & Lustenberger, C. (2025). Sleep and cardiac autonomic modulation in older adults: Insights from an at-home study with auditory deep sleep stimulation. *Journal of Sleep Research*, 34(2), e14328.

Iber, C., Ancoli-Israel, S., Chesson, A. & Quan, S. (2007). *The AASM manual for the scoring of sleep and associated events: rules, terminology, and technical specification* (ed. 1st). Westchester, IL: American Academy of Sleep Medicine.

Irwin, M. R. (2015a). Why sleep is important for health: a psychoneuroimmunology perspective. *Annu Rev Psychol*, 66, 143-72. doi: 10.1146/annurev-psych-010213-115205.

Irwin, M. R. (2015b). Why Sleep Is Important for Health: A Psychoneuroimmunology Perspective. *Annual Review of Psychology*, 66(Volume 66, 2015), 143-172. doi: https://doi.org/10.1146/annurev-psych-010213-115205.

Ivanov, P. C., Liu, K. K. L. & Bartsch, R. P. (2016). Focus on the emerging new fields of Network Physiology and Network Medicine. *New J Phys*, 18(10), 100201. doi: 10.1088/1367-2630/18/10/100201.

Ketz, N., Jones, A. P., Bryant, N. B., Clark, V. P. & Pilly, P. K. (2018). Closed-loop slow-wave tACS improves sleep-dependent long-term memory generalization by modulating endogenous oscillations. *Journal of Neuroscience*, 38(33), 7314–7326.

Khan, M. A. & Al-Jahdali, H. (2023). The consequences of sleep deprivation on cognitive performance. *Neurosciences Journal*, 28(2), 91–99.

Kräuchi, K., Fattori, E., Giordano, A., Falbo, M., Iadarola, A., Aglì, F., Tribolo, A., Mutani, R. & Cicolin, A. (2018). Sleep on a high heat capacity mattress increases conductive body heat loss and slow wave sleep. *Physiology & behavior*, 185, 23-30.

Legault, G. (2011). Sleep and heat related changes in the cognitive performance of underground miners: a possible health and safety concern. *Minerals*, 1(1), 49–72.

Leminen, M. M., Virkkala, J., Saure, E., Paajanen, T., Zee, P. C., Santostasi, G., Hublin, C., Muller, K., Porkka-Heiskanen, T., Huotilainen, M. & Paunio, T. (2017). Enhanced Memory Consolidation Via Automatic Sound Stimulation During Non-REM Sleep. *Sleep*, 40(3). doi: 10.1093/sleep/zsx003.

Light, G. A., Williams, L. E., Minow, F., Sprock, J., Rissling, A., Sharp, R., Swerdlow, N. R. & Braff, D. L. (2010). Electroencephalography (EEG) and Event-Related Potentials (ERPs) with Human Participants. *Current Protocols in Neuroscience*, 52(1), 6.25.1-6.25.24. doi: https://doi.org/10.1002/0471142301.ns0625s52.

Lima, G. S., Savi, M. A. & Bessa, W. M. (2023). Intelligent control of cardiac rhythms using artificial neural networks. *Nonlinear Dynamics*, 111(12), 11543–11557.

Lustenberger, C. (2025). Enhancing deep sleep and heart function with auditory stimulation. *Brain Stimulation: Basic, Translational, and Clinical Research in Neuromodulation*, 18(1), 233.

Määttä, S., Landsness, E., Sarasso, S., Ferrarelli, F., Ferreri, F., Ghilardi, M. F. & Tononi, G. (2010). The effects of morning training on night sleep: a behavioral and EEG study. *Brain research bulletin*, 82(1-2), 118–123.

Mander, B. A., Winer, J. R. & Walker, M. P. (2017). Sleep and Human Aging. *Neuron*, 94(1), 19-36. doi: https://doi.org/10.1016/j.neuron.2017.02.004.

Massimini, M., Huber, R., Ferrarelli, F., Hill, S. & Tononi, G. (2004). The sleep slow oscillation as a traveling wave. *Journal of Neuroscience*, 24(31), 6862-6870.

Massimini, M., Ferrarelli, F., Esser, S. K., Riedner, B. A., Huber, R., Murphy, M., Peterson, M. J. & Tononi, G. (2007). Triggering sleep slow waves by transcranial magnetic stimulation. *Proceedings of the National Academy of Sciences*, 104(20), 8496-8501.

Mikutta, C., Wenke, M., Spiegelhalder, K., Hertenstein, E., Maier, J. G., Schneider, C. L., Fehér, K., Koenig, J., Altorfer, A., Riemann, D. et al. (2022). Co-ordination of brain and heart oscillations during non-rapid eye movement sleep. *Journal of Sleep Research*, 31(2), e13466.

Monstad, P. & Guilleminault, C. (1999). Cardiovascular changes associated with spontaneous and evoked K-complexes. *Neurosci Lett*, 263(2-3), 211-3. doi: 10.1016/s0304-3940(99)00142-1.

Naji, M., Krishnan, G. P., McDevitt, E. A., Bazhenov, M. & Mednick, S. C. (2019). Coupling of autonomic and central events during sleep benefits declarative memory consolidation. *Neurobiol Learn Mem*, 157, 139-150. doi: 10.1016/j.nlm.2018.12.008.

Navarrete, M., Schneider, J., Ngo, H.-V. V., Valderrama, M., Casson, A. J. & Lewis, P. A. (2020). Examining the optimal timing for closed-loop auditory stimulation of slow-wave sleep in young and older adults. *Sleep*, 43(6), zsz315.

Ngo, H.-V. V., Martinetz, T., Born, J. & Mölle, M. (2013). Auditory closed-loop stimulation of the sleep slow oscillation enhances memory. *Neuron*, 78(3), 545–553.

Ngo, H.-V. V., Miedema, A., Faude, I., Martinetz, T., Mölle, M. & Born, J. (2015). Driving sleep slow oscillations by auditory closed-loop stimulation—a self-limiting process. *Journal of Neuroscience*, 35(17), 6630–6638.

Niizeki, K. & Saitoh, T. (2018). Association between phase coupling of respiratory sinus arrhythmia and slow wave brain activity during sleep. *Frontiers in physiology*, 9, 1338. Retrieved from: https://www.ncbi.nlm.nih.gov/pmc/articles/PMC6167474/pdf/fphys-09-01338.pdf.

Ong, J. L., Patanaik, A., Chee, N., Lee, X. K., Poh, J. H. & Chee, M. W. L. (2018a). Auditory stimulation of sleep slow oscillations modulates subsequent memory encoding through altered hippocampal function. *Sleep*, 41(5), zsy031. doi: 10.1093/sleep/zsy031.

Ong, J. L., Lo, J. C., Chee, N. I., Santostasi, G., Paller, K. A., Zee, P. C. & Chee, M. W. (2016). Effects of phase-locked acoustic stimulation during a nap on EEG spectra and declarative memory consolidation. *Sleep Medicine*, 20, 88-97. doi: https://doi.org/10.1016/j.sleep.2015.10.016.

Ong, J. L., Patanaik, A., Chee, N. I. Y. N., Lee, X. K., Poh, J.-H. & Chee, M. W. L. (2018b). Auditory stimulation of sleep slow oscillations modulates subsequent memory encoding through altered hippocampal function. *Sleep*, 41(5), zsy031. doi: 10.1093/sleep/zsy031.

Papalambros, N. A., Weintraub, S., Chen, T., Grimaldi, D., Santostasi, G., Paller, K. A., Zee, P. C. & Malkani, R. G. (2019). Acoustic enhancement of sleep slow oscillations in mild cognitive impairment. *Ann Clin Transl Neurol*, 6(7), 1191-1201. doi: 10.1002/acn3.796.

Papalambros, N. A., Santostasi, G., Malkani, R. G., Braun, R., Weintraub, S., Paller, K. A. & Zee, P. C. (2017). Acoustic enhancement of sleep slow oscillations and concomitant memory improvement in older adults. *Frontiers in human neuroscience*, 11, 247563.

Porta, A. & Faes, L. (2015). Wiener–Granger causality in network physiology with applications to cardiovascular control and neuroscience. *Proceedings of the IEEE*, 104(2), 282-309.

Prehn-Kristensen, A., Munz, M., Göder, R., Wilhelm, I., Korr, K., Vahl, W., Wiesner, C. D. & Baving, L. (2014). Transcranial oscillatory direct current stimulation during sleep improves declarative memory consolidation in children with attention-deficit/hyperactivity disorder to a level comparable to healthy controls. *Brain stimulation*, 7(6), 793–799.

Purcell, S., Manoach, D., Demanuele, C., Cade, B., Mariani, S., Cox, R., Panagiotaropoulou, G., Saxena, R., Pan, J., Smoller, J. et al. (2017). Characterizing sleep spindles in 11,630 individuals from the National Sleep Research Resource. *Nature communications*, 8(1), 15930.

Purves, D., Augustine, G., Fitzpatrick, D., Hall, W., LaMantia, A., Mooney, R. & White, L. (2018). *Neuroscience*. Sinauer. Retrieved from: https://books.google.ca/books?id=YwY7kAEACAAJ.

Rasch, B. & Born, J. (2013). About Sleep's Role in Memory. *Physiological Reviews*, 93(2), 681-766. doi: 10.1152/physrev.00032.2012.

Rundo, J. V. & Downey III, R. (2019). Polysomnography. *Handbook of clinical neurology*, 160, 381–392.

Saebipour, M. R., Joghataei, M. T., Yoonessi, A., Sadeghniiat-Haghighi, K., Khalighinejad, N. & Khademi, S. (2015). Slow oscillating transcranial direct current stimulation during sleep has a sleep-stabilizing effect in chronic insomnia: A pilot study. *Journal of sleep research*, 24(5), 518-525.

Santostasi, G., Malkani, R., Riedner, B., Bellesi, M., Tononi, G., Paller, K. A. & Zee, P. C. (2016). Phase-locked loop for precisely timed acoustic stimulation during sleep. *J Neurosci Methods*, 259, 101-114. doi: 10.1016/j.jneumeth.2015.11.007.

Schade, M. M., Mathew, G. M., Roberts, D. M., Gartenberg, D. & Buxton, O. M. (2020). Enhancing slow oscillations and increasing N3 sleep proportion with supervised, non-phase-locked pink noise and other non-standard auditory stimulation during NREM sleep. *Nature and science of sleep*, 411–429.

Schreiner, S. J., Imbach, L. L., Valko, P. O., Maric, A., Maqkaj, R., Werth, E., Baumann, C. R. & Baumann-Vogel, H. (2021a). Reduced Regional NREM Sleep Slow-Wave Activity Is Associated With Cognitive Impairment in Parkinson Disease. *Front Neurol*, 12, 618101. doi: 10.3389/fneur.2021.618101.

Schreiner, S. J., Imbach, L. L., Valko, P. O., Maric, A., Maqkaj, R., Werth, E., Baumann, C. R. & Baumann-Vogel, H. (2021b). Reduced Regional NREM Sleep Slow-Wave Activity Is Associated With Cognitive Impairment in Parkinson Disease. *Frontiers in Neurology*, Volume 12 - 2021. doi: 10.3389/fneur.2021.618101.

Shaffer, F. & Ginsberg, J. (2017). An Overview of Heart Rate Variability Metrics and Norms. *Frontiers in Public Health*, 5, 258. doi: 10.3389/fpubh.2017.00258.

Sharon, O. & Nir, Y. (2018). Attenuated fast steady-state visual evoked potentials during human sleep. *Cerebral cortex*, 28(4), 1297-1311.

Stankovski, T., Pereira, T., McClintock, P. V. E. & Stefanovska, A. (2017a). Coupling functions: Universal insights into dynamical interaction mechanisms. *Rev. Mod. Phys.*, 89, 045001. doi: 10.1103/RevModPhys.89.045001.

Stankovski, T., Pereira, T., McClintock, P. V. & Stefanovska, A. (2017b). Coupling functions: universal insights into dynamical interaction mechanisms. *Reviews of Modern Physics*, 89(4), 045001.

Stanyer, E. C., Baniqued, P. D. E., Awais, M., Kouara, L., Davies, A. G., Killan, E. C. & Mushtaq, F. (2021). The impact of acoustic stimulation during sleep on memory and sleep architecture: A meta-analysis. *Journal of sleep research*, e13385.

Staresina, B. P., Bergmann, T. O., Bonnefond, M., Van Der Meij, R., Jensen, O., Deuker, L., Elger, C. E., Axmacher, N. & Fell, J. (2015). Hierarchical nesting of slow oscillations, spindles and ripples in the human hippocampus during sleep. *Nature neuroscience*, 18(11), 1679–1686.

Stefanovska, A., Lotric, M., Strle, S. & Haken, H. (2001). The cardiovascular system as coupled oscillators? *Physiological measurement*, 22(3), 535-50.

Steriade, M. (2006). Grouping of brain rhythms in corticothalamic systems. *Neuroscience*, 137(4), 1087-1106. doi: https://doi.org/10.1016/j.neuroscience.2005.10.029.

Swapna, G., Soman, K. & Vinayakumar, R. (2019). Diabetes detection using ecg signals: An overview. *Deep learning techniques for biomedical and health informatics*, 299–327.

Thayer, J. F., Åhs, F., Fredrikson, M., Sollers III, J. J. & Wager, T. D. (2012). A meta-analysis of heart rate variability and neuroimaging studies: implications for heart rate variability as a marker of stress and health. *Neuroscience & Biobehavioral Reviews*, 36(2), 747-756.

Tiriac, A. & Blumberg, M. (2016). The Case of the Disappearing Spindle Burst. *Neural Plasticity*, 2016, 1-7. doi: 10.1155/2016/8037321.

Tononi, G. & Cirelli, C. (2006). Sleep function and synaptic homeostasis. *Sleep Medicine Reviews*, 10(1), 49-62. doi: https://doi.org/10.1016/j.smrv.2005.05.002.

Tononi, G., Riedner, B., Hulse, B., Ferrarelli, F. & Sarasso, S. (2010). Enhancing sleep slow waves with natural stimuli. *Medicamundi*, 54(2), 73–79.

Vyazovskiy, V. V. & Harris, K. D. (2013). Sleep and the single neuron: the role of global slow oscillations in individual cell rest. *Nature Reviews Neuroscience*, 14(6), 443-451. doi: 10.1038/nrn3494.

Whitehurst, L. N., Chen, P.-C., Naji, M. & Mednick, S. C. (2020). New directions in sleep and memory research: the role of autonomic activity. *Current Opinion in Behavioral Sciences*, 33, 17-24. doi: 10.1016/j.cobeha.2019.11.001.

Wilckens, K. A., Ferrarelli, F., Walker, M. P. & Buysse, D. J. (2018). Slow-Wave Activity Enhancement to Improve Cognition. *Trends in Neurosciences*, 41(7), 470-482. doi: 10.1016/j.tins.2018.03.003.

Wunderlin, M., Zeller, C. J., Wicki, K., Nissen, C. & Züst, M. A. (2024). Acoustic stimulation during slow wave sleep shows delayed effects on memory performance in older adults. *Frontiers in Sleep*, 2, 1294957.

Yamatsu, A., Yamashita, Y., Maru, I., Yang, J., TATSUZAkI, J. & Kim, M. (2015). The improvement of sleep by oral intake of GABA and apocynum venetum leaf extract. *Journal of nutritional science and vitaminology*, 61(2), 182-187.

Yoon, H. & Baek, H. J. (2022). External Auditory Stimulation as a Non-Pharmacological Sleep Aid. *Sensors*, 22(3), 1264.